NATIONAL CENTER FOR EARTHQUAKE ENGINEERING RESEARCH

ISSN 1088-3800

3D-BASIS - Nonlinear Dynamic Analysis of Three-Dimensional Base Isolated Structures: Part II

by

S. Nagarajaiah, A.M. Reinhorn and M.C. Constantinou

Technical Report NCEER-91-0005

February 28, 1991

This research was conducted at the University at Buffalo, State University of New York and was supported in whole or in part by the National Science Foundation under grant number ECE 86-07591.

NOTICE

This report was prepared by the University at Buffalo, State University of New York as a result of research sponsored by the National Center for Earthquake Engineering Research (NCEER) through a grant from the National Science Foundation, and other sponsors. Neither NCEER, associates of NCEER, its sponsors, the University at Buffalo, State University of New York nor any person acting on their behalf:

a. makes any warranty, express or implied, with respect to the use of any information, apparatus, method, or process disclosed in this report or that such use may not infringe upon privately owned rights; or

b. assumes any liabilities of whatsoever kind with respect to the use of, or the damage resulting from the use of, any information, apparatus, method, or process disclosed in this report.

Any opinions, findings, and conclusions or recommendations expressed in this publication are those of the author(s) and do not necessarily reflect the views of NCEER, the National Science Foundation, or other sponsors.

3D-BASIS
Nonlinear Dynamic Analysis of Three-Dimensional Base Isolated Structures: Part II

by

S. Nagarajaiah[1], A.M. Reinhorn[2] and M.C. Constantinou[3]

February 28, 1991

Technical Report NCEER-91-0005

NCEER Project Number 89-2102

NSF Master Contract Number ECE 86-07591

1 Research Assistant Professor, Department of Civil Engineering, State University of New York at Buffalo
2 Professor, Department of Civil Engineering, State University of New York at Buffalo
3 Associate Professor, Department of Civil Engineering, State University of New York at Buffalo

NATIONAL CENTER FOR EARTHQUAKE ENGINEERING RESEARCH
State University of New York at Buffalo
Red Jacket Quadrangle, Buffalo, NY 14261

PREFACE

The National Center for Earthquake Engineering Research (NCEER) is devoted to the expansion and dissemination of knowledge about earthquakes, the improvement of earthquake-resistant design, and the implementation of seismic hazard mitigation procedures to minimize loss of lives and property. The emphasis is on structures and lifelines that are found in zones of moderate to high seismicity throughout the United States.

NCEER's research is being carried out in an integrated and coordinated manner following a structured program. The current research program comprises four main areas:

- Existing and New Structures
- Secondary and Protective Systems
- Lifeline Systems
- Disaster Research and Planning

This technical report pertains to Program 2, Secondary and Protective Systems, and more specifically, to protective systems. Protective Systems are devices or systems which, when incorporated into a structure, help to improve the structure's ability to withstand seismic or other environmental loads. These systems can be passive, such as base isolators or viscoelastic dampers; or active, such as active tendons or active mass dampers; or combined passive-active systems.

Passive protective systems constitute one of the important areas of research. Current research activities, as shown schematically in the figure below, include the following:

1. Compilation and evaluation of available data.
2. Development of comprehensive analytical models.
3. Development of performance criteria and standardized testing procedures.
4. Development of simplified, code-type methods for analysis and design.

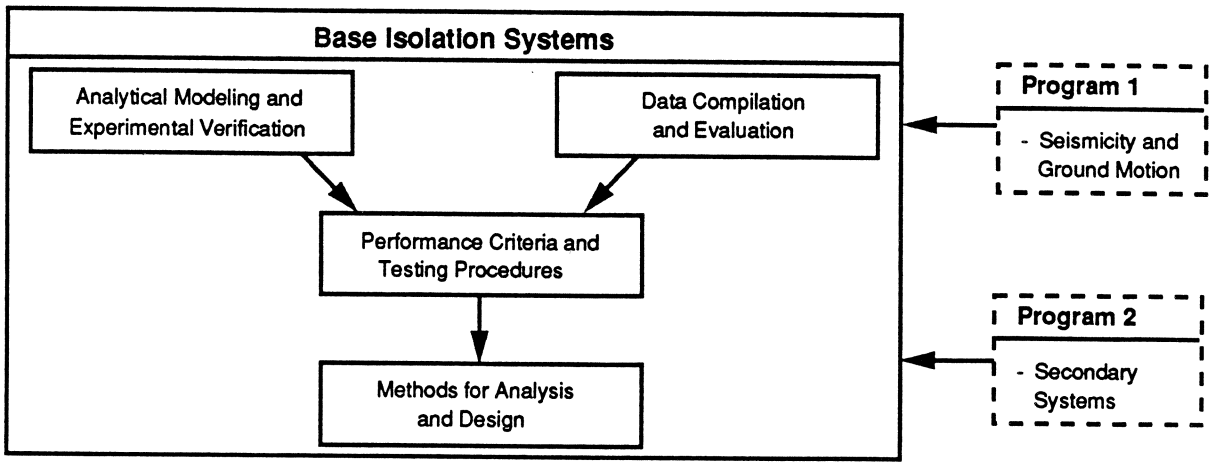

In this study, the capabilities of the computer program 3D-BASIS have been extended and an updated user's guide is presented. 3D-BASIS is used for analysis of three-dimensional base isolated buildings. The superstructure is treated as linear. The isolation system may consist of combinations of hysteretic and frictional devices. Response quantities computed using 3D-BASIS are compared with results obtained from other existing programs and experimental results.

ABSTRACT

Structures can be designed to withstand severe earthquake forces by providing ductility and energy dissipation capacity to the structural elements, thus allowing damage in the structural elements and invariably in the nonstructural elements. Another approach which is being rapidly adopted all-around the world is the concept of base isolation, wherein the flexibility and the energy dissipation capacity are provided by a specially designed isolation system that is placed between the superstructure and the foundation. These isolation systems can be designed to essentially limit the nonlinear behavior to the isolation level, imposing little or no ductility demand on the superstructure.

The study of three dimensional behavior of base isolated structures requires a comprehensive analytical model. The analytical model should be capable of addressing highly nonlinear behavior of isolation systems such as sliding systems and elastomeric bearing systems (with biaxial effects). The existing analytical models and solution algorithms cannot accurately analyze sliding systems or combined elastomeric-sliding systems.

This report deals with the development of a comprehensive analytical model and solution algorithm for nonlinear dynamic analysis of three dimensional base isolated structures and the development of computer program 3D-BASIS.

A new analytical model and solution algorithm involving the pseudo-force method is developed. New biaxial and uniaxial models of isolation elements are developed. The novelty of the analytical

model and solution algorithm is its capability to capture the highly nonlinear frictional behavior of sliding isolation systems in plane motion.

Nonlinear behavior is restricted to the base and the superstructure is considered to be elastic at all times. The nonlinear isolation system may consist of elastomeric and/or sliding bearings, linear springs and viscous elements. The solution algorithm consists of the pseudo-force method with iteration. Comparison of the computed results with experimental results is presented for verification. A six story reinforced concrete base isolated structure is analyzed to demonstrate the efficiency of the algorithm.

ACKNOWLEDGEMENTS

This work has been supported by the National Center for Earthquake Engineering Research (Which is supported by the National Science Foundation Grant No. ECE 86-07591 and the State of New York). This support is gratefully acknowledged.

TABLE OF CONTENTS

LIST OF FIGURES

LIST OF TABLES

SECTION 1

INTRODUCTION

The fundamental frequency of vibration of low-to-medium rise buildings is often in the range of frequencies where earthquake energy is the strongest. As a result these buildings amplify the ground vibration. The accelerations increase with the height of the building inducing higher interstory drifts and causing more damage or eventual collapse. One way to avoid severe damage and collapse in such situations is by providing ductility and energy dissipation capacity to the structural elements. Damage can still be substantial with this approach during severe inelastic excursions of the structural elements, eventhough collapse may not occur. Furthermore, the nonstructural elements and contents of the building are invariably damaged.

An improved solution for design of low-to-medium rise buildings is base isolation which is being adopted rapidly all-around the world. The concept of base isolation (Kelly 1986b,1988; Buckle 1990) is one in which flexibility and energy dissipation capacity are provided by a specially designed isolation system that is placed between the superstructure and the foundation. The isolation system reduces the seismic force input into the superstructure. The isolation system can be designed to restrict all the nonlinear behavior to the isolation level, thus imposing little or no ductility demand on the superstructure.

The idea or concept of base isolation is not new and many proposals have been made since the turn of the century. Excellent account of these and the development of base isolation to the present stage can be found in Kelly (1986b,1988) and Buckle (1990).

Acceptance of base isolation as a viable alternative and implementation of base isolation for aseismic structures is mainly because of the experimental work in the form of numerous shake table tests of base isolated models with various isolation systems. Eventhough none have to date been tested as-built by a strong tremor, evidence of their performance under mild to moderate earthquakes exist (Buckle 1990).

Analysis capability and code provisions of base isolated buildings are still in a developmental stage. Only tentative code provisions have been developed by Structural Engineering Association of California (1990). A comprehensive analysis capability for base isolated structures, with elastomeric and/or sliding isolation systems, with uplift resistant mechanisms and fail-safe systems, is still lacking.

The existing algorithms specifically developed for base isolated structures such as NPAD by Way and Jeng (1988), used for the analysis of Foothill Communities Law and Justice Center, California or a general purpose finite element program such as ANSR by Mondkar and Powell (1975), have plasticity based nonlinear elements that can be used to model elastomeric isolation elements. However these

elements cannot model sliding isolation elements accurately. Hence these algorithms cannot analyze base isolated structures with sliding isolation systems accurately.

Three dimensional behavior such as lateral-torsional response and effect of biaxial interaction in isolation bearings on the response of base isolated structures needs to be investigated. The study of three dimensional behavior of base isolated structures with highly nonlinear components in the isolation system, requires a comprehensive analytical model, and an accurate and efficient solution algorithm. The analytical model and the solution algorithm should be developed specifically for base isolated structures and verified.

1.1 Scope of Investigation

This report deals with the nonlinear dynamic analysis of three dimensional base isolated structures as follows:

a. Seismic response of three dimensional base isolated structures: (i) with sliding isolation systems including biaxial effects; (ii) with elastomeric isolation systems including biaxial effects; (iii) combined elastomeric and sliding isolation systems including biaxial effects.

In order to achieve the above objective a new generalized analytical model and solution algorithm is developed as follows:

a. Unified analytical modeling of: (i) sliding bearings with biaxial interaction, including variation of coefficient of friction with velocity and bearing pressure; and (ii) elastomeric bearings with biaxial interaction, including variation of shear stiffness with shear strain and axial load.

b. Development of a generalized analytical model, and an accurate and efficient solution algorithm to analyze all the above mentioned cases.

c. Verification and demonstration of accuracy of the developed solution algorithm by comparison with: (i) experimental results; (ii) response computed using predictor-corrector method; and (iii) response computed using general purpose finite element programs.

d. Demonstration of efficiency of the developed solution algorithm by analyzing a real structure.

The developed analytical model and solution algorithm have been implemented in the computer program 3D-BASIS (Nagarajaiah et al. 1989,1990c).

1.2 Organization of the Report

Organization and summary of various sections is as follows:

Section 2 reviews the various base isolation systems.

Section 3 presents a comprehensive review of the existing analytical models. This section also describes the existing capa-

bilities of modeling isolation components, the analytical models used for the base isolated structures and existing code provisions/recommendations.

The review in section 3 clearly highlights the limitations that exist and the need to develop a comprehensive algorithm and modeling procedure which can account for most if not all the features necessary for analyzing various kinds and aspects of base isolated structures.

Section 4 deals with the analytical model for base isolated structures. Aspects of full three dimensional representation of the superstructure are described.

Section 5 describes the uniaxial and biaxial models developed for representing the various isolation components. The biaxial effects in isolation bearings are accounted for by a discrete model with nonlinear characteristics. The validity of the hysteretic model considered is established by comparison with experimental results.

Section 6 describes the analytical model and the solution algorithm.

Section 7 presents the verification of solution algorithm by comparison with: (i) experimental results; (ii) solution using predictor-corrector method; and (iii) response computed using the general purpose finite element program ANSR (Mondkar and Powell 1975).

Section 8 presents the analysis of a six story reinforced concrete building on different isolation systems.

Section 9 presents the conclusions.

SECTION 2

BASE ISOLATION SYSTEMS

The essential components of an isolation system are components which provide flexibility, energy dissipation capacity, rigidity under low levels of lateral loads due to wind or minor earthquakes, recentering capability in the case of sliding systems, uplift resistant devices and fail-safe mechanism.

Flexible components of the isolation system may be unreinforced rubber blocks, elastomeric bearings (reinforced rubber blocks), sliding bearings, springs, sleeved piles, cable suspension systems or pneumatic bearings. However because of the flexibility at the base, base displacements are larger and to limit the base displacement to acceptable design levels additional damping or energy absorbing devices are added to the isolation systems. Damping or energy absorption may be due to plastic deformation of metal, friction damping, high damping elastomers, or viscous fluid damping.

Rigidity under low levels of lateral load is provided to prevent perceptible vibrations under frequently occurring loads such as minor earthquakes or wind loads. Such rigidity is provided by high shear modulus or high shear stiffness at low strains in high damping elastomeric bearings, high initial or elastic stiffness of lead in lead-rubber bearings, or devices designed to fail if these low levels of lateral load are exceeded. Recentering devices are provided to prevent large permanent displacements that could occur in a

freely sliding system. These devices could be helical springs, rubber blocks or specially designed bearings that use structural weight for recentering.

Uplift resistant devices are provided to prevent uplift of a portion of the structure due to large overturning moments. These could be devices enclosed in a circular hole in the middle of elastomeric bearings. These devices are activated if the bearings go into tension due to excessive overturning moments in the structure. Fail-safe mechanisms could be concrete or steel pedestals provided on either side of the bearing on which the structure comes to rest in case bearing displacements become excessive and the bearing becomes unstable.

2.1 Elastomeric Bearing Isolation Systems

Elastomeric bearings are made by bonding sheets of rubber to thin steel reinforcing plates. The bearings are very stiff in the vertical direction and very flexible in the horizontal direction. Damping that is inherent in usual rubber compounds as well as neoprene used in elastomeric bearings is rather low for use in aseismic base isolation. As an answer to this shortcoming researchers in New Zealand have developed several energy dissipators that could be used to enhance damping in elastomeric bearing systems (Buckle 1990). Of these, the lead-rubber bearing system is the most highly developed and extensively used system (Buckle 1990). This consists

of a lead core in a cylindrical hole at the center of an elastomeric bearing. The lead plug produces substantial increase in damping (Built 1982), from approximately 3% of critical damping in usual rubber compounds to about 10-15% and also increases resistance to wind loading by providing high initial stiffness (before yielding) to the bearing.

High damping rubber bearings (Kelly 1986b) used in the first base isolated building in the United states, Foothill Communities Law and Justice Center, San Bernardino, California, have a high degree of inherent damping. The shear stiffness of this rubber is high for small strains but decreases by a factor of about four or five as the strain increases, reaching a minimum value at a shear strain of 50%. For strains greater than 100% the stiffness begins to increase again. Thus for small loading caused by wind or mild earthquake the system has high stiffness and short period and as the lateral load increases the stiffness drops. For very high load, say above the maximum credible earthquake, the stiffness increases again providing a fail-safe system. The damping follows the same pattern but less dramatically, decreasing from an initial value of 20% to a minimum of 10% and then increasing again. In addition the energy dissipation capacity remains unaffected by variation of the vertical load that the bearing carries.

Conventional reinforced rubber bearings have been used for earthquake protection in France (Delfosse 1986) despite the low

damping. This system carries the trade name GAPEC. Mild steel rods have been added to this system for additional damping. Another system by trade name SEISMAFLOAT (Staudacher 1985) consists of unreinforced rubber bearings.

The elastomeric bearing systems shift the fundamental frequency of the isolated structure to values lower than the predominant earthquake frequencies. This effect coupled with increased energy dissipation capacity results in significant reductions of the earthquake forces imparted to the structural system above the isolation interface. The prime consideration in the design of elastomeric isolation systems is stability. Furthermore, these systems are sensitive to frequency content of ground motion.

2.2 Sliding Isolation Systems

Spie-Batignolles (SBTP) and Electricite de France (EDF) have developed a sliding-elastomeric isolation system for nuclear power plants (Plichon 1978; 1980). The system uses laminated neoprene bearings with lead-bronze-stainless steel sliding plates on top of each bearing. The sliding interface provides a friction coefficient of 0.2. The design of the power plant is for 0.2g and is standardised regardless of the seismicity of the area. The idea of a sliding joint as an isolation system is an attractive one for low cost housing since it can be constructed using no more complicated

technology or skilled labour other than that required for a conventional building. Hence this has been developed in India (Arya 1984) and China.

2.3 Sliding Isolation Systems with Recentering Devices

Sliding isolation systems with recentering devices consist of sliding bearings (Teflon slider sliding on a stainless steel plate) with recentering devices. Sliding bearings support and decouple the structure from the ground. The bearings further provide an energy dissipation mechanism by virtue of their frictional behavior. Recentering devices are provided to prevent large permanent displacements that could occur in a freely sliding system. These devices can be helical springs, rubber blocks or specially designed bearings that use structural weight for recentering.

Several sliding isolation systems with recentering devices have been proposed. The most notable are, the Earthquake Barrier System (Caspe and Reinhorn 1986), the Sliding Disc Bearing and Helical Spring System (Constantinou, Mokha and Reinhorn 1990a), the Resilient-Friction Base Isolator System (Mostaghel et al 1988), the Friction Pendulum System (Zayas et al. 1987), the TASS system (Hisano et al. 1988), and Alexsismon (Ikonomou 1985).

The Earthquake Barrier System uses Teflon sliding bearings with yielding steel beams for recentering. The Sliding Disc Bearing and Helical Spring System uses Teflon sliding bearings with helical

spring units for recentering. In the Resilient-Friction Base Isolator system, bearings consist of several Teflon-steel interfaces fitted in the center with a rubber core which provides the recentering capability. In the Friction Pendulum System the sliding interface takes a spherical shape so that the recentering capability is provided by the weight of the structure during rising along the spherical surface. In the TASS system, rubber blocks used in parallel with elastomeric-TFE sliding bearings provide the recentering capability.

Sliding isolation systems with weak restoring force provide isolation by limiting the force at the isolation interface and not by shifting the fundamental frequency of the system to low values (Constantinou et al. 1990a). These systems have low sensitivity to the frequency content of excitation and are stable.

2.4 Systems with Combined Elastomeric and Sliding Isolation Systems

Recently a 9 story model on a combined elastomeric and sliding isolation system was tested (Chalhoub and Kelly 1990) at U. C. Berkeley. An uplift resistant mechanism was also incorporated in the elastomeric bearings. These tests revealed that the combined system is effective in isolating the structure. When excessive displacements occurred the uplift resistant devices were activated increasing the horizontal stiffness of the isolation system thus limiting the displacements.

2.5 Other Systems

Another system which goes by the trade name GERB (Huffmann 1986) consists of helical steel springs and viscous dampers. Flexibility and energy absorption capability is provided in all directions. The other notable system used in New Zealand is the sleeved pile system (Boardman 1983).

SECTION 3

REVIEW OF EXISTING ANALYTICAL MODELS

Many existing general purpose finite element computer programs like ANSR (Mondkar and Powell 1975) and DRAIN-2D (Kannan and Powell 1975) can be used directly if the isolation system exhibits bilinear force-displacement behavior (eg. lead-rubber bearing system). However when the isolation system is comprised of sliding system or combined elastomeric and sliding isolation system, or high damping elastomeric bearing isolation system, with uplift resistant mechanisms and fail-safe systems, then the above mentioned computer programs cannot accurately analyze such systems.

Earliest studies on buildings with a soft first story reported are by Chopra and Clough (1973) and Jagdish and Raghuprasad (1979). Several studies with single-degree and multi-degree of freedom representation have been reported the most notable being by Su et al. (1989) on comparative analysis of various isolation systems. Many studies on optimization and random vibration of base isolated structures (Constantinou 1984) have been reported.

3.1 Models for Isolation Components

(i) Uniaxial Models

The essential features that need to be modeled for uniaxial behavior of elastomeric bearings are: (i) the appropriate shear stiffness representation in the pre-and-post yielding range; (ii) representation of the strain dependence of shear stiffness appro-

priately; and (iii) representation of the loss of shear stiffness with increase in axial load ($P-\Delta$ effects). Furthermore, the energy dissipated or hysteretic damping, the strain dependency of hysteretic damping, and the increase in damping with increasing axial load ($P-\Delta$ effects) should be accurately represented. Eventhough stiffness and damping of the elastomeric isolators is frequency dependent, this seems to be of lesser importance in the range of frequencies encountered in base isolation (Fujita et al. 1989).

Bilinear or trilinear models can be used to model isolation elements like lead-rubber bearings, mild steel dampers. Lee (1980) has used the bilinear model for modeling lead-rubber bearings. Many Japanese researchers (Yasaka et al. 1988 and others) have used the bilinear model for modeling Lead-rubber bearings and steel dampers. Fujita et al. (1989) have used the bilinear model with modifications for modeling high damping elastomeric bearings. The trilinear model has been used by Miyazaki et al.(1988) for modeling lead-rubber bearings. The Ramberg-Osgood model (1943) has been used for modeling high damping elastomeric bearings by Yasaka et al. (1988) and Fujita et al.(1989). It is difficult to capture all the essential features mentioned before by these simple models.

The Coulomb model in which the transition from stick to sliding mode and vice versa is controlled by stick-slip conditions described by Mostaghel et al. (1988) and Su et al. (1989) has been used for modeling sliding bearings. The viscoplastic model for sliding bearings proposed by Constantinou et al. (1990b) has been used for

modeling sliding bearings. The viscoplastic model proposed by Ozdemir and Kelly (1976) has been used for modeling steel dampers by Bhatti et al. (1981) and by Fujita et al. (1989) with modifications for modeling high damping elastomeric bearings and lead-rubber bearings. The visoplastic or the rate model captures most of the features.

The differential equation model developed by Wen et al. (1976) collapses to the viscoplasticity model under certain conditions (Constantinou et al. 1990b) and captures most of the features. This model has the advantage of computational efficiency. Hence this model has been adapted in the present study for modeling lead-rubber bearings, high damping elastomeric bearings, steel dampers, and sliding bearings.

Finally, plasticity based yield surface models have been used to model lead-rubber bearings and high damping elastomeric bearings (Tarics et al. 1984). It is difficult to modify these models to capture the essential features mentioned before.

(ii) Biaxial Models

Experimental evidence in tests on steel dampers and high damping bearings (Yasaka et al. 1988) reveal the importance of biaxial effects on force-displacement characteristics. Biaxial interaction coupled with all the effects mentioned for uniaxial behavior complicates modeling.

Japanese researchers (Wada et al. 1988, Yasaka et al. 1988, Nakamura et al. 1988) have used the multiple shear spring model to account for biaxial effects in steel dampers, lead-rubber bearings and high damping elastomeric bearings. This model consists of a series of shear springs arranged in a radial pattern. The plasticity based yield surface model has been used by Tarics et al. (1984) for modeling lead-rubber bearings and by Mizukoshi et al. (1989) for modeling laminated rubber bearings and hysteretic dampers. However multiple shear spring model and yield surface models when used in large number of bearings can be computationally intensive.

The differential equation model for biaxial interaction proposed by Park et al. (1986), is an extension of the model by Wen (1976) for uniaxial behavior. Constantinou et al. (1990b) have used this model for modeling biaxial effects in sliding bearings. In the present study this model has been adapted for modeling biaxial behavior of lead-rubber bearings, high damping elastomeric bearings, steel dampers, and sliding bearings. The model is very effective in capturing most of the essential features which will be demonstrated by comparison with experimental results in section 5.

3.1.1 Models for Axial Load Effects ($P-\Delta$ Effects)

Many models have been proposed for $P-\Delta$ effects in elastomeric isolation bearings. The most notable one is the mechanical model proposed by Koh et al. (1988;1989). This model takes into account

the reduction in horizontal stiffness, reduction in height and the increase in damping due to $P-\Delta$ effects.

Axial load effects in elastomeric bearings and sliding bearings are accounted for in the present study by adjusting the appropriate parameters of the model considered.

3.1.2 Models for Uplift and Fail-safe Systems

If uplift resistant mechanisms are enclosed inside elastomeric bearings (Chalhoub and Kelly 1990) or high damping elastomeric bearings are used, then the increase in shear stiffness at large strains has to be accurately captured.

Beucke and Kelly (1985) have proposed a model which is a combination of linear viscous, constant coulomb and linear coulomb damping appropriate for friction type fail-safe mechanism. However this model proves to be computationally intensive. Hence they have also suggested equivalent linearization methods.

3.1.3 Models for Visco-dampers and Accelerated Liquid Mass Dampers

Huffmann (1986) has described the characteristics of damping resistance of GERB viscodampers. Kawamata (1988) has described the analysis of liquid mass dampers. An equivalent stiffness and damping ratio neglecting the frequency dependency of the properties of the viscodamper has also been used. Schwahn et al. (1987) have presented the use of an equivalent rheological model for viscodampers and

discussed the implications of using these models. In the present study the frequency independent viscous-dashpot and elastic element are used for modeling viscodampers.

3.2 Analytical Models for Base Isolated Structures

3.2.1 Equivalent Linear Method of Analysis

The nonlinear behavior of the isolation system is linearized by assuming an equivalent stiffness (essentially the post yielding stiffness of the bearings) and an appropriate damping ratio (10% to 15% of critical). Both the superstructure and the isolation system are considered to be elastic. The elastomeric isolators are represented as equivalent short columns. Either two or three dimensional representation is used. This approach has been used for the design of base isolated structures and for assessing forces in the structural elements. In most cases general purpose computer programs like ETABS (Wilson et al. 1975), SAP (Wilson 1980) and other programs have been used for this purpose.

A site specific response spectrum is reduced to the nonlinear version by accounting for the hysteretic damping (Walters et al. 1987) and used for linear response spectrum analysis. Such analyses yield good results, but since modal superposition method is used for establishing the peak responses a certain degree of approximation is involved in the estimation of peak values of response. However these methods cannot be used when sliding isolators are present in

the isolation system.

Kelly, Buckle and Tsai (1986a,1989) have used a linear viscous method to predict the response of base isolated structures on elastomeric bearings. The effective stiffness and the damping factor/loss factor are evaluated based on a parameter identification applied to the linear viscous model.

Pan and Kelly (1983,1984) have used the equivalent linear representation with appropriate damping to study the lateral-torsional response and vertical-rocking response of base isolated structures.

Beucke and Kelly (1989) have suggested an equivalent linearization method to analyze systems with fail-safe mechanisms. Novak and Henderson (1989) have used equivalent linearization for a soil structure interaction study of base isolated structures.

The results of such equivalent linear methods of analysis yield good results in most cases, but have to be considered with caution because of the nature of nonlinearities involved.

3.2.2 Two Dimensional Nonlinear Dynamic Analysis

Two dimensional analysis can be used but at the expense of excluding torsional response and biaxial effects. Eventhough coupled lateral-torsional response is reduced in base isolated structures, it cannot be overlooked in practical design due to the fact that torsional response can cause excessive displacements at the corner bearings and can lead to instability of the bearings.

The superstructure and the isolation system are modeled using either elastic elements or inelastic elements. The advantage in a two dimensional analysis is the ease with which both the superstructure and the isolation system can be represented by inelastic elements. Thus ductility demand - if any - on the structural elements (superstructure) can be estimated. Biaxial effects in isolation bearings are absent, which makes the analysis much simpler as compared to full three dimensional representation. The computational effort needed is lesser.

Wang and Reinhorn (1989) have analyzed sliding isolated structures using conventional stick-slip conditions. Constantinou et al. (1990a) have used a predictor-corrector method for analyzing sliding base isolated structures. Mostaghel et al. (1988) have used the conventional stick-slip conditions to analyze the response of structures supported on R-FBI system. Sveinsson et al. (1990) have used the computer program DRAIN2D (Kannan and Powell 1975) to evaluate the seismic response of a base isolated structure, considering ductility demand on the structural members. Koh and Balendra (1989) have analyzed base isolated structures including $P-\Delta$ effects in elastomeric isolation bearings.

Base isolated buildings in New Zealand, the Wellington Central Police station (Charleson et al. 1987) with sleeved pile/damper isolation system and the William Clayton building (Megget 1978) with lead-rubber bearing isolation system, were analyzed using the computer program DRAIN-2D (Kannan and Powell 1975). The bilinear

model was used for modeling the isolation elements. Union House (Boardman et al.1983) a twelve story building in New Zealand with the sleeve pile/damper isolation system was analyzed by a two dimensional nonlinear dynamic analysis computer program developed by Sharpe and Carr (1979).

Nuclear power plants with the French EDF isolation system have been analyzed by Plichon et al. (1978,1980) using elasto-plastic model to represent the isolation system. Several Japanese researchers (Miyazaki et al. 1988, Wada et al. 1988 and others) have studied two dimensional behavior.

Constantinou et al. (1987,1988) have analyzed base isolated structures on laminated rubber bearings considering soil structure interaction and have also developed simplified method of analysis. Wolf et al. (1983) have analyzed the Koeberg nuclear power plant including soil structure interaction.

In symmetric structures two dimensional nonlinear dynamic analysis is adequate and yields response quantities of interest for design of base isolated structures. This is the prime motivation for all the above mentioned studies. However for asymmetric base isolated structures three dimensional nonlinear dynamic analysis is necessary.

3.2.3 Three Dimensional Nonlinear Dynamic Analysis

Tarics et al. (1984) have analyzed the Foothill communities law and justice center, the first base isolated structure to be built in United States with the high damping elastomeric bearing isolation system. The computer program NPAD (Way et al. 1988) developed specifically for three dimensional nonlinear dynamic analysis of this base isolated structure, is the first program of its kind suitable for elastomeric isolation systems (lead-rubber bearing and high damping elastomeric bearing isolation systems). In the analysis a linear elastic three dimensional superstructure was considered. The high damping rubber isolators were represented as bilinear elastic springs with biaxial interaction and the hysteretic damping in the isolators was accounted for by using a viscous element with damping ratio of 10% to 15% of critical. For a comparative analysis a lead-rubber isolation system was also considered initially and the lead-rubber bearings were modeled using plasticity based non-linear elements. However this program cannot accurately analyze base isolated structures with sliding isolation systems or combined sliding-elastomeric isolation systems.

The city and county building in salt lake city, the first building in the world to be retrofitted with isolation bearings (Walters et al. 1987) was analyzed using a linear elastic three dimensional superstructure. Plasticity based nonlinear beam-column elements in the general purpose finite element program ANSR (Mondkar and Powell 1975) were used to model the lead-rubber isolators.

Asher et al. (1990) have used ANSR to analyze the USC university hospital which is isolated using lead-rubber isolators and elastomeric bearings. Sveinsson et al. (1990) have used ANSR to analyze an existing eight story building to be retrofitted using the lead-rubber isolation system. Buckle et al. (1987) have used ANSR to analyze base isolated nuclear power stations with lead-rubber isolation systems. Mizukoshi et al. (1989) have analyzed nuclear reactor building on lead-rubber isolation system, including soil-structure interaction, to study the torsional response. The isolation system consisting of lead-rubber isolators and dampers was modeled using plasticity based bilinear element.

The computer program ANSR can be used to analyze base isolated structures with elastomeric isolation systems, particularly lead-rubber isolation system. The bilinear properties of the lead-rubber system with biaxial effects can be easily captured using the plasticity based nonlinear elements available. Hence ANSR is very popular amongst the designers. However this is a program written for general purpose finite element analysis and hence does not cater for the specific needs of the analysis of base isolated structures and cannot accrately analyze base isolated structures with sliding isolation systems or combined sliding-elastomeric isolation systems.

3.3 Code provisions

The Structural Engineers Association of California (SEAOC 1990) has put forth 'Tentative general requirements for the design and construction of seismic isolated structures'. The general design philosophy of the document is that: (i) the base isolated structure remain stable for required design displacements; (ii) the isolation system should provide resistance which increases with increasing displacement; (iii) the system should be capable of repeated cyclic loads without any significant degradation; and (iv) the isolation system should have quantifiable engineering properties so that reliable estimates of response quantities can be obtained.

Two design procedures are permitted under the proposed design guidelines in the document:

a. The use of a set of simple equations that prescribe design values of displacement and base shear. These formulae are similar to the seismic lateral force formulae now in use for conventional building design. This procedure is intended for stiff buildings of regular configuration which are located on stiff soils or rock sites and away from active faults.

b. Dynamic analysis, which could be either nonlinear time history analysis or linear response spectrum analysis is required for all other situations. In particular nonlinear time history analysis is required when the isolated structure is located on a soil profile with site factor S_4 and/or when the isolation system is not capable of producing restoring force as specified

in the requirements, or when the force-displacement properties of the isolation system are either dependent on the rate of loading or dependent on the vertical and the bilateral load. Also **the document recommends that the analytical model be three dimensional and should include both the superstructure and the isolation system.** Furthermore, the force-displacement characteristics of the isolation system used in the analyses should be substantiated by tests. The document recommends that the analysis shall be performed with seismic input in both orthogonal directions of the building.

3.4 Remarks

The review clearly highlights the limitations that exist and the need to develop a comprehensive algorithm for nonlinear dynamic analysis of three dimensional base isolated structures, which can account for most if not all the above mentioned features necessary for analyzing various kinds and aspects of base isolated structures.

SECTION 4

STRUCTURE MODELING

The three dimensional superstructure is considered to be elastic. The isolation system is considered to be nonlinear. The nonlinear force-displacement characteristics of the isolation components are modeled explicitly. In this section the superstructure modeling is described, in section 5 the models for isolation components are described and in section 6 the analytical model and the solution algorithm for the combined system are described.

4.1 Superstructure Modeling

The three dimensional superstructure is modeled with the assumption that it remains elastic at all times. This assumption is reasonable in the context of base isolation and has been exploited by several investigators (Tarics et al. 1984, Asher et al. 1990 and others) to reduce the computational effort. However it may be necessary to consider the structure also to be inelastic in some cases. This is not dealt with in the present study.

Multistory buildings with eccentric centers of mass and resistance respond in coupled lateral-torsional motions to earthquake ground motion, even when the motion is uniform over the base and contains no rotational components (Reinhorn et al. 1977, Kan and Chopra 1977). Analysis of such buildings requires torsional degrees of freedom in addition to translational degrees of freedom. Hence, a three-dimensional building with three degrees of freedom per floor is assumed to adequately represent the elastic super-

structure. As explained in the following section, two options are considered. In option one, the elastic superstructure is assumed to be a three-dimensional shear building, and in option two, the elastic superstructure is assumed to be a fully three-dimensional building.

The two options considered are based on the following assumptions:

a. Each floor has three degrees of freedom, X and Y translations and rotation about the center of mass of the floor. These degrees of freedom are attached to the center of mass of each floor.

b. There exists a rigid slab at the base level that connects all isolation elements. The three degrees of freedom at the base are attached to the center of mass of the base.

c. Since three degrees of freedom per floor are required in the three-dimensional representation of the superstructure, the number of modes required for modal reduction is always a multiple of three. The minimum number of modes required is three.

In the first option, the stiffness matrix of the three dimensional shear building is explicitly considered (this stiffness matrix is described in section 4.1.1). The following additional assumptions are made:

a. The centers of mass of the floors and the base lie on a vertical axis and the centers of resistance of the floors and the base are arbitrarily located.

b. Since a three dimensional shear building representation is used for the superstructure, floor diaphragms are considered to be rigid, and walls and columns are considered to be inextensible.

In the second option, the eigenvalues and eigenvectors (for the fixed base condition) of the fully three dimensional superstructure are considered. Hence the superstructure stiffness matrix is not considered explicitly. The following additional assumption is made:

a. ETABS (Wilson et al. 1975) or a similar computer program, is used for eigenvalue analysis of the superstructure (for fixed base condition).

4.1.1 Shear Building Representation

The N-story idealized superstructure consists of rigid floor slabs supported on massless axially inextensible columns and walls. It is assumed that the centers of mass of the floors and the base lie on the same vertical axis, however, the centers of resistance need not lie on the vertical axis. Furthermore it is assumed that the principal axes of resistance of all stories are identically oriented. In this section, the superstructure stiffness matrix needed for shear building representation is described. The salient features of the idealized system are shown in Figs. 4-1 (for the present option the centers of mass of floors and the base lie on the reference axis) and 4-2.

The static eccentricities, e_{xi} and e_{yi} , between the center of resistance and center of mass of story i are defined by:

$$e_{xi} = \frac{1}{K_{yi}} \sum_j x_{ij} k_{yij} \tag{4.1}$$

$$e_{yi} = \frac{1}{K_{xi}} \sum_j y_{ij} k_{xij} \tag{4.2}$$

where

$$K_{xi} = \sum_j k_{xij}$$

$$K_{yi} = \sum_j k_{yij}$$

k_{xij} and k_{yij} represent the translational stiffnesses of the resisting elements (column or wall) of story i along the principal axes of resistance X and Y, respectively. x_{ij} and y_{ij} define the location of the resisting element j with respect to the origin at the center of mass. The torsional stiffness of the story i is defined with respect to the center of mass:

$$K_{\theta i} = \sum_j k_{xij} y_{ij}^2 + \sum_j k_{yij} x_{ij}^2 \tag{4.3}$$

The resulting stiffness matrix of the superstructure is presented in Table 4.1. The associated mass matrix is diagonal and involves the masses and rotational moments of inertia of each floor. The eigenvalues and eigenvectors from the eigenvalue analysis are used in the analytical model which includes the nonlinear isolation system (refer section 6). The dynamic response and the peak response values are computed by 3D-BASIS.

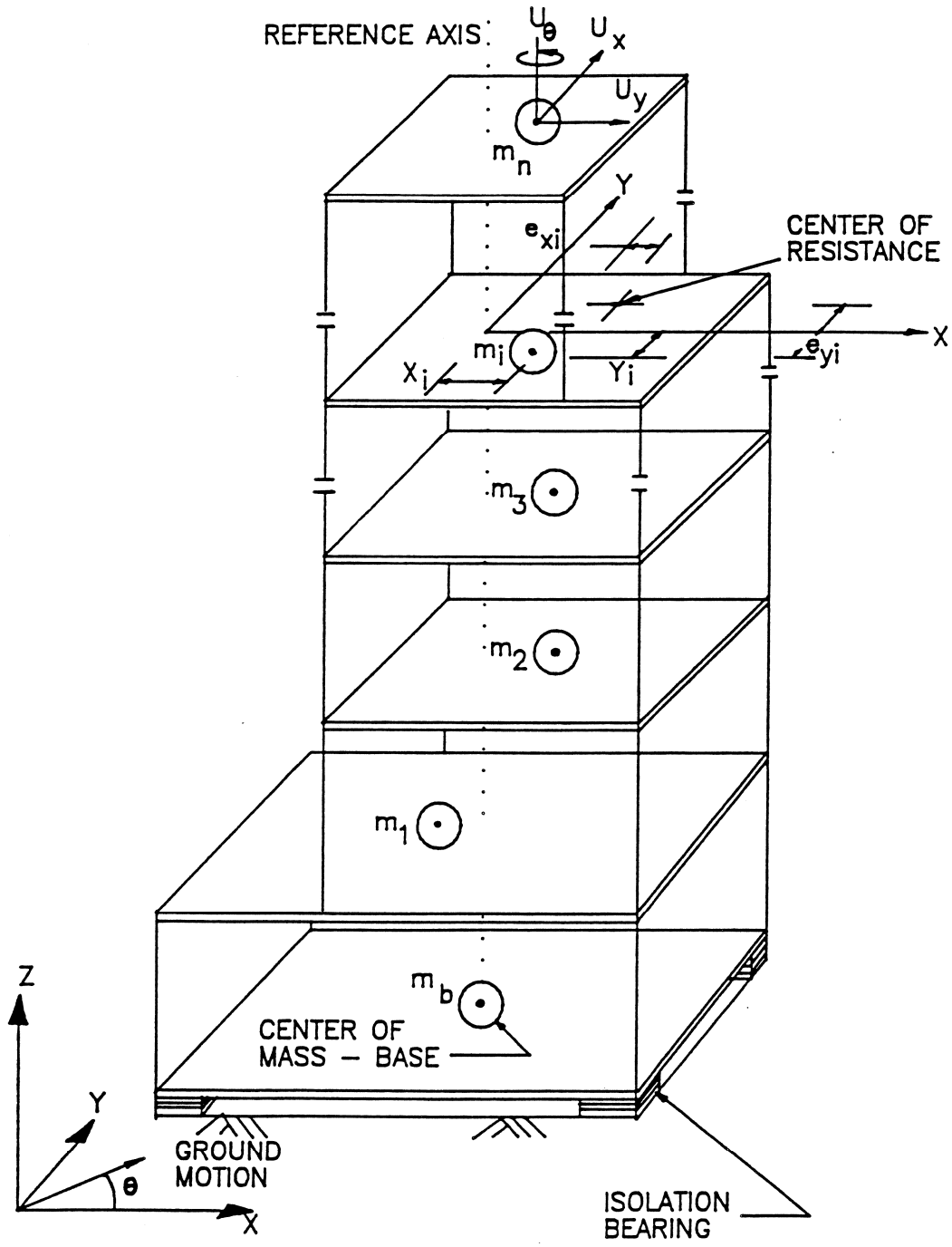

FIG. 4.1. Asymmetric Base Isolated Structure Excited by Bidirectional Ground Motion

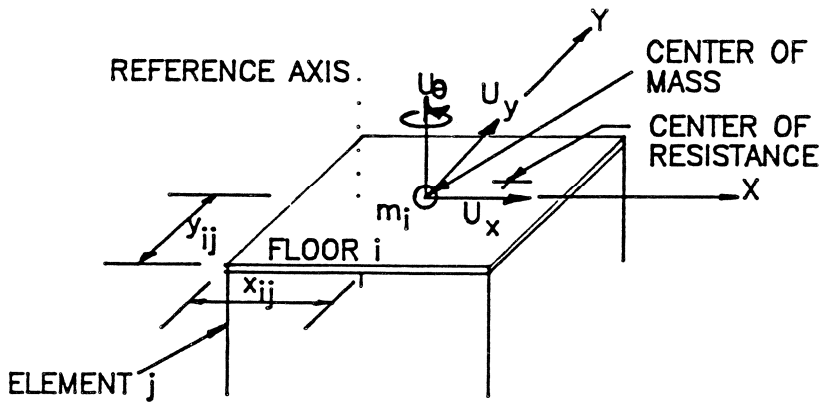

(a)

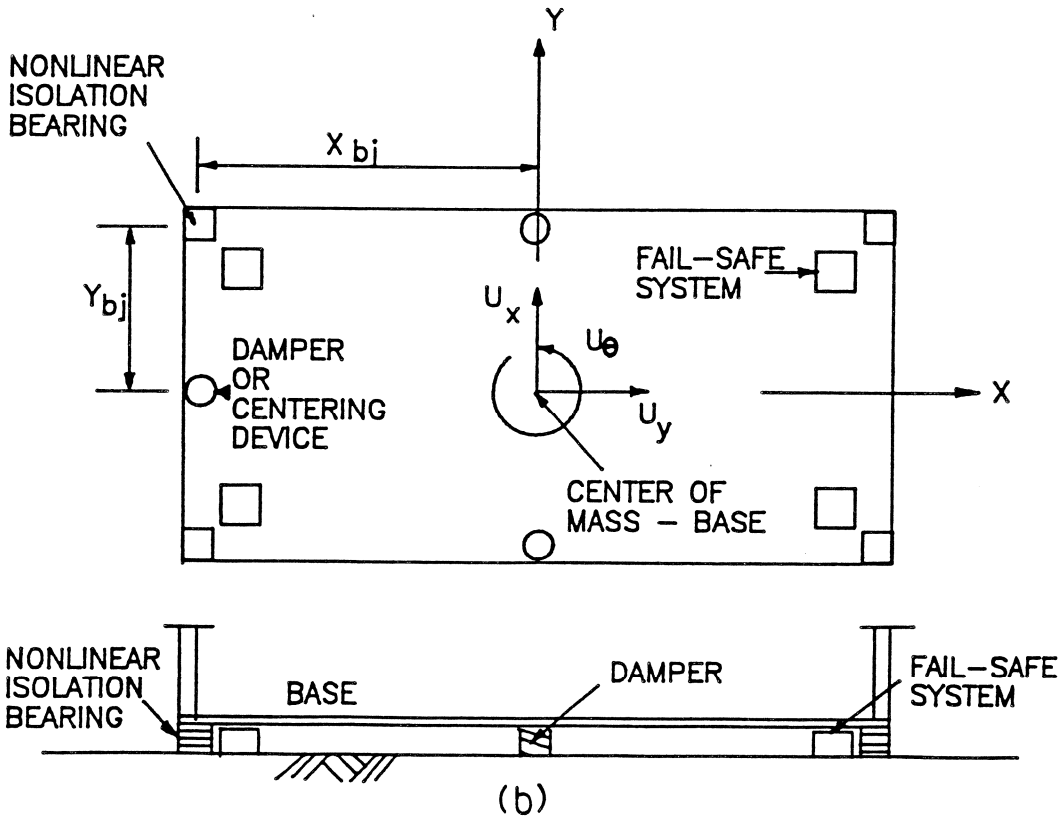

(b)

FIG. 4.2. Degrees of Freedom and Details of a typical floor and base: (a) Isometric View of Floor *i*; (b) Plan and Section of Base

TABLE 4.1
SUPERSTRUCTURE STIFFNESS MATRIX
FOR A THREE DIMENSIONAL SHEAR BUILDING

$$
\begin{bmatrix}
K_{xn} & 0 & -K_{xn}e_{yn} & -K_{xn} & 0 & K_{xn}e_{yn} & & & & & & \\
0 & K_{yn} & K_{yn}e_{xn} & 0 & -K_{yn} & -K_{yn}e_{xn} & & 0 & & & 0 & \\
-K_{xn}e_{yn} & K_{yn}e_{xn} & K_{\theta n} & K_{xn}e_{yn} & -K_{yn}e_{xn} & -K_{tn} & & & & & & \\
 & & & K_{xn}+K_{xn-1} & 0 & -K_{xn}e_{yn}-K_{xn-1}e_{yn-1} & & & & & & \\
 & SYM. & & 0 & K_{yn}+K_{yn-1} & K_{yn}e_{xn}+K_{yn-1}e_{xn-1} & & SYM. & & & 0 & \\
 & & & -K_{xn}e_{yn}-K_{xn-1}e_{yn-1} & K_{yn}e_{xn}+K_{yn-1}e_{xn-1} & K_{\theta n}+K_{\theta n-1} & & & & & & \\
 & & & & & & K_{x3}+K_{x2} & 0 & -K_{x3}e_{y3}-K_{x2}e_{y2} & & & \\
 & 0 & & & SYM. & & 0 & K_{y3}+K_{y2} & K_{y3}e_{x3}+K_{y2}e_{x2} & & SYM. & \\
 & & & & & & -K_{x3}e_{y3}-K_{x2}e_{y2} & K_{y3}e_{x3}+K_{y2}e_{x2} & K_{\theta 3}+K_{\theta 2} & & & \\
 & & & & & & & & & K_{x2}+K_{x1} & 0 & -K_{x2}e_{y2}-K_{x1}e_{y1} \\
 & 0 & & & 0 & & & SYM. & & 0 & K_{y2}+K_{y1} & K_{y2}e_{x2}+K_{y1}e_{x1} \\
 & & & & & & & & & -K_{x2}e_{y2}-K_{x1}e_{y1} & K_{y2}e_{x2}+K_{y1}e_{x1} & K_{\theta 2}+K_{\theta 1}
\end{bmatrix}
$$

4.1.2 Three Dimensional Representation

The elastic superstructure is modeled as a full three dimensional structure using ETABS (Wilson et al. 1975). The eigenvalues and orthonormal eigenvectors of the superstructure (for fixed base condition) from ETABS analysis are used in the analytical model which includes the nonlinear isolation system (refer section 6). In the present case the centers of mass of floors need not lie on the reference axis as shown in Fig. 4.1.

After the completion of the analysis including the nonlinear isolation system (the complete formulation will be presented in section 6), displacement, velocity and acceleration response at the centers of mass of floors computed in 3D-BASIS are used in ETABS to arrive at the peak member forces, drift and other relevant information.

4.2 Isolation System Modeling

The isolation system is considered to be nonlinear. The nonlinear force-displacement characteristics of the isolation components are modeled explicitly. The models for isolation components are described in section 5. The following assumption is made for modeling the isolation system:

a. The isolation system is rigid in the vertical direction and torque resistance of individual bearing is neglected.

SECTION 5

MODELS FOR ISOLATION COMPONENTS

The differential equation model for the uniaxial behavior developed by Wen (1976) and the differential equation model for the biaxial behavior developed by Park et al. (1986) are adapted in the present study. The biaxial model by Park et al. (1986) is an extension of the model by Wen (1976) for uniaxial behavior. With the modifications proposed in the present study the models for uniaxial and biaxial behavior can be adapted for modeling lead-rubber bearings, high damping elastomeric bearings, and steel dampers. Constantinou et al. (1990b) have adapted the differential equation model for modeling uniaxial and biaxial effects in sliding bearings. These models for sliding bearings are adopted in the present study.

The essential features that need to be modeled for uniaxial behavior of elastomeric bearings are the appropriate shear stiffness representation in the pre-and-post yielding range, representation of the strain dependence of shear stiffness appropriately, and representation of the loss of shear stiffness because of $P-\Delta$ effects. Furthermore, the energy dissipated or hysteretic damping, the strain dependency of hysteretic damping, and the increase in damping because of $P-\Delta$ effects should be accurately represented. Eventhough the frequency dependence of stiffness and damping is present this seems to be of lesser importance in the range of frequencies encountered in base isolation (Fujita et al. 1989).

Experimental evidence in tests on steel dampers and high damping rubber bearings (Yasaka et al. 1988) reveal the importance of biaxial effects on force-displacement characteristics. Biaxial effects in elastomeric isolation systems have been accounted for, but its effect on the response has not been studied in detail. Japanese researchers (Yasaka et al. 1988; Nakamura et al. 1988; Wada et al. 1988) have accounted for biaxial effects in elastomeric isolation systems by using the multiple spring model - to model elastomeric bearings - in which a number of nonlinear springs are arranged in a radial pattern. Tarics et al. (1984) have accounted for biaxial effects in elastomeric isolation systems by using plasticity based nonlinear model to model elastomeric bearings.

The essential features that need to be modeled for uniaxial behavior of sliding bearings are the velocity dependence of the coefficient of friction and the influence of bearing pressure on the coefficient of friction. The change of coefficient of friction with direction can be neglected (Constantinou et al. 1990b).

For sliding isolation systems, Younis et al. (1983) have analyzed plane motion of two rigid bodies in contact with coulomb friction. The biaxial model for sliding bearings used in the present study is capable of reproducing multiple stick-slip conditions that arise in sliding isolation systems, wherein each bearing is subjected to different motion.

5.1 Aspects of Modeling Isolation Components

The isolation system often experiences multidirectional motion under multidirectional excitation, wherein each isolation element experiences a different motion and when sliding bearings are present in the isolation system multiple stick-slip conditions result. In such cases the conventional method of keeping track of transition from stick to sliding mode and vice versa described by Mostaghel et al. (1988) and Su et al. (1989) results in complications. Hence in the presented analytical model a hysteretic model is used to represent the stick-slip behavior of sliding bearings. Sliding bearings are usually made of Teflon - Steel interface and Teflon undergoes a small elastic shear deformation (of the order of 0.1 to 0.2 mm as shown in Fig. 5.1) before sliding commences (Constantinou et al. 1990b). Eventhough the hysteretic model presented cannot capture rigid-plastic behavior, the small shear deformation of Teflon renders a finite but high elastic stiffness to the hysteretic loop, which can be captured by the hysteretic model.

The isolation elements presented in this report can model both uniaxial and biaxial behavior of either elastomeric or sliding bearings. The model for sliding bearings can account for the variation of coefficient of friction with velocity (evident in Fig. 5.1) and bearing pressure observed in Teflon sliding bearings (Constantinou et al. 1990b). The model for elastomeric bearings can account for the change in energy dissipation capacity due to the variation of axial force observed in lead-rubber bearings (Built 1982).

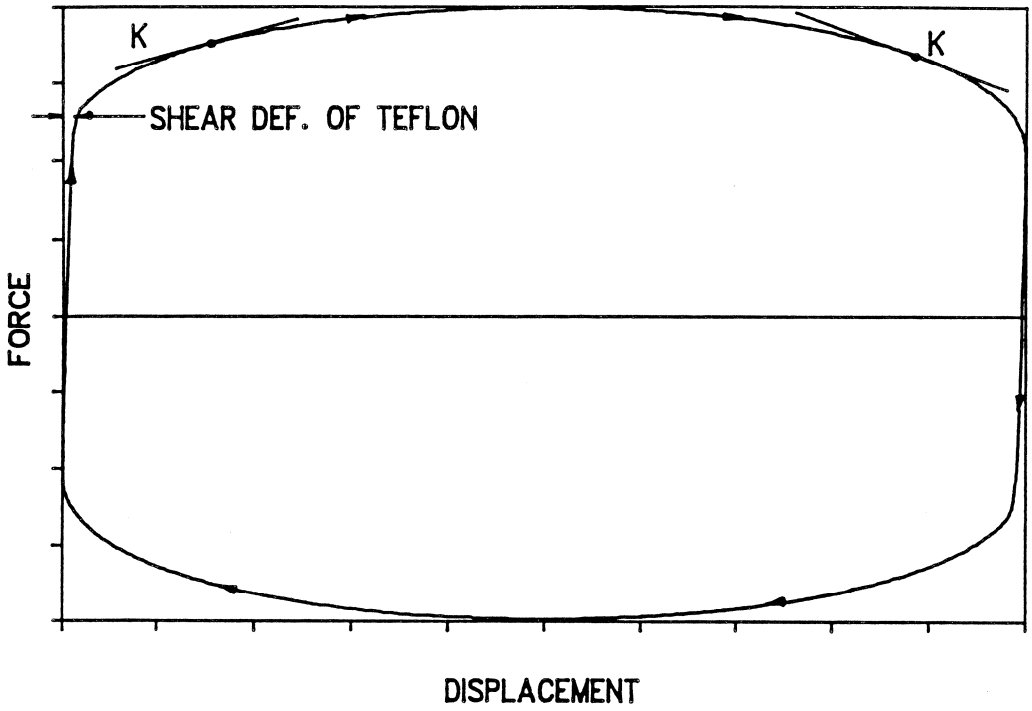

FIG. 5.1. Force-displacement characteristic of Teflon-steel interface

5.2 Elements for Modeling Isolation Components

Several isolation elements are considered so that any combination of these can be used to model the isolation system completely. The isolation elements are:

(i) Elastic elements

(ii) Viscous elements

(iii) Hysteretic element for elastomeric bearings

  a. uniaxial

  b. biaxial

(iv) Hysteretic element for sliding bearings

  a. uniaxial

  b. biaxial

(i) Elastic element: This element can be used to approximately simulate the behavior of elastomeric bearings along with the viscous element.

(ii) Viscous element: This element can be used to model the equivalent damping in elastomeric bearings.

(iii) Hysteretic element for elastomeric bearings: This element can be used to simulate the behavior of high damping rubber bearings, lead-rubber bearings, lead extrusion devices, and mild steel dampers in the form of torsional or flexural beams. Both uniaxial and biaxial behavior can be modeled.

(iv) Hysteretic element for sliding bearings: This element can be used to simulate the behavior Teflon-steel interfaces and other frictional interfaces. Both uniaxial and biaxial behavior can be modeled.

5.3 Models for Isolation Components

Modeling elastic elements is straight forward and will not be dealt with here. The viscous element is described briefly first. Then the biaxial isolation element is described, followed by the description of the uniaxial element which is a particular case of the biaxial element. The isolation elements and their verification described herein have been presented more extensively in previous publications (Nagarajaiah et al. 1989;1990b;1990c), however the description which follows is made for the sake of completeness.

5.3.1 Model for Viscous elements

The viscous element is for modeling the equivalent hysteretic damping of isolation components. The damping coefficient at each isolation component defines the viscous dashpot element. This element along with elastic element can be used to approximately model the behavior of elastomeric bearings.

5.3.2 Model for Biaxial Isolation Elements

At a bearing undergoing plane motion with displacement components U_x and U_y and velocity components $\dot{U}_x$ and $\dot{U}_y$ in the X and Y directions, lateral forces develop and these forces exhibit biaxial

interaction. In addition a torsional moment develops at the bearing. The contribution of this torsional moment to the total torque exerted to the structure supported by several bearings is insignificant.

The direction of the resultant force at the bearing opposes the direction of the motion given by:

$$\theta = \tan^{-1}\left(\frac{\dot{U}_y}{\dot{U}_x}\right) \tag{5.1}$$

The model presented herein accounts for the direction and magnitude of the resultant hysteretic force.

The model for biaxial interaction is based on the following set of equations proposed by Park, Wen and Ang (1986):

$$\begin{Bmatrix} \dot{Z}_x Y \\ \dot{Z}_y Y \end{Bmatrix} = \begin{Bmatrix} A\dot{U}_x \\ A\dot{U}_y \end{Bmatrix} - \begin{pmatrix} Z_x^2(\gamma Sign(\dot{U}_x Z_x)+\beta) & Z_x Z_y(\gamma Sign(\dot{U}_y Z_y)+\beta) \\ Z_x Z_y(\gamma Sign(\dot{U}_x Z_x)+\beta) & Z_y^2(\gamma Sign(\dot{U}_y Z_y)+\beta) \end{pmatrix} \begin{Bmatrix} \dot{U}_x \\ \dot{U}_y \end{Bmatrix} \tag{5.2}$$

in which, Z_x and Z_y are hysteretic dimensionless quantities, Y is the yield displacement, A, γ and β are dimensionless quantities that control the shape of the hysteresis loop. The values of $A = 1$, $\gamma = 0.9$ and $\beta = 0.1$ are used in this report. When yielding commences, Eq. 5.2 has the following solution provided that $A/(\beta+\gamma) = 1$ (Constantinou et al. 1990b):

$$Z_x = \cos\theta, \quad Z_y = \sin\theta \tag{5.3}$$

Z_x and Z_y are bounded by values ± 1 and account for the direction and biaxial interaction of hysteretic forces. The interaction curve given by Eq. 5.2 is circular.

(i) Biaxial Model for Sliding Bearings

For a sliding bearing, the mobilized forces are described by the equations (Constantinou et al. 1990b):

$$F_x = \mu_s W Z_x, \quad F_y = \mu_s W Z_y \tag{5.4}$$

in which, W is the vertical load carried by the bearing and μ_s is the coefficient of sliding friction which depends on the value of bearing pressure, angle θ and the instantaneous velocity of sliding $\dot{U}$:

$$\dot{U} = (\dot{U}_x^2 + \dot{U}_y^2)^{1/2} \tag{5.5}$$

Z_x and Z_y which are bounded by the values ± 1, account for the conditions of separation and reattachment (instead of a signum function) and also account for the direction and biaxial interaction of frictional forces.

The coefficient of sliding friction is modeled by the following equation (Constantinou et al. 1990b):

$$\mu_s = f_{max} - \Delta f \quad \exp(-a|\dot{U}|) \tag{5.6}$$

in which, f_{max} is the maximum value of the coefficient of friction and Δf is the difference between the maximum and minimum (at $\dot{U} \sim 0$) values of the coefficient of friction. f_{max}, Δf and a are functions of bearing pressure and angle θ (Constantinou et al. 1990b). To account for the effects of axial load, the parameters are adjusted based on experimental results (Mokha et al. 1990a). The dependency on the angle θ is negligible and hence neglected.

(ii) Biaxial Model for Elastomeric Bearings and Steel Dampers

For a elastomeric bearing, the mobilized forces are described by the equations:

$$F_x = \alpha \frac{F^y}{Y} U_x + (1-\alpha) F^y Z_x, \quad F_y = \alpha \frac{F^y}{Y} U_y + (1-\alpha) F^y Z_y \tag{5.7}$$

in which, α is the postyielding to preyielding stiffness ratio, F^y is the yield force and Y is the yield displacement. Z_x and Z_y account for the direction and biaxial interaction of hysteretic forces. To account for the effects of axial load, parameter α, yield force F^y and yield displacement Y are adjusted based on experimental results (Built 1982).

5.3.3 Model for Uniaxial Isolation Elements

The biaxial interaction can be neglected when the off-diagonal elements of the matrix in Eq. 5.2 are replaced by zeros. This results in a uniaxial model with two either frictional or bilinear independent elements in the two orthogonal directions. Eq. 5.2 collapses to the uniaxial model governed by the following equation (Wen 1976):

$$\dot{Z}Y = A\dot{U} - |Z|^{\eta}(\gamma Sgn(\dot{U}Z) + \beta)\dot{U} \tag{5.8}$$

where $\eta = 2$ in the biaxial case and this parameter controls the transition from elastic range to the post yielding range. The value of this parameter can be increased to achieve near-bilinear behavior rather than smooth bilinear behavior. When the ratio $A/(\beta+\gamma) = 1$ the model reduces (Constantinou et al. 1990b) to model of viscoplasticity (Ozdemir and Kelly 1976).

The interaction curve in the uniaxial case is effectively square. In the case of uniaxial sliding element the velocity used for calculation of the coefficient of friction from Eq. 5.6 is either $\dot{U}_x$ or $\dot{U}_y$.

5.4 Verification of the Hysteretic Model

Two comparisons are considered:

1. Comparison with tests conducted by Yasaka et al. (1988) on a steel damper and high damping rubber bearing.

2. Comparison with experimental results obtained by Mokha et al (1990a) for Teflon-steel interfaces.

Tests by Yasaka et al. (1988) were conducted on a cantilever steel damper and high damping rubber bearing. These specimens were of 1/7 scale. The vertical actuator in the test set up was controlled to hold the axial load at 4 ton (39.24 kN), for the high damping rubber bearing. The horizontal actuators were controlled to obtain the desired motion in the horizontal plane.

The Teflon-steel interface experiment (Mokha et al. 1990a) was conducted on highly polished stainless steel-unfilled Teflon interfaces at 1000 psi pressure.

The properties used for simulation of the uniaxial and biaxial hysteresis loops are extracted from the experimental results.

5.4.1 Verification Procedure

Harmonic motion of a given frequency and amplitude is considered

to be the input. The biaxial and uniaxial models presented are considered for simulation. The simulated and test results in the form of force-displacement loops are considered for comparison.

5.4.2 Steel Damper

Comparison with biaxial tests on a 1/7 scale steel damper by Yasaka et al. (1988) is considered. The tested cantilever steel damper was 17 mm in diameter and had an effective height of 100 mm. The steel damper had a lateral elastic stiffness of 2.58 ton/cm (2.53 kN/mm; 1 Metric ton = 9.81 kN), yield force of 0.286 ton (2.8056 kN) and yield displacement of 0.111 cm (1.11 mm). The hysteresis loops are simulated using Eqs. 5.2 and 5.7, with α = 0.023. The simulated and experimental hysteresis loops shown in Fig. 5.2 indicate good agreement. The bidirectional motion shown in Fig. 5.2 is given by:

$$U_x = U_o \sin \omega t; \quad U_y = U_o \sin 2\omega t \tag{5.9}$$

in which, U_O = 2.93 cm (29.3 mm) and ω = 1.57 radian/sec. In Fig. 5.2, Q_X and Q_Y represent forces and U_X and U_Y represent the displacements, in the X and Y directions respectively.

5.4.3 High Damping Rubber Bearing

The tested high damping rubber bearing had 24 layers of rubber - hardness 50 - 0.12 cm (1.2 mm) thick, with 24 steel reinforcing

plates of 0.05 cm (0.5 mm) thickness. Design dead weight was 4 ton (39.24 kN), post yielding horizontal stiffness was 0.281 ton/cm (0.276 kN/mm), and vertical stiffness was 451 ton/cm (442 kN/mm).

The following parameters are used for simulation of results for the high damping rubber bearing: elastic horizontal stiffness of 1.1 ton/cm (1.079 kN/mm); yield force 0.165 ton/cm (0.16186 kN/mm); yield displacement of 0.15 cm (1.5 mm); and $\alpha = 0.3$. Shear stiffness degradation is incorporated as follows:

$$\alpha^* = \alpha(0.5 + 0.5e^{(-5|U|/t_s)}) \tag{5.10}$$

where U is the resultant displacement, t_s is the thickness of the rubber, α^* is the modified post-to-preyielding stiffness ratio. The simulated and experimental hysteresis loops shown in Fig. 5.3 indicate good agreement. The bidirectional motion shown in Fig. 5.3 is based on Eq. 5.9 (U_o = 2.93 cm (29.3 mm) and ω = 1.57 radian/sec). In Fig. 5.3, Q_x and Q_y represent forces and U_x and U_y represent the displacements, in the X and Y directions respectively.

5.4.4 Sliding Bearing

Experiment conducted by Mokha et al. (1990a) on a highly polished stainless steel-unfilled Teflon interface at 1000 psi pressure is considered. The parameters in Eq. 5.6 are f_{max} = 0.1193, Δf = 0.0927 and a = 0.6 sec/in (0.02363 sec/mm) (Constantinou et al. 1990b). The uniaxial hysteresis loops are simulated using Eq. 5.4 and 5.8, with Y = 0.01 inch (0.254 mm) based on Constantinou et al. (1990b).

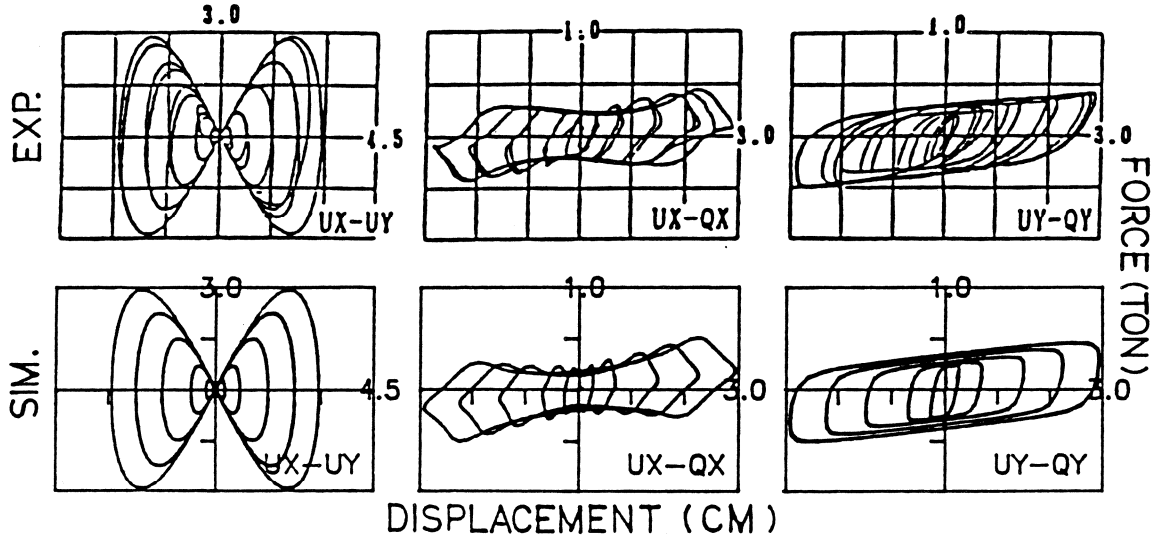

FIG. 5.2. Comparison of Experimental and Simulated Results of the Bidirectional Tests on Steel Damper for Lemniscate Motion

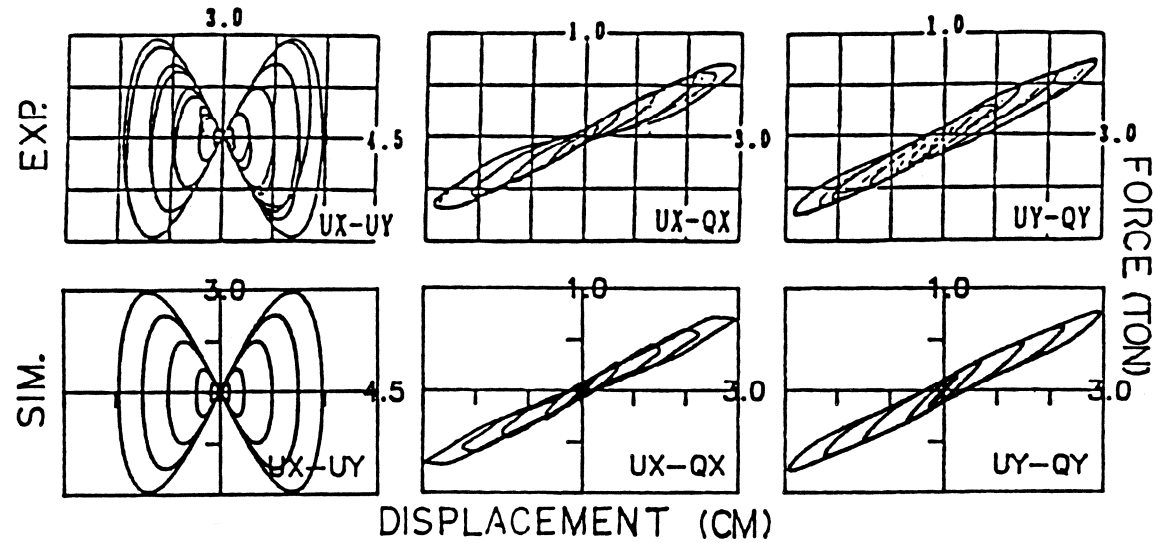

FIG. 5.3. Comparison of Experimental and Simulated Results of the Bidirectional Tests on High Damping Rubber Bearing for Lemniscate Motion

The input motion was unidirectional sinusoidal wave of 1.0 inch (25.4 mm) amplitude and frequency 0.16 Hz. Fig. 5.4 shows the simulated and experimental hysteresis loops. The model captures the features exhibited by the experimental force-displacement loops.

5.4.5 Verification and Features of the Biaxial Model

The satisfactory comparison with experimental results in the case of steel damper and high damping bearing validates the biaxial model considered.

Experimental data is not available for biaxial sliding behavior, hence only indirect verification (Constantinou et al. 1990b) is presented for the biaxial model for sliding bearings. Teflon-steel interface at 1000 psi (6.9 N/mm^2) is considered. The parameters in Eq. 5.6 from Constantinou et al. (1990b) are f_{max} = 0.1193, Δf = 0.0927 and a = 0.6 sec/in (0.02363 sec/mm). The hysteresis loops are simulated using Eqs. 5.2 and 5.4, with Y = 0.01 inch (0.254 mm) based on Constantinou et al. (1990b). The simulated results for the bidirectional motion are shown in Fig. 5.5 along with the uniaxial case (results in the Y direction are partially shown only for the biaxial case for clarity). The bidirectional motion shown in the upper left corner of Fig. 5.5 is based on Eq. 5.9 with U_o = 1 inch (25.4 mm) and ω = 1 radian/sec. The results shown in Fig. 5.5 have the following features: the biaxial force in X direction approaches the uniaxial force in X direction, when the biaxial force in Y direction approaches zero value indicating appropriate interaction. This can be observed at points 2 and 4 in Fig. 5.5 (b). Furthermore,

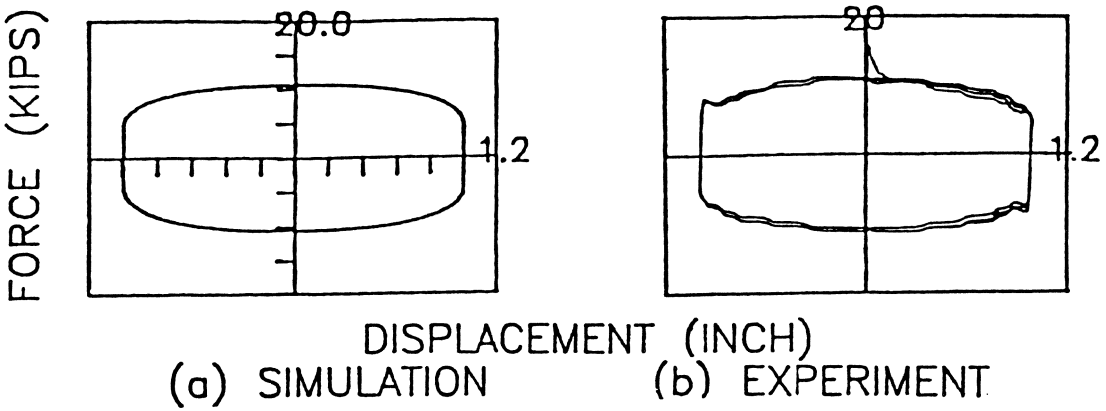

FIG. 5.4. Comparison of Results of Experiment Conducted on Unfilled Teflon-steel Interface at 1000 psi Pressure: (a) Simulation; (b) Experiment

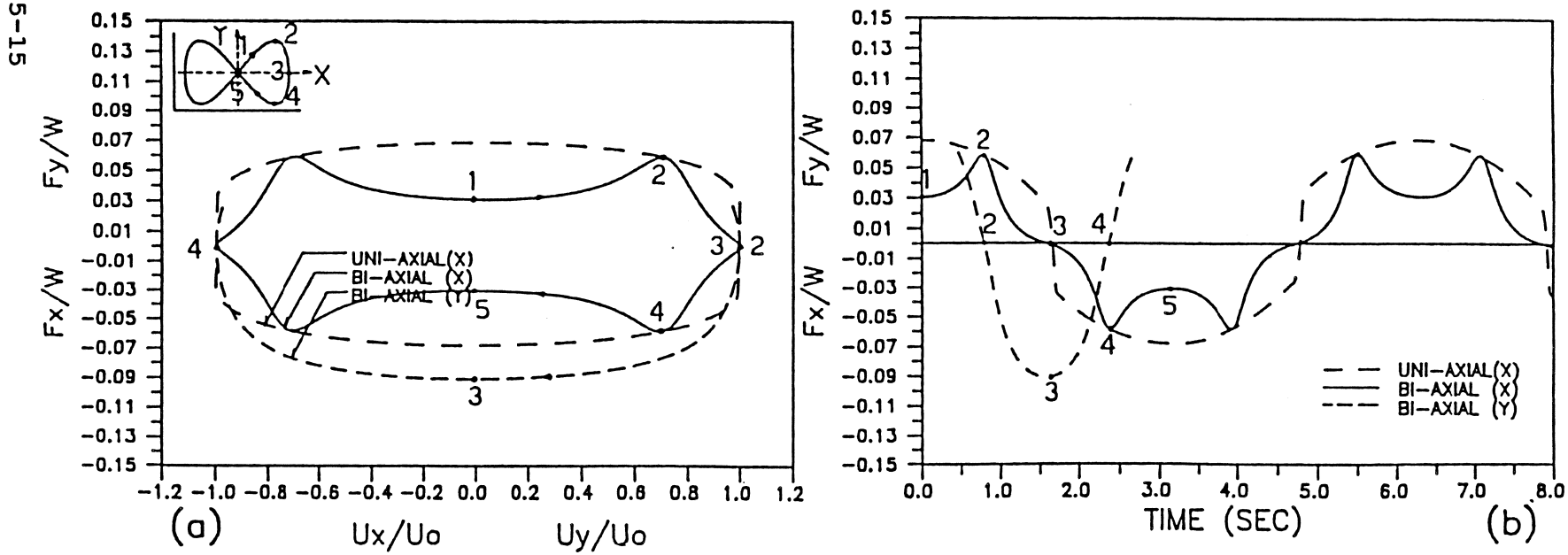

FIG. 5.5. Simulated Biaxial Friction Behavior of Teflon-steel Interface under Bidirectional Motion: (a) Force-Displacement Loop; (b) Force Time History (1 Ton = 9.801 kN).

the biaxial force in X direction is zero at point 3 wherein the motion is only in the Y direction. Note the marked similarity of the simulated hysteresis loops in Fig. 5.5 with experimental hysteresis loops of the steel damper shown in Fig. 5.2. Further verification of both biaxial and uniaxial models can be found in Nagarajaiah (1990b).

Hence the uniaxial and biaxial models described above are used for modeling lead-rubber bearings, high damping bearings, steel dampers, and sliding bearings.

SECTION 6

ANALYTICAL MODEL AND SOLUTION ALGORITHM FOR BASE ISOLATED STRUCTURES

This section presents the analytical model and the solution algorithm involving the pseudo-force method. It also describes briefly the reasons for using pseudo-force method of solution, instead of the widely used Modified Newton-Raphson method of solution. The analytical model considers an elastic superstructure and nonlinear isolation system. Furthermore, modal reduction of the elastic superstructure is adopted since it leads to computational efficiency and due to the well known fact that only the first few modes are adequate to model the superstructure in base isolated structures. The following analytical model has been presented in a previous publication (Nagarajaiah et al. 1989), however the solution algorithm has been modified by using unconditionally stable semi-implicit Runge-Kutta method, suitable for stiff differential equations, instead of the fourth order Runge-Kutta method used previously (Nagarajaiah et al. 1989). The modified solution algorithm is presented in detail and the analytical model is presented briefly for the sake of completeness.

6.1 Analytical Model and Equations of Motion

A typical base isolated multistory building and the displacement coordinates that will be used in the formulation are shown in Fig. 6.1 (U_i, U_b, U_g may be in X or Y direction). The superstructure is modeled as an elastic frame-wall structure with three degrees

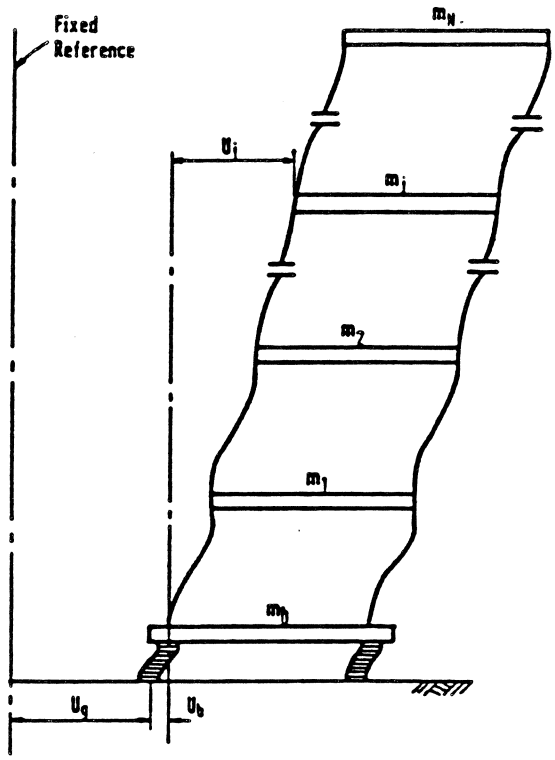

FIG. 6.1. Displacement Coordinates of the base isolated structure

of freedom per floor. The three degrees of freedom are attached to the center of mass of each floor and base. The floors and the base are assumed to be infinitely rigid inplane. The isolation system may consist of elastomeric and/or sliding isolation bearings, linear springs and viscous elements.

The equations of motion for the elastic superstructure are expressed in the following form:

$$M_{nxn}\ddot{u}_{nx1} + C_{nxn}\dot{u}_{nx1} + K_{nxn}u_{nx1} = -M_{nxn}R_{nx3}\{\ddot{u}_g + \ddot{u}_b\}_{3x1} \qquad (6.1)$$

in which, n is three times the number of floors, M is the diagonal superstructure mass matrix, C is the superstructure damping matrix, K is the superstructure stiffness matrix and R is the matrix of earthquake influence coefficients i.e. the matrix of displacements and rotation at the center of mass of the floors resulting from a unit translation in the X and Y directions and unit rotation at the center of mass of the base. Furthermore, $\ddot{u}$, $\dot{u}$ and u represent the floor acceleration, velocity and displacement vectors relative to the base, $\ddot{u}_b$ is the vector of base acceleration relative to the ground and $\ddot{u}_g$ is the vector of ground acceleration.

The equations of motion for the base are as follows:

$$R^T_{3xn}M_{nxn}\{\{\ddot{u}\} + R\{\ddot{u}_b + \ddot{u}_g\}\}_{nx1} + M_{b3x3}\{\ddot{u}_b + \ddot{u}_g\}_{3x1} + C_{b3x3}\{\dot{u}_b\}_{3x1} + K_{b3x3}\{u_b\}_{3x1} + \{f\}_{3x1} = 0 \qquad (6.2)$$

in which, M_b is the diagonal mass matrix of the rigid base, C_b is the resultant damping matrix of viscous isolation elements, K_b is the resultant stiffness matrix of elastic isolation elements and

f is the vector containing the forces mobilized in the nonlinear elements of the isolation system such as the presented elements for sliding or elastomeric bearings. Employing modal reduction:

$$\mathbf{u}_n = \Phi_{nxm}\mathbf{u}^*_{mxl} \tag{6.3}$$

in which, Φ is the modal matrix normalized with respect to the mass matrix and $\mathbf{u}^*$ is the modal displacement vector relative to the base and m is the number of eigenvectors retained in the analysis, and combining Eqs. 6.1 to 6.3 the following equation is derived:

$$\begin{pmatrix} [I] & [\Phi^T M R] \\ [R^T M \Phi] & [R^T M R + M_b] \end{pmatrix}_{(m+3)x(m+3)} \begin{Bmatrix} \ddot{u}^* \\ \ddot{u}_b \end{Bmatrix}_{(m+3)xl} + \begin{pmatrix} [2\xi_i\omega_i] & 0 \\ 0 & [C_b] \end{pmatrix}_{(m+3)x(m+3)} \begin{Bmatrix} \dot{u}^* \\ \dot{u}_b \end{Bmatrix}_{(m+3)xl}$$

$$+ \begin{pmatrix} [\omega_i^2] & 0 \\ 0 & [K_b] \end{pmatrix}_{(m+3)x(m+3)} \begin{Bmatrix} u^* \\ u_b \end{Bmatrix}_{(m+3)xl} + \begin{Bmatrix} 0 \\ f \end{Bmatrix}_{(m+3)xl} = -\begin{bmatrix} \Phi^T M R \\ R^T M R + M_b \end{bmatrix}_{(m+3)x3} \ddot{u}_{g\,3xl} \tag{6.4}$$

in which, ξ_i = the modal damping factor and ω_i = the natural frequency, of the fixed base structure in the mode i. In Eq. 6.4 matrices $[2\xi_i\omega_i]$ and $[\omega_i^2]$ are diagonal.

Eq. 6.4 can be written as follows:

$$\bar{M}\ddot{\bar{u}}_t + \bar{C}\dot{\bar{u}}_t + \bar{K}\bar{u}_t + f_t = \bar{P}_t \tag{6.5}$$

At time $t+\Delta t$

$$\bar{M}\ddot{\bar{u}}_{t+\Delta t} + \bar{C}\dot{\bar{u}}_{t+\Delta t} + \bar{K}\bar{u}_{t+\Delta t} + f_{t+\Delta t} = \bar{P}_{t+\Delta t} \tag{6.6}$$

Written in incremental form

$$\bar{M}\Delta\ddot{\bar{u}}_{t+\Delta t} + \bar{C}\Delta\dot{\bar{u}}_{t+\Delta t} + \bar{K}\Delta\bar{u}_{t+\Delta t} + \Delta f_{t+\Delta t} = \bar{P}_{t+\Delta t} - \bar{M}\ddot{\bar{u}}_t - \bar{C}\dot{\bar{u}}_t - \bar{K}\bar{u}_t - f_t \tag{6.7}$$

In which, $\bar{M}$, $\bar{C}$, $\bar{K}$ and $\bar{P}$ represent the reduced mass, damping, stiffness and load matrices (see Eq. 6.4). Furthermore, the state of motion of modal superstructure and base is represented by vectors

$\ddot{u}_t$, $\dot{u}_t$ and u_t (see Eq. 6.4).

6.2 Method of Solution

The incremental nonlinear force vector $\Delta f_{t+\Delta t}$ in Eq. 6.7 is unknown. Two methods can be used to represent this incremental nonlinear force vector: the first method is by using a tangent stiffness representation with modified Newton-Raphson solution procedure; and the second method is by representing the nonlinear forces as pseudo-forces and considering them as additional loads (by bringing them to the right hand side of the equation of motion and adding them to the load vector) and using an iterative solution procedure.

When sliding elements are present in the isolation system the force-displacement behavior of the isolation system consists of near-rigid plastic behavior and involves abrupt changes in tangent stiffness. Furthermore, when biaxial effects are included the force-displacement loops are highly nonlinear. Hence the problem at hand is highly nonlinear and requires a stable and accurate solution procedure.

6.2.1 Modified Newton-Raphson Procedure

Modified Newton-Raphson procedure is widely used for nonlinear dynamic analysis and converges to the correct solution rapidly when the nonlinearities are mild. However when the nonlinearities are

severe the method fails to converge (Stricklin et al. 1977).

The tangent stiffness formulation was investigated and is reported in Nagarajaiah et al. 1989. The study revealed that:

a. The method converged for three dimensional response of structures with elastomeric isolation systems.
b. The method did not converge for three dimensional response of structures with sliding isolation systems because of the severe nonlinearities involved.

In addition the method has the following disadvantage:

a. The tangent stiffness matrix representing the nonlinear forces and the coefficient or effective-stiffness matrix (Newmark's method) has to be updated at every time step and hence the solution procedure is computationally intensive. The small time step needed to achieve the desired accuracy in the present context (response of sliding base isolated structures) makes this method computationally inefficient.

6.2.2 Pseudo-force Method

The pseudo-force method has been used for nonlinear dynamic analysis of shells by Stricklin et al. (1971) and by Darbre and Wolf (1988) for soil structure interaction problems. The method has the following advantages:

a. The coefficient or the effective-stiffness matrix (Newmark's method) is formulated only once for constant time step and used

repeatedly for the entire analysis, which makes the method extremely efficient in the present context (response of sliding base isolated structures).

b. The method converges even in the case of highly nonlinear problems (Stricklin et al. 1971;1977).

In addition the following advantages were found in the present study:

a. The pseudo-force method converges to the correct solution even when severe nonlinearities such as planar sliding behavior along with biaxial effects are present.

b. The method yields results of comparable accuracy of the predictor-corrector method. These comparisons are presented in section 7.

c. The method along with the solution algorithm presented is extremely efficient. This will be demonstrated in sections 7 and 8.

Hence the pseudo-force method is used in the solution algorithm.

6.3 Solution Algorithm

The incremental nonlinear force vector $\Delta f_{t+\Delta t}$ in Eq. 6.7 is unknown. This vector is brought on to the right hand side of Eq. 6.7 and treated as a pseudo-force vector. The two step solution algorithm developed is as follows:

(i) The solution of equations of motion using unconditionally stable Newmark's constant-average-acceleration method (the Newmark's

method is chosen as it is unconditionally stable for both positive and negative tangent stiffness - Cheng 1988).

(ii) The solution of differential equations governing the behavior of the nonlinear isolation elements using unconditionally stable semi-implicit Runge-Kutta method (Rosenbrock 1964) suitable for solution of stiff differential equations.

Furthermore, a iterative procedure consisting of corrective pseudo-forces is employed within each time step until equilibrium is achieved. The developed solution algorithm is shown in Table 6.1.

6.4 Varying Time Step for Accuracy

The solution algorithm has the option of using a constant time step or variable time step. The time step is reduced from Δt_{slip} - the time step at high velocity dictated by standard requirements of numerical accuracy and stability - to a fraction of its value at low velocities to maintain accuracy, especially in sliding isolated structures (Nagarajaiah 1990b). The time step is reduced based on the magnitude of the resultant velocity at the center of mass of the base:

$$\Delta t_{stick} = \Delta t_{slip}\left[1 - \exp\left(-\frac{\dot{u}^2}{a}\right)\right] \tag{6.8}$$

in which, $\dot{u}$ = resultant velocity at the center of mass of the base, Δt_{stick} = reduced time step used when the structure velocity is low ($\Delta t_{slip} > \Delta t_{stick} > \Delta t_{slip}/nl$; nl = integer to introduce the desired reduction) and a = constant to define the range of velocity over

TABLE 6.1 SOLUTION ALGORITHM

A.Initial Conditions:

1. Form stiffness matrix $\bar{K}$, mass matrix $\bar{M}$, and damping matrix $\bar{C}$. Initialize $\bar{u}_0$, $\dot{u}_0$ and $\ddot{u}_0$.

2. Select time step Δt, set parameters $\delta = 0.25$ and $\theta = 0.5$, and calculate the integration constants:

$$a_1 = \frac{1}{\delta(\Delta t)^2};\quad a_2 = \frac{1}{\delta \Delta t};\quad a_3 = \frac{1}{2\delta};\quad a_4 = \frac{\theta}{\delta \Delta t};\quad a_5 = \frac{\theta}{\delta};\quad a_6 = \Delta t\left(\frac{\theta}{2\delta} - 1\right)$$

3. Form the effective stiffness matrix $\quad K^* = a_1\bar{M} + a_4\bar{C} + \bar{K}$

4. Triangularize K^* using Gaussian elimination (only if the time step is different from the previous step).

B.Iteration at each time step:

1. Assume the pseudo-force $\Delta f^i_{t+\Delta t} = 0$ in iteration i = 1.

2. Calculate the effective load vector at time $t + \Delta t$:

$$P^*_{t+\Delta t} = \Delta \bar{P}_{t+\Delta t} - \Delta f^i_{t+\Delta t} + \bar{M}(a_2\dot{u}_t + a_3\ddot{u}_t) + \bar{C}(a_5\dot{u}_t + a_6\ddot{u}_t)$$

$$\Delta \bar{P}_{t+\Delta t} = \bar{P}_{t+\Delta t} - (\bar{M}\ddot{u}_t + \bar{C}\dot{u}_t + \bar{K}\bar{u}_t + f_t)$$

3. Solve for displacements at time $t + \Delta t$: $\quad K^*\Delta u^i_{t+\Delta t} = P^*_{t+\Delta t}$

4. Update the state of motion at time $t + \Delta t$:

$$\ddot{u}_{t+\Delta t} = \ddot{u}_t + a_1\Delta\bar{u}^i_{t+\Delta t} - a_2\dot{u}_t - a_3\ddot{u}_t;\quad \dot{u}_{t+\Delta t} = \dot{u}_t + a_4\Delta\bar{u}^i_{t+\Delta t} - a_5\dot{u}_t - a_6\ddot{u}_t;\quad \bar{u}_{t+\Delta t} = \bar{u}_t + \Delta\bar{u}^i_{t+\Delta t}$$

5. Compute the state of motion at each bearing and solve for the nonlinear force at each bearing using semi-implicit Runge-Kutta method.

6. Compute the resultant nonlinear force vector at the center of mass of the base $\Delta f^{i+1}_{t+\Delta t}$.

7. Compute

$$Error = \frac{|\Delta f^{i+1}_{t+\Delta t} - \Delta f^i_{t+\Delta t}|}{Ref.\,\mathrm{Max}.\,Moment}$$

Where $|.|$ is the euclidean norm

8. If Error $\geq$ tolerance, further iteration is needed, iterate starting form step B-1 and use $\Delta f^{i+1}_{t+\Delta t}$ as the pseudo-force and the state of motion at time t, $\bar{u}_t$, $\dot{u}_t$ and $\ddot{u}_t$.

9. If Error $\leq$ tolerance, no further iteration is needed, update the nonlinear force vector: $f_{t+\Delta t} = f_t + \Delta f^{i+1}_{t+\Delta t}$

reset time step if necessary, go to step B-1 if the time step is not reset or A-2 if the time step is reset.

which the reduction takes place. The time step is not reduced continuously as implied by Eq. 6.8, but rather at discrete intervals of velocity, for computational efficiency.

6.5 Implementation of the Analytical Model and the Solution Algorithm

The analytical model and the solution algorithm have been implemented in computer programs 3D-BASIS and BASETAB.

6.5.1 Computer Program 3D-BASIS

The analytical model with the elastic superstructure (with both the three dimensional shear building option and the option in which eigenvalues and eigenvectors are used) and the nonlinear isolation system, and the solution algorithm have been implemented in the computer program 3D-BASIS (Nagarajaiah et al. 1989;1990b;1990c).

6.5.2 Computer Program BASETAB

BASETAB (Nagarajaiah 1990b) is a computer program which has been developed by combining the computer program 3D-BASIS and the computer program ETABS (Wilson et al. 1975). ETABS computes the eigenvalues and eigenvectors (for fixed base condition) and returns the eigenvalues and eigenvectors to 3D-BASIS. 3D-BASIS computes the displacement, velocity and acceleration response at the centers of mass of floors and returns these response values to ETABS. Finally ETABS computes the peak member forces, drift and other relevant response quantities of interest.

SECTION 7

VERIFICATION OF THE ALGORITHM

Comparisons with experimental results from shake table tests on a model base isolated structure on sliding isolation system is considered. Furthermore, comparison with results from the rigorous mathematical solution involving Gear's predictor-corrector method is considered. Finally the comparison with results obtained using the general purpose finite element program ANSR (Mondkar and Powell 1975) is considered. The accuracy and efficiency of the algorithm are demonstrated by comparison.

7.1 Comparison with Experimental Results of a Six Story Sliding Base Isolated Model

Comparison with experimental results of a shake table test (Mokha et al. 1990b) performed on a 1/4 scale artificial mass simulation model (total weight 228.6 kN) of a six story steel moment-resisting frame with a sliding isolation system called Friction Pendulum System (FPS) is considered. The model had three bays of 4 ft (1219.2 mm) in the longer direction and one bay of 4 ft (1219.2 mm) in the shorter direction. The height of the model was 18 ft (6 x 3 ft = 5486.4 mm). The fundamental period of the model in fixed base condition, determined experimentally, was 2.34 Hz. The weight distribution, was 7.65 Kips (34.03 kN) at the 6^{th} floor, 7.84 Kips (34.9 kN) at the 5^{th} to 1^{st} floors and 4.56 Kips

(20.3 kN) at the base. A complete description of the dynamic properties of the model are reported by Mokha et al. (1990b). The Friction Pendulum isolation system, consisted of four sliding bearings. The sliding bearings comprised of an articulated slider - faced with a bearing material - sliding on a smooth spherical concave chrome surface. When set in motion the bearing develops a lateral force equal to the combination of the mobilized frictional force and the restoring force which develops as a result of the induced rising of the structure along the spherical surface.

The period of vibration in the sliding mode which is independent of the mass of the structure and related only to the radius of curvature of the spherical surface is:

$$T_b = 2\pi\left(\frac{R}{g}\right)^{1/2} \tag{7.1}$$

in which, g is the acceleration due to gravity. T_b is - of course - the natural period of a pendulum of length R. The radius of curvature of the bearing was 9.75 inch (247.65 mm) resulting in a period of 1 sec (2 sec in prototype scale). The 'stiffness' K_b of each bearing due to the pendulum action is:

$$K_b = \frac{W}{R} \tag{7.2}$$

in which W is the normal force or weight on the bearing.

The bearing material of the slider was Techmet-B with parameters in Eq. 5.6, f_{max} = 0.095, Δf = 0.045 and a =0.9 sec/in (35.4

sec/meter). El Centro S00E component (scaled peak shake table acceleration of 0.78 g and time scaled by a factor of two to satisfy similitude requirements) applied in the longer direction of the steel frame is considered for comparison.

The dynamic properties used for 3D-BASIS analysis are based on the properties reported by Mokha et al. (1990b). The model for sliding bearings accounts for the nonlinear forces in the sliding bearings and the restoring forces due to the pendulum action are modeled by linear elastic spring elements. The shear displacement of Techmet-B before sliding or the yield displacement Y = 0.005 inch (0.127 mm) is considered (Mokha et al. 1990b). Fig. 7.1 shows the base (bearing) displacement time history and base shear-displacement loop, recorded in the experiment and computed using 3D-BASIS. The loop is for the entire system of bearings. The comparison shows not only good agreement but almost every detail of the observed response is reproduced in the 3D-BASIS analysis.

7.2 Comparison with Rigorous Mathematical Solution Using Predictor-Corrector Method

Comparison with solution using Gear's predictor-corrector method is considered. The equations of motion and the differential equations governing the behavior of sliding isolation element are reduced to a system of first order differential equations and numerically integrated using an adaptive integration technique with

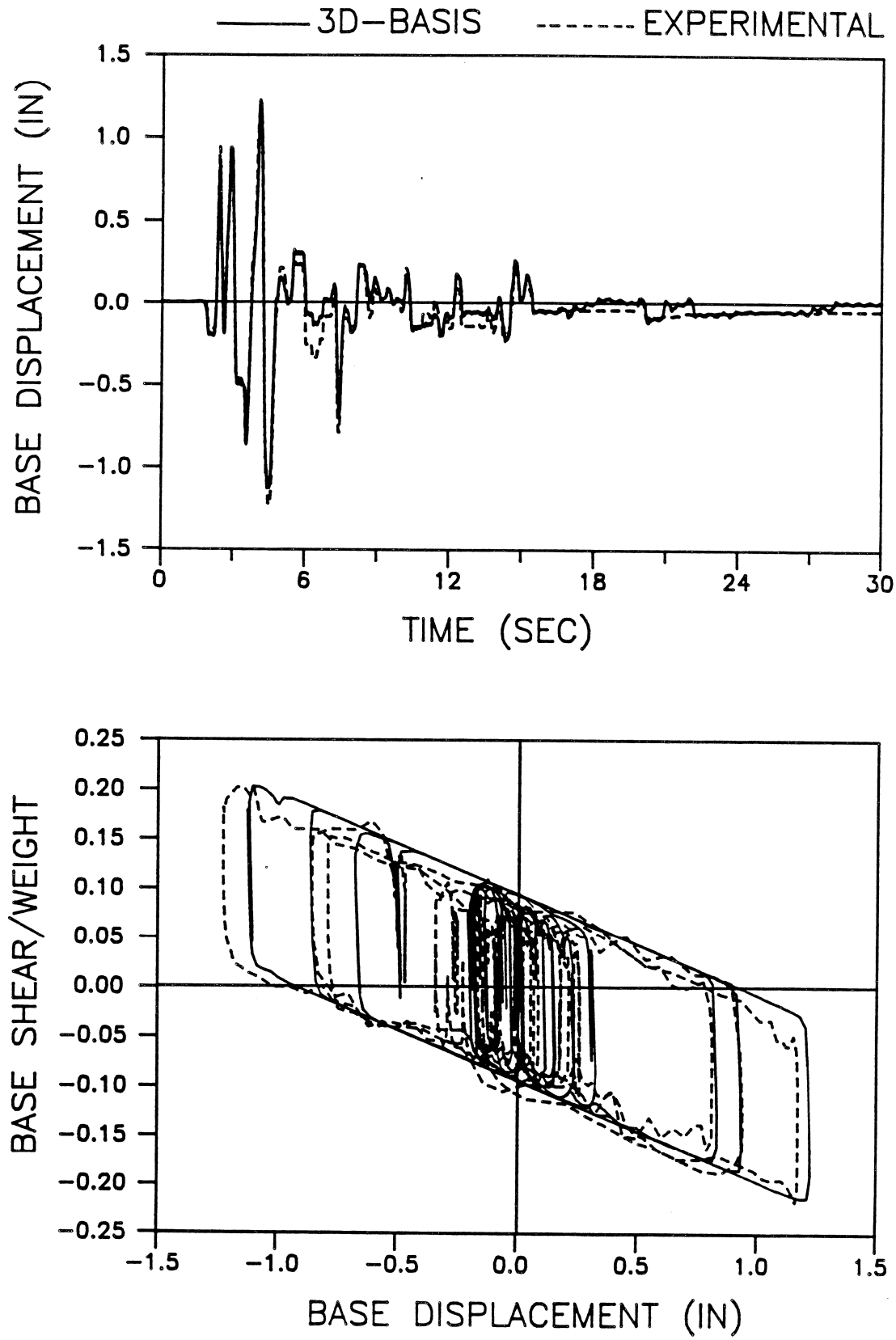

FIG. 7.1. Comparison of Experimental and Computed Response of the Six Story Scaled Model on Friction Pendulum Isolation System Subjected to 1940 El Centro Earthquake with Scaled Peak Shake Table Acceleration of 0.78 g (1 in = 25.4 mm)

truncation error control which is appropriate for stiff differential equations (Gear 1971). The same procedure has been used to compute the response of sliding base isolated structure by Constantinou et al. (1990a). The model sliding base isolated structure described in section 7.1 and the corresponding parameters are used in this comparison also. El Centro S00E component (scaled peak acceleration of the shake table = 0.34 g) applied in the longer direction is considered for comparison. Fig. 7.2 shows the base displacement and normalized base shear computed using Gear's method. Fig. 7.2 also shows the response computed using 3D-BASIS for the same set of parameters and excitation. The comparison shows the accuracy of the solution procedure. The time step of computation was constant time step of 0.005 sec in 3D-BASIS as against 0.005 sec and lower for predictor-corrector method. Fig. 7.3 shows the comparison of response computed using 3D-BASIS and experimental results for the same set of parameters and excitation.

7.3 Comparison with Analysis using General Purpose Finite Element Program ANSR

The structural system considered is a single storey structure. The structure has equal base dimensions L=480 inch (12192 mm) and is supported on four corner columns, has a height of 180 inch (4572 mm) and a total weight of 480 Kips (2135 kN). Equal floor and base weight is considered. The center of mass of both the floor and the

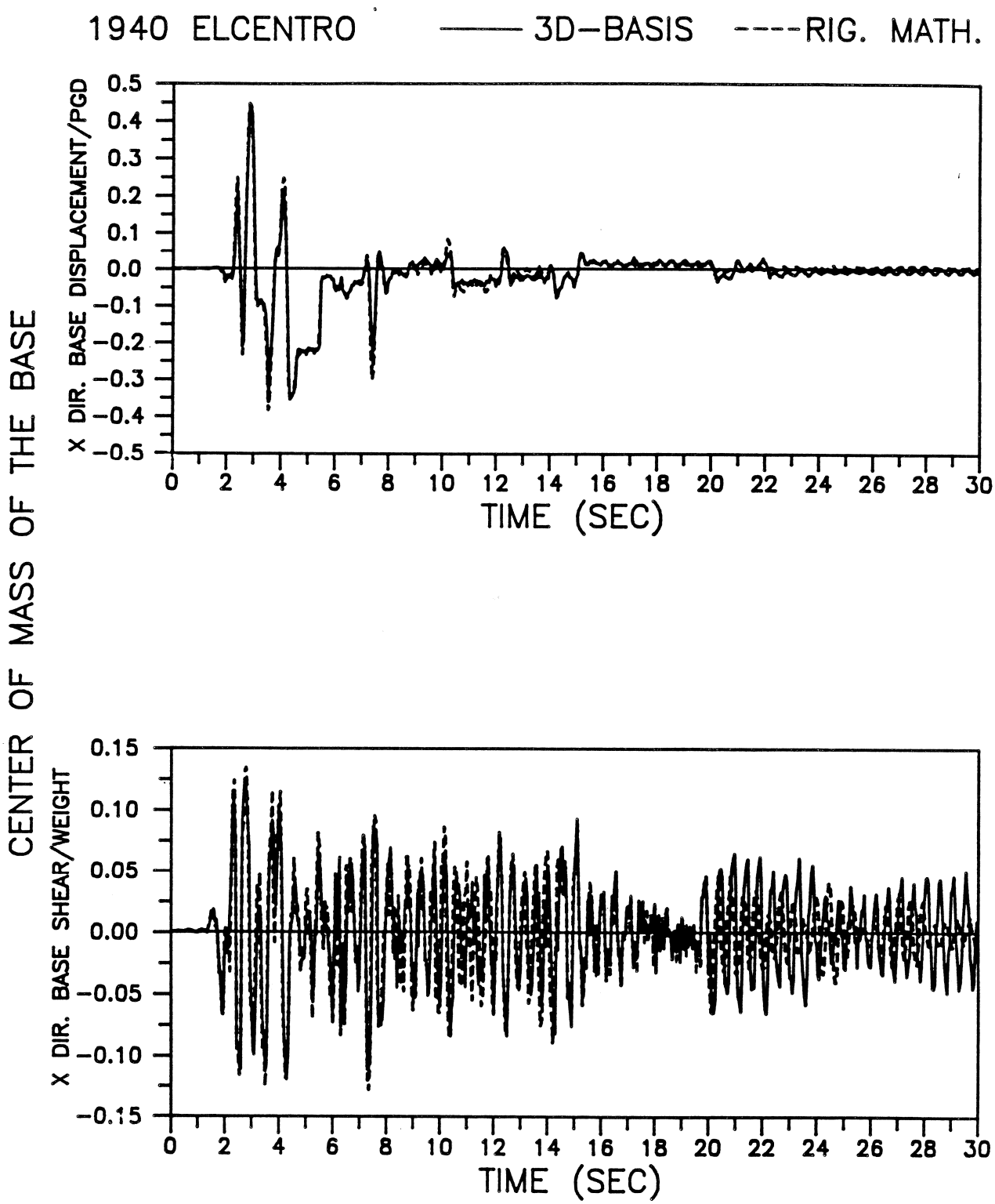

FIG. 7.2. Comparison of Computed Response of the Six Story Scaled Model on Friction Pendulum Isolation System Subjected to 1940 El Centro Earthquake with Scaled Peak Shake Table Acceleration of 0.34 g

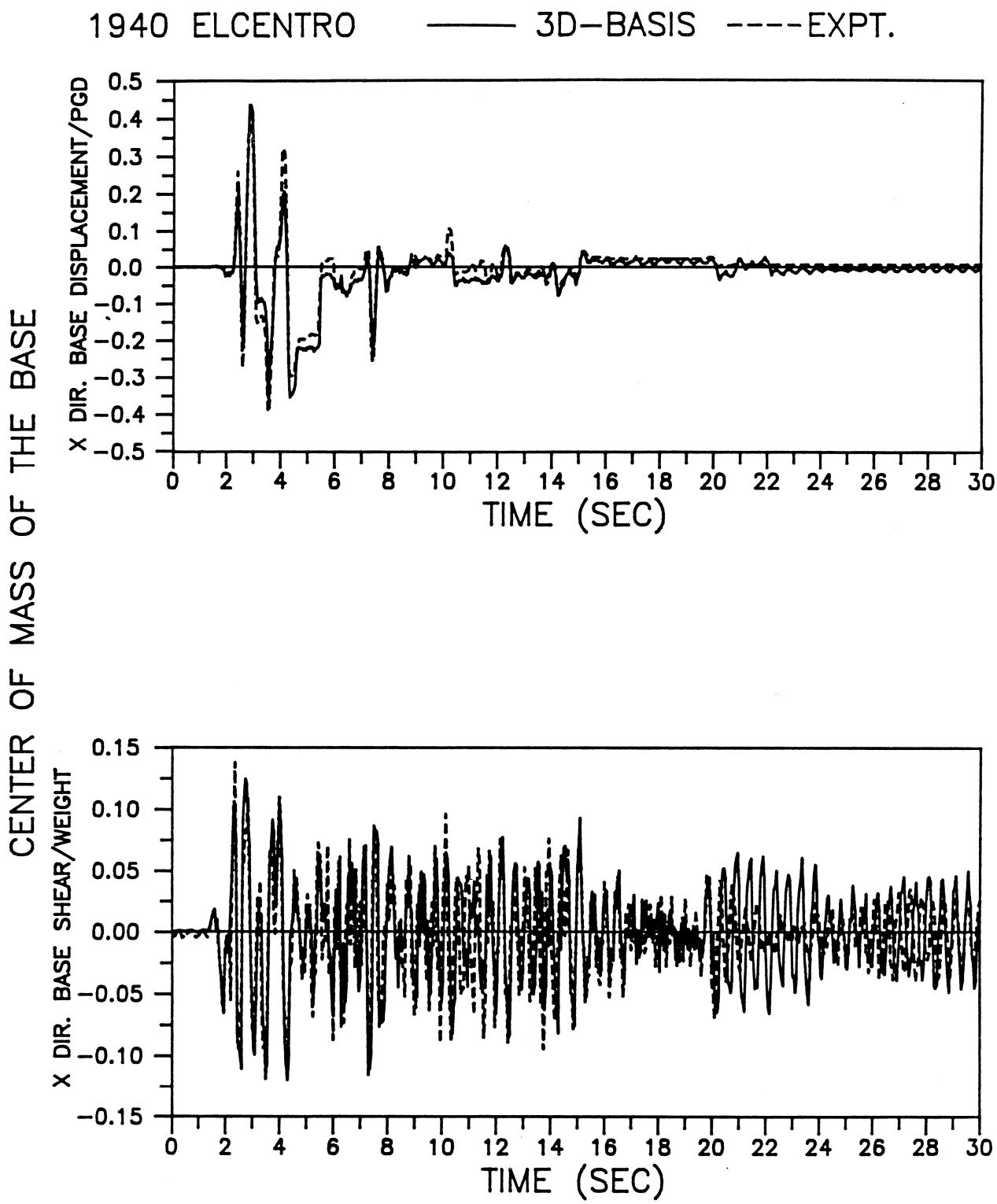

FIG. 7.3. Comparison of Experimental and Computed Response of the Six Story Scaled Model on Friction Pendulum Isolation System Subjected to 1940 El Centro Earthquake with Scaled Peak Shake Table Acceleration of 0.34 g

base are assumed to be on the same vertical axis. The vertical axis of centers of mass is offset from the geometric center of the building for inducing a mass eccentricity of 0.083L in the Y direction. Eccentricities $e_x = e_y = 0.1L$ of the center of resistance of the superstructure from the center of mass are considered. The uncoupled translational period of the superstructure T_s is 0.3 sec in both X and Y directions. The uncoupled torsional period of the superstructure T_θ is equal to T_s. Viscous damping of 2 percent of critical is used for the superstructure in all the three modes.

An isolation system consisting of four lead-rubber bearings placed below the columns is considered. The design of the isolation system was based on a ground motion with the characteristics of the ATC 0.4g S2 spectrum and on the procedure developed by Dynamic Isolation Systems (1983). The torsional response was not accounted for in the design. A design live load of 200 Kips (889.6 kN) was considered in addition to the total dead load of 480 Kips (2135 kN). The bearings chosen were of 13 inch (330.2 mm) diameter and comprised of 18 layers of natural rubber (hardness 50) of 0.375 inch (9.53 mm) thickness. Lead plugs of 2.5 inch (63.5 mm) diameter were placed in all four bearings. The properties of bearings determined were the initial elastic stiffness of 17.8 K/in (3.12 kN/mm), the postyielding stiffness of 2.74 K/in (0.48 kN/mm) and the yield strength F^Y of 6.6 Kip (29.36 kN). The total yield strength of the isolation system is 5.5% the structural weight. The stiffness

and yield strength of each bearing was adjusted based on experimental results of Built (1982) to account for the effect of changes in axial load. The rigid body mode period is:

$$T_b = 2\pi\left(\frac{W}{K_b g}\right)^{1/2} \tag{7.3}$$

in which, W is the total weight and K_b is the total post yielding stiffness of four Lead-rubber bearings. T_b in the present case is 2.12 sec. The biaxial model for elastomeric bearings is used to model the lead-rubber bearings.

The ground motion considered is 1940 El Centro. The S00E component is input in the X direction and S90W is input in the Y direction. Fig. 7.4 shows the base displacement response at a corner bearing where maximum response occurred. The peak ground displacement (PGD) of 4.29 inch (108.96 mm) is used for normalizing the displacement response. The comparison shows good agreement between response computed using 3D-BASIS and ANSR, with completely different modeling and solution procedures. The time step of computation was kept constant at 0.01 sec in both analyses (3D-BASIS and ANSR). The CPU time on a VAX 8700 was 16 sec for 3D-BASIS analysis and 14 sec for ANSR analysis.

7.4 Conclusion

Several comparisons presented with both experimental and analytical results reveal the accuracy and efficiency of the

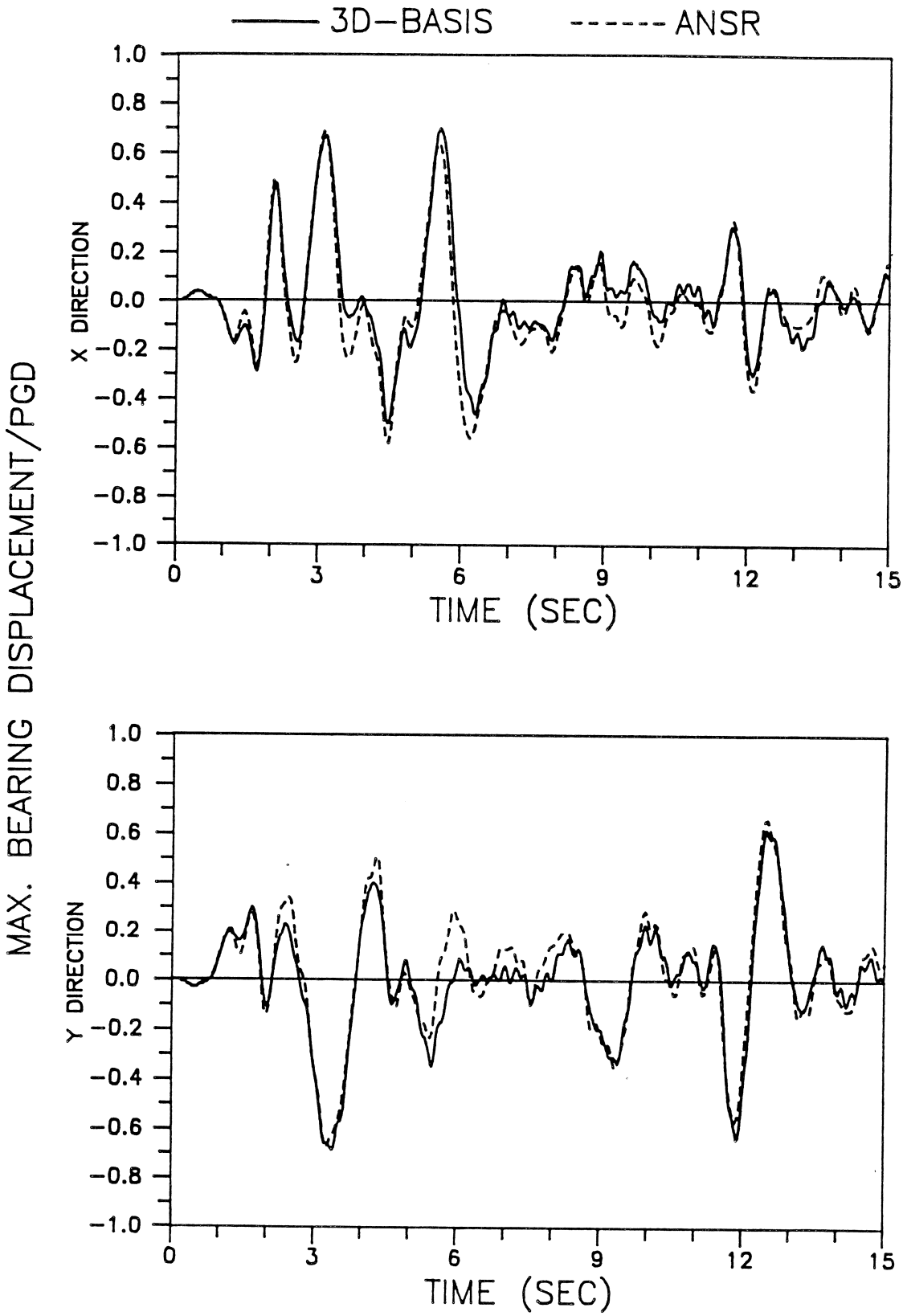

FIG. 7.4. Comparison of Response Computed using 3D-BASIS and ANSR of a Single Story Structure on Lead-rubber Isolation System Subjected to El Centro Earthquake with Component S00E in X Direction and Component S90W in Y Direction (PGD = 108.9 mm)

algorithm. The solution algorithm is very stable and works with comparable accuracy of a predictor-corrector method (wherein the time step may reduce to a millionth of a second during the adaptive integration), but with a much larger time step. This is the attractive feature of the algorithm and leads to considerable computational saving when a large number of bearings are present.

SECTION 8

ANALYSIS OF SIX STORY REINFORCED CONCRETE BASE ISOLATED STRUCTURE

8.1 General Description

The analysis of a six story reinforced concrete base isolated structure to be constructed in Greece is considered. Two types of isolation systems that are considered are the lead-rubber bearing isolation system and the Friction Pendulum System. The plan and section of the building are shown in Fig. 8.1. The reinforced concrete superstructure has been designed to resist lateral loads equivalent to a seismic base shear coefficient of 0.15 g (at working stress level) using shear walls.

The lead-rubber bearing isolation system designed based on the procedure developed by Dynamic Isolation Systems (1983) consists of 22 lead-rubber bearings (see Fig. 8.1(b) and Table 8.1 for details). A site specific response spectrum shown in Fig. 8.2 was used in the design of the structure/isolation system. The average isolation yield level Q_d was set to 0.045W, where W is the total weight of the structure = 25143 kN. The rigid body isolation period T_b (see Eq. 7.3) is 1.65 sec.

The Friction Pendulum System consists of 22 articulated sliders. The design of the sliding isolation system was based completely on experimental results of Mokha et al. (1990b). The bearing material of the slider was Techmet-B with parameters in Eq. 5.6 from Mokha et al. (1990b) being f_{max} = 0.095, Δf = 0.045 and a =0.9 sec/in (35.4 sec/meter). The radius of curvature of the

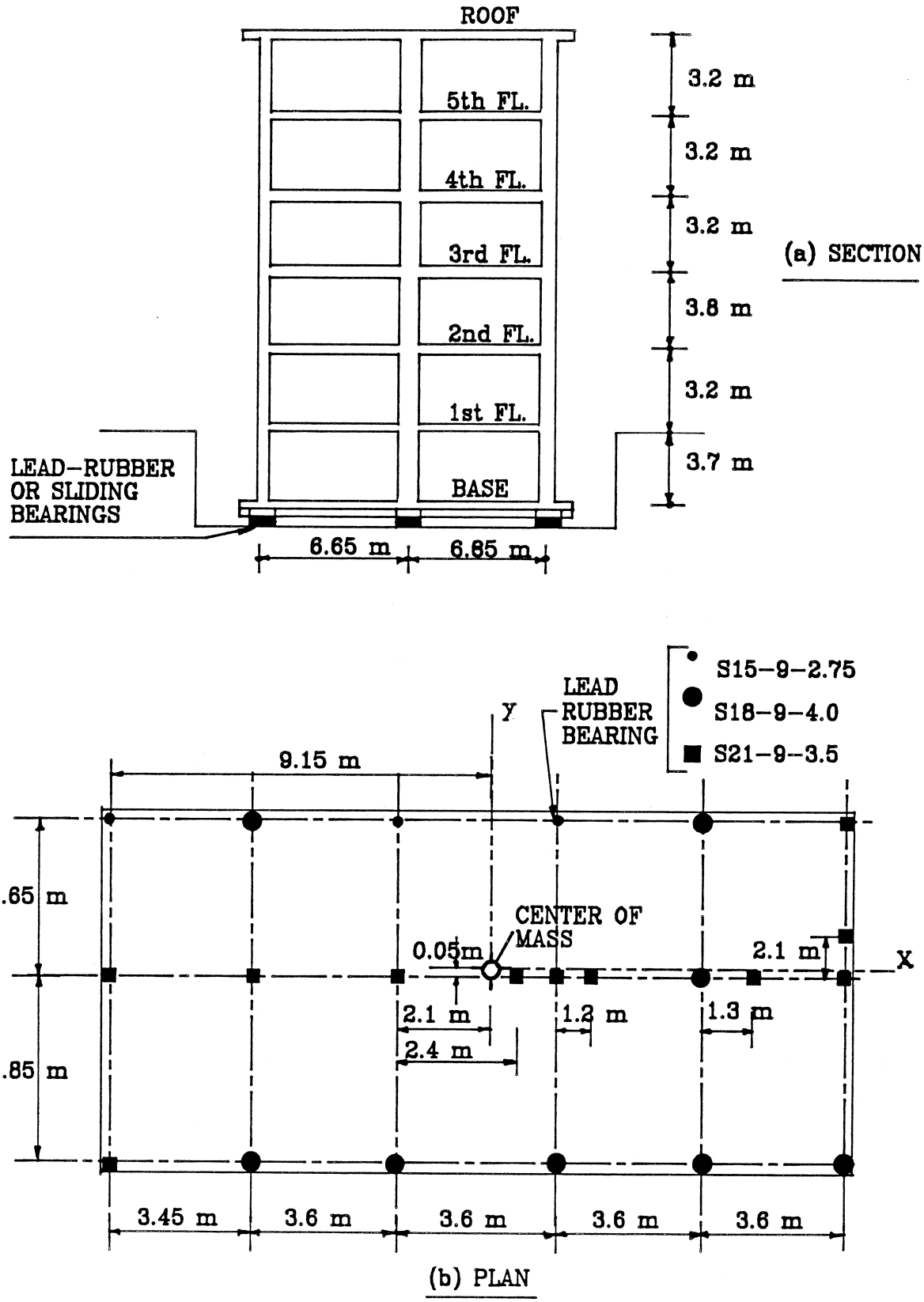

FIG. 8.1. Six Story Reinforced Concrete Base Isolated Structure: (a) Section; (b) Plan

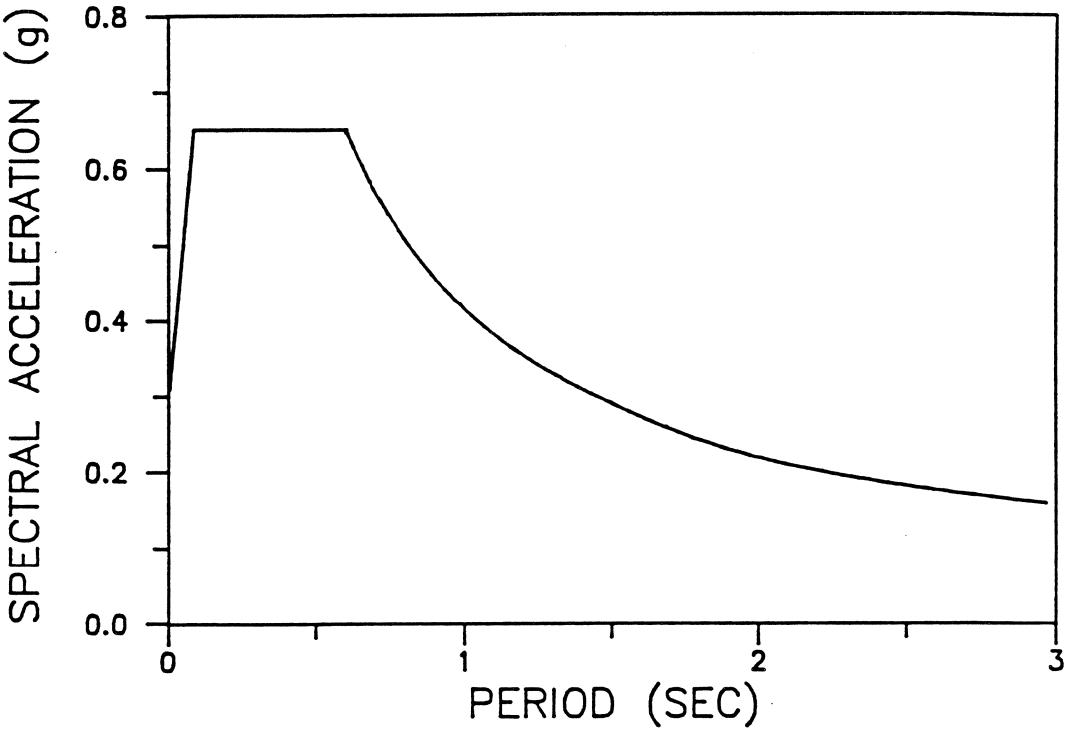

FIG. 8.2. Site Specific Response Spectrum used for the Analysis and Design of Six Story Reinforced Concrete Structure on Different Isolation Systems

TABLE 8.1 LEAD-RUBBER BEARING ISOLATION SYSTEM

LEAD-RUBBER BEARING PROPERTIES			
Bearing	S15-9-2.75	S18-9-4	S21-9-3.5
Number of Bearings	3	8	11
Plan Size (mm x mm)	380 x 380	460 x 460	530 x 530
Bearing Height (mm x mm)	220	220	220
Number of Rubber Layers	13	13	13
Rubber Layer Thickness (mm)	9.525	9.525	9.525
Lead Core Diameter (mm)	70	100	90
K_u - Preyielding stiffness (kN/m)	6828	10744	13308
K_d - Postyielding stiffness (kN/m)	999	1665	1917
Q_d Yield Level (kN)	30.2	64.0	49.0
PARAMETERS USED FOR MODELING LEAD-RUBBER BEARINGS			
Postyielding to Preyielding stiffness ratio α	0.147	0.154	0.144
Yield Force (kN)	35.7	75.8	58
Yield Displacement (mm)	5.2	7.0	4.3

spherical concave surface was chosen to be 1 meter so that the period of vibration in the sliding mode (see Eq. 7.1) is 2 sec. The equivalent 'stiffness' K_b (see Eq. 7.2) of the articulated slider was calculated based on the normal force at each bearing.

8.2 Response of Structure with Lead-rubber Bearing Isolation System

The superstructure is modeled as a three dimensional building using ETABS (Wilson et al. 1975). The frequencies and mode shapes of the first six modes (shown in Table 8.2) are used to model the superstructure is 3D-BASIS. Damping of 5% of critical is used for the superstructure in all the modes. The lead-rubber bearings are modeled using the biaxial model for elastomeric bearings (see Table 8.1 for details of the parameters). The dynamic response is computed for three artificial accelerograms, of 20 sec duration. These artificial accelerograms are realized from the site specific response spectrum.

The peak response values due to one of the three earthquakes (shown in Fig. 8.3) which gave the maximum response, are shown in Table 8.3. The same earthquake gave maximum response in the X and Y directions. In Table 8.3 the response in the X direction is shown when the ground motion is applied in the X direction (case X) and the response in the Y direction is shown when the ground motion is applied in the Y direction (case Y). The Y direction base displacement and rotational response at the center of mass of the base for case

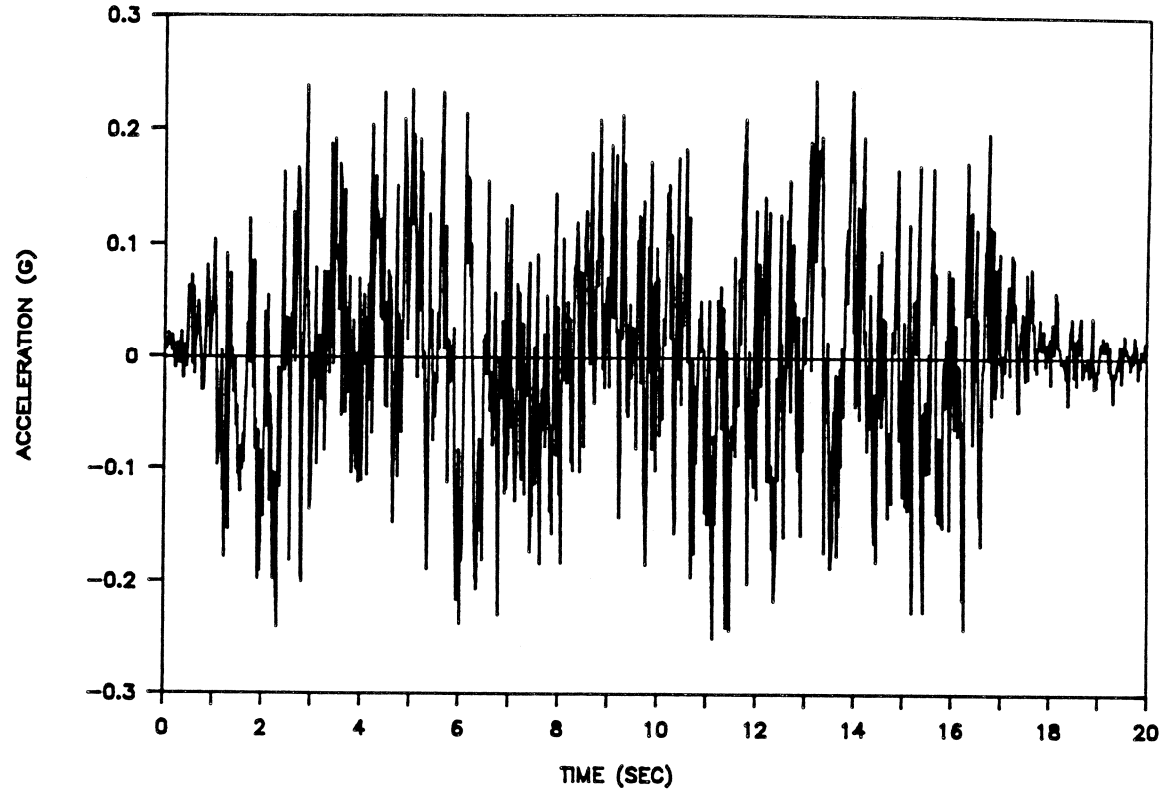

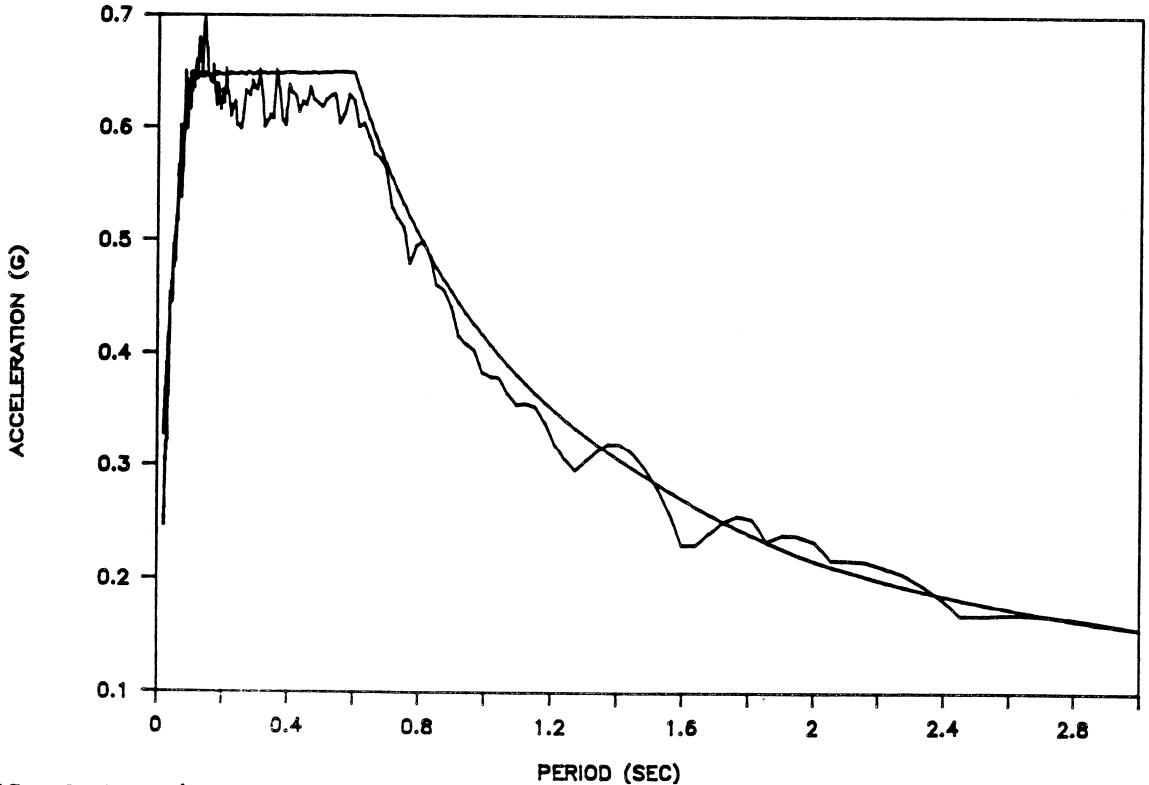

FIG. 8.3. Simulated Ground Motion used for the Analysis: (a) Artificial Accelerogram; (b) Corresponding Response Spectrum in Comparison with the Site Specific Response Spectrum

TABLE 8.2 DYNAMIC CHARACTERISTICS OF SIX STORY REINFORCED CONCRETE BUILDING (FIXED BASE)

MODE			1	2	3	4	5	6
FREQUENCY (Hz)			1.147	1.202	2.503	3.833	4.268	7.446
Fl.	Mass *	Dir	MODE 1	MODE 2	MODE 3	MODE 4	MODE 5	MODE 6
6	350	X	-0.0095	0.1009	0.0043	0.0956	0.0071	-0.0066
	350	Y	0.1057	0.0133	-0.0427	0.0058	-0.0773	0.0014
	15311	ROT	0.0055	0.0007	0.0138	0.0001	-0.0068	-0.0006
5	350	X	-0.0098	0.0881	0.0014	0.0222	0.0042	0.0436
	350	Y	0.0851	0.0098	-0.0286	-0.0014	-0.0007	0.0023
	15311	ROT	0.0045	0.0004	0.0125	-0.0005	-0.0012	0.0001
4	350	X	-0.0094	0.0726	-0.0017	-0.0469	-0.0003	0.0849
	350	Y	0.0634	0.0065	-0.0162	-0.0057	0.0594	0.0000
	15311	ROT	0.0035	0.0002	0.0109	-0.0009	0.0027	0.0004
3	385	X	-0.0078	0.0543	-0.0032	-0.0855	-0.0056	0.0106
	385	Y	0.0403	0.0034	-0.0101	-0.0060	0.0859	-0.0034
	17466	ROT	0.0022	0.0001	0.0082	-0.0008	0.0046	0.0003
2	411	X	-0.0046	0.0298	-0.0027	-0.0745	-0.0068	-0.0871
	411	Y	0.0166	0.0009	-0.0078	-0.0030	0.0656	-0.0051
	17997	ROT	0.0007	-0.0001	0.0043	-0.0004	0.0034	0.0002
1	359	X	-0.0018	0.0118	-0.0011	-0.0373	-0.0035	-0.0722
	359	Y	0.0062	0.0003	-0.0036	-0.0015	0.0319	-0.0030
	15701	ROT	0.0002	0.0000	-0.0018	-0.0002	0.0015	0.0001

* Translational mass in kN-sec^2/meter
Mass moment of inertia in kN-meter-sec^2

TABLE 8.3 RESPONSE OF SIX STORY REINFORCED CONCRETE BASE ISOLATED STRUCTURE

	Fl.	Lead-Rubber Isolation System		Friction Pendulum Isolation System	
		Case X	Case Y	Case X	Case Y
		Ground Motion and Response in X dir	Ground Motion and Response in Y dir	Ground Motion and Response in X dir	Ground Motion and Response in Y dir
Ratio of Peak Corner Interstory Drift to Height of the story	6	0.0015	0.0035	0.0025	0.0050
	5	0.0018	0.0037	0.0028	0.0051
	4	0.0022	0.0043	0.0029	0.0052
	3	0.0026	0.0039	0.0031	0.0050
	2	0.0023	0.0019	0.0027	0.0023
	1	0.0014	0.0010	0.0015	0.0012
Peak Corner Base Disp. (mm) (Translation ± Rotational disp.)		77 ± 8	83 ± 9	44 ± 5	33 ± 8
Peak Floor acceleration (g)	6	0.256	0.255	0.415	0.312
	5	0.205	0.202	0.289	0.244
	4	0.193	0.194	0.276	0.188
	3	0.185	0.169	0.236	0.205
	2	0.183	0.161	0.245	0.187
	1	0.207	0.166	0.245	0.216
	Base	0.218	0.194	0.329	0.299
Ratio of Structure Shear to Total Weight	Top of Base	0.136	0.146	0.139	0.116

Y, are shown in Fig. 8.4(a).

To verify the response in case Y, the structural stiffness properties are condensed to six degrees of freedom (one per floor in the Y direction) and used for a two dimensional analysis using DRAIN-2D (Kannan and Powell 1975). The properties of the isolation system are lumped with F^y= 1328 kN, Y= 0.00525 meters, α = 0.148, and Q_d = 0.045W in a single isolation element, resulting in T_b=1.6 sec. The artificial accelerogram (shown in Fig. 8.3) that gave the maximum response in case Y - 3D-BASIS - analysis is used as the excitation. The base displacement response (Y direction) is shown in Fig. 8.5(a). The time step of computation was kept constant at 0.01 sec in both analyses (3D-BASIS and DRAIN-2D). The CPU time on VAX 8700 was 74 sec for the three dimensional 3D-BASIS analysis -with 22 lead-rubber bearings- capturing the lateral-torsional response and was 32 sec for the two dimensional DRAIN-2D analysis -with all the nonlinear isolation properties lumped in a single element- capturing only the translational response in the Y direction.

8.3 Response of Structure with Friction Pendulum Isolation System

The superstructure is modeled in the same way as described for the case with lead-rubber bearing isolation system. The biaxial model for sliding bearings, along with a linear spring is used to model the articulated sliders. The shear displacement of Techmet-B

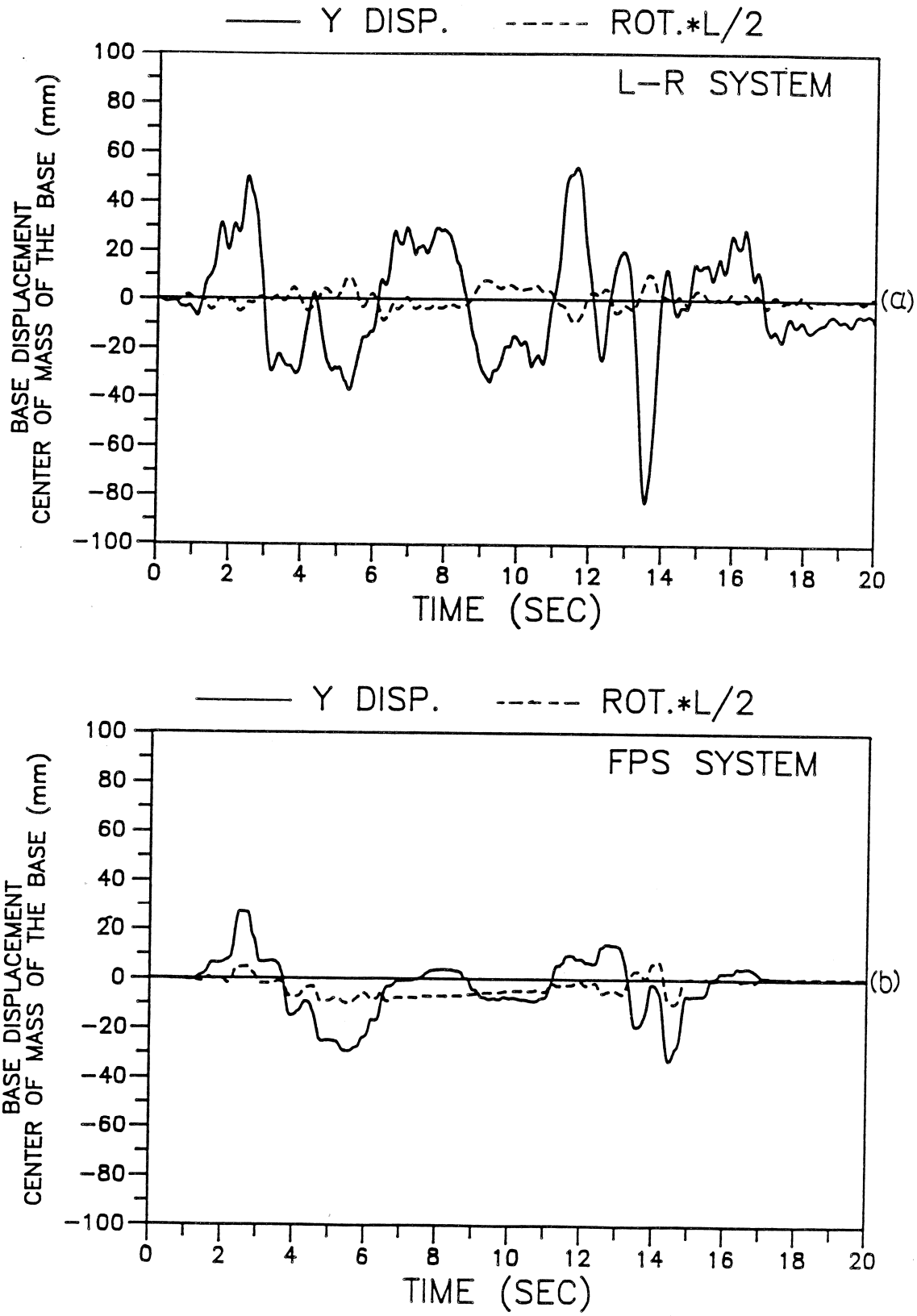

FIG. 8.4. Response of Six Story Reinforced Concrete Structure to Simulated Earthquake: (a) Lead-rubber Isolation System; (b) Friction Pendulum Isolation System

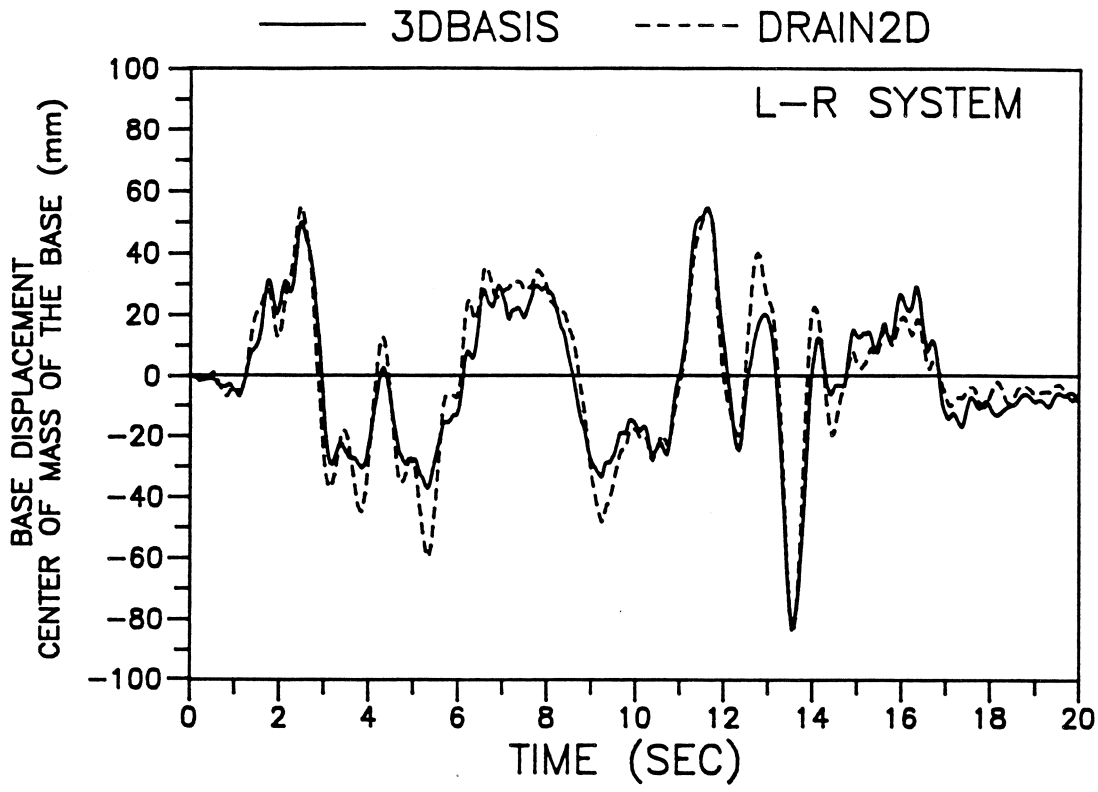

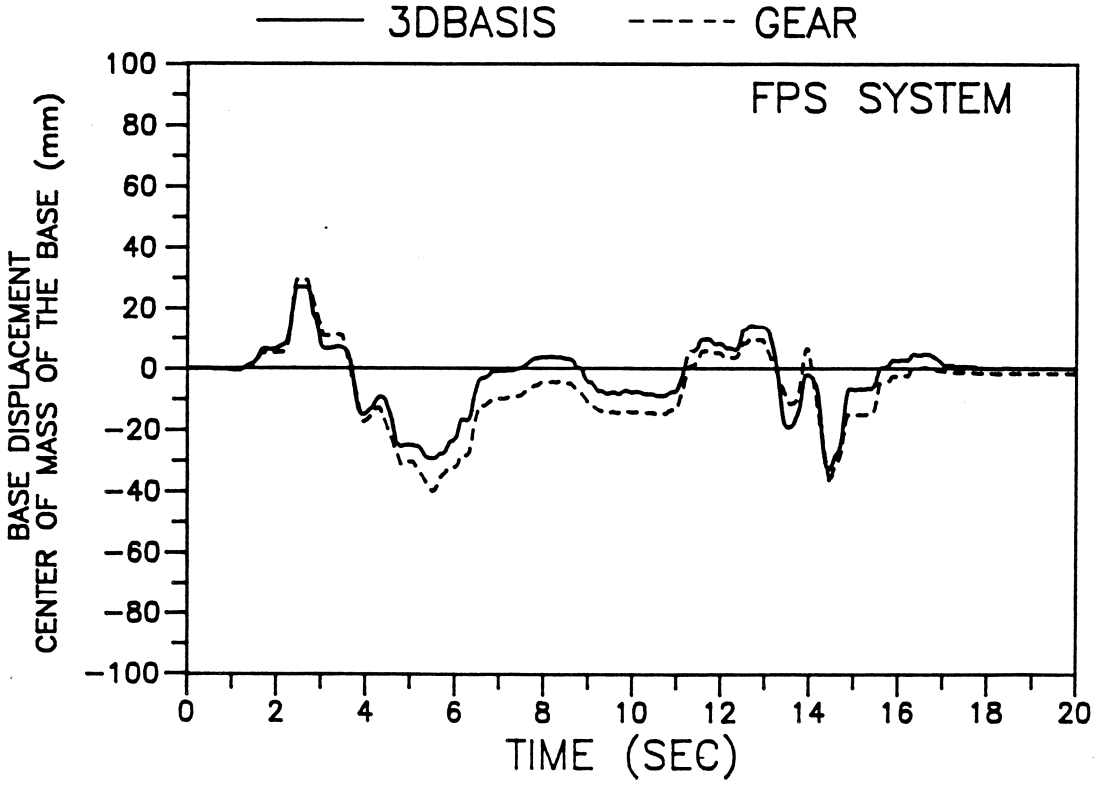

FIG. 8.5. Response of Six Story Reinforced Concrete Structure to Simulated Earthquake: (a) Lead-rubber Isolation System; (b) Friction Pendulum Isolation System

before sliding commences or the yield displacement Y = 0.005 inch (0.127 mm) is considered based on Mokha et al. (1990b). The artificial accelerogram (shown in Fig. 8.3) which gave the maximum response in the lead-rubber bearing isolation system is considered in the analysis. The peak response values are shown in Table 8.3. The Y direction base displacement and rotational response at the center of mass of the base for case Y, is shown in Fig. 8.4(b).

To verify the response in case Y, the structural stiffness properties are condensed to six degrees of freedom (one per floor in the Y direction) and used for a two dimensional analysis. The properties of the isolation system are lumped in a single isolation element. The equivalent 'stiffness' K_b (see Eq. 7.2) is based on the total normal force on all bearings. However the parameters in Eq. 5.6 specified before continue to be the same. The equations of motion and the differential equation governing the behavior of sliding isolation element are reduced to a system of first order differential equations and numerically integrated using Gear's (1971) predictor-corrector method appropriate for stiff differential equations. The base displacement response (Y direction) is shown in Fig. 8.5(b). The time step of computation was kept constant at 0.01 sec in 3D-BASIS analysis and was 0.01 sec and lower (since the time step is adjusted automatically) in Gear's method of analysis. The CPU time on DEC VAX 8700 was 258 sec for three dimensional

3D-BASIS analysis -with 22 sliding bearings- capturing the lateral-torsional response and was 93 sec for the two dimensional GEAR analysis -with all the nonlinear isolation properties lumped in a single element- capturing only the translational response in the Y direction.

Comparison of the response of the structure with Lead-rubber bearing system (LR) and Friction Pendulum System (FPS) is considered. The peak acceleration in case X, for FPS system is 0.415g (see Table 8.3) as against 0.256g (see Table 8.3) for LR system. But the resulting structure shear in FPS system is nearly the same as in the LR system, indicating higher mode response. This is evident in Fig. 8.6 which shows the displacement and acceleration profiles, at selected times, for case X. The times at which the profiles are plotted correspond to the instances at which the peak acceleration, peak base shear, peak base displacement and peak interstory drift occur. These profiles clearly demonstrate that when the peak acceleration in the structure with FPS isolation system occurs, the response is dominated by higher mode response. The peak corner base displacement is much smaller (nearly half) in the FPS system, compared to the LR system, for nearly the same or lesser structure shear at the top of base. The peak interstory drift in the LR system is smaller than the peak interstory drift in the FPS system.

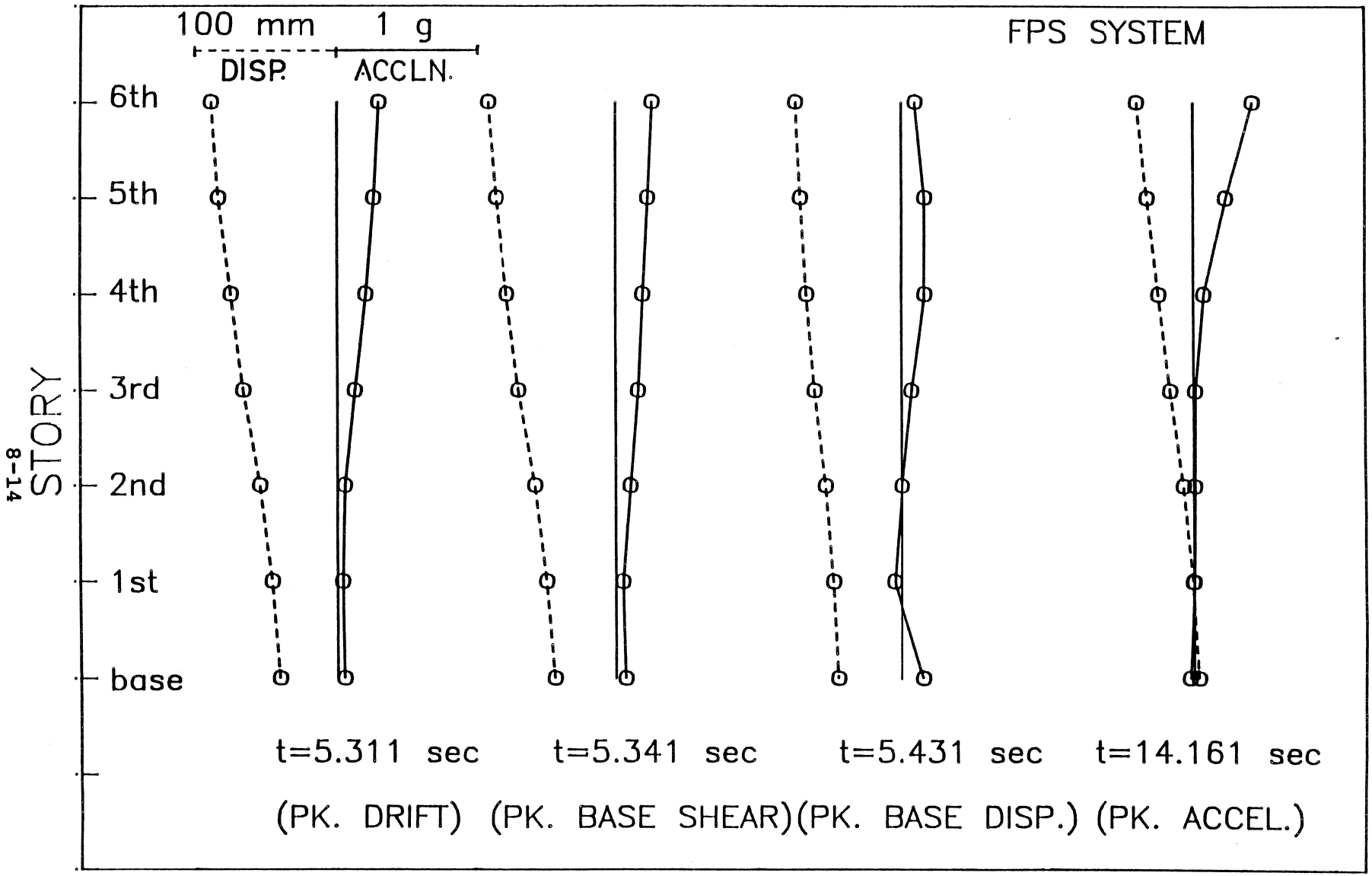

FIG. 8.6. Peak Drift, Base Shear, Base Displacement, and Peak Acceleration Profiles of the Six Story Reinforced Concrete Structure on Friction Pendulum Isolation System

8.4 Conclusion

The analysis of the six story structure presented reveals the capability of the algorithm to solve base isolated structures with large number of isolators accurately. It also reveals the efficiency of the solution algorithm.

CHAPTER 9

DISCUSSION AND CONCLUSIONS

The behavior of isolation components in base isolated structures is nonlinear. Lead-rubber bearings exhibit bilinear hysteretic behavior. Sliding bearings exhibit hysteretic behavior which is similar to rigid-plastic behavior. Coefficient of sliding friction in Teflon sliding bearings is velocity dependent. In addition the hysteretic behavior of the isolation bearings is highly nonlinear when biaxial interaction between lateral forces is present.

In this report a unified analytical model for isolation components, a generalized analytical model to address highly nonlinear isolation systems and a suitable solution algorithm have been presented. The generalized analytical model considers the superstructure to be elastic (which is a valid assumption in the case of base isolated structures) and the isolation system to be nonlinear. The three dimensional superstructure and isolation system is integrated in the analytical model.

The analytical model and the solution algorithm presented are suitable for high rigidities and sharp softening exhibited by sliding bearings. The solution algorithm involving conventional modified Newton-Raphson method is not suitable when sliding systems are considered. The solution algorithm involving predictor-corrector method is inefficient in computing the response of large base isolated structural systems. The new solution algorithm involving

pseudo-force method along with the time marching procedure, presented in this report, has proven to be both adequate and efficient for large base isolated structures.

The following conclusions are derived from the development of the generalized analytical model and the solution algorithm:

a. The biaxial and uniaxial models of isolation elements presented can model the force-displacement characteristics needed adequately.

b. The generalized analytical model and the solution algorithm developed involving the pseudo-force method is accurate and efficient.

c. Pseudo-force method converges to the correct solution even when severe nonlinearities such as planar sliding behavior along with biaxial effects are present.

d. Pseudo-force method yields results of comparable accuracy of highly accurate predictor-corretor method.

The comparisons with test results proves the accuracy of the analytical model and solution algorithm. The comparison with results obtained using Gear's method, ANSR and DRAIN2D demonstrates the accuracy and efficiency of the algorithm. The analysis of six story reinforced concrete structure on Friction Pendulum System further demonstrates the efficiency. The analytical model and solution algorithm developed offers a significant analysis capability.

SECTION 10
REFERENCES

Arya, A. S. (1984). "Sliding concept for mitigation of earthquake disaster of masonry buildings." 8th World Conf. on Earthquake Engrg., San Francisco, 5, 951-958.

Asher, J. W. et al. (1990). "Seismic isolation design of the USC university hospital." Proc. of Fourth U.S. National Conf. on Earthquake Engrg., California, Vol. 3, 529-538.

Beucke, K. E. and Kelly, J. M. (1985). "Equivalent linearizations for practical hysteretic systems." Int. J. Non-Linear Mech., 23(4), 211-238.

Bhatti, M. A. and Pister, K. S. (1981). "Transient response analysis of structural systems with nonlinear behavior." Computers and Structures, 13, 181-188.

Boardman, P. R., Wood, B. J. and Carr, A. J. (1983). "Union House - A cross braced structure with energy dissipators." Bull. of the New Zealand National Society for Earthquake Engrg., 16(2), 83-97.

Buckle, I. G., Kelly, T. E. and Jones, L. R. (1987). "Basic concepts of seismic isolation and their application to nuclear structures." ASME Pressure Vessels and Piping Conference, PVP-vol. 127, 429-437.

Buckle, I. G. and Mayes, R. L. (1990). "Seismic isolation: history, application, and performance - A world overview." Earthquake Spectra, 6(2), 161-202.

Built, S. M. (1982). "Lead-rubber dissipators for the base isolation of bridge structures." Report No. 289, Dept. of Civil Engineering, University of Auckland, New Zealand.

Caspe, M. S. and Reinhorn, A. M. (1986). "The earthquake barrier. A solution for adding ductility to otherwise brittle buildings." Proc. of ATC-17 Seminar on Base Isolation and Passive Energy Dissipation, Applied Technology Council, Palo Alto, Calif., 331-342.

Chalhoub, M. S. and Kelly, J. M. (1990). "Sliders and tension controlled reinforced elastomeric bearings combined for earthquake isolation." Earthquake Engrg. and Struct. Dyn., 19(3), 333-344.

Charleson, A. W., Wright, P. D. and Skinner, R. I. (1987). "Wellington Central Police Station base isolation of an essential facility." Pacific Conf. on Earthquake Engrg., New Zeland, 377-388.

Cheng, M. (1988). "Convergence and stability of step by step integration for model with negative stiffness." Earthquake Engrg. Struct. Dyn., 16(1), 227-244.

Chopra, A. K., Clough, D. P. and Clough, R. W. (1973). "Earthquake resistance of buildings with a soft first story." Earthquake Engrg. and Struct. Dyn., 1(4), 347-355.

Constantinou, M. C. (1984). "Random vibration and optimization of design of aseismic base isolation systems," thesis presented to the Rensselaer Polytechnic Institute, New York, in partial fulfillment of the degree of the Doctor of Philosophy.

Constantinou, M. C. (1987). "A simplified analysis procedure for base-isolated structures on flexible foundation." Earthaquake Engrg. and Struct. Dyn., 15(8), 963-983.

Constantinou, M. C. and Kneifati, M. C. (1988). "Dynamics of soil-base-isolated-structure systems." J. Struct. Engrg., 114(1), 211-221.

Constantinou, M. C., Mokha, A. and Reinhorn, A. M. (1990a). "Experimental and analytical study of a combined sliding disc bearing and helical steel spring isolation system." Report No. NCEER-90-19, National Center for Earthquake Engineering, State Univ. of New York, Buffalo, New York, in print.

Constantinou, M. C., Mokha, A. and Reinhorn, A. M. (1990b). "Teflon bearings in base isolation II: Modeling." J. Struct. Engrg. ASCE, 116(2), 455-474.

Darbre, G. R. and Wolf, J. P. (1988). "Criterion of stability and implementation issues of hybrid frequency-time domain procedure for nonlinear dynamic analysis." Earthquake Engrg. and Struct. Dyn., 16(4), 569-582.

Delfosse, G. C. (1986). "Construction and testing of an experimental dwelling-house on rubber bearings." 2nd World Cong. on Joints and Bearings, ACI-SP-94, 1, 222-232.

Den Hartog, J. P. (1931). "Forced vibration with combined coulomb and viscous friction." Transactions of ASME, APM-53-9, 107-115.

Dynamic Isolation Systems, Inc. (1983). Seismic Base Isolation Using Lead-rubber Bearings, Berkeley, Calif.

Fujita, T., Suzuki, S. and Fujita, S. (1989). "Hysteretic restoring force characteristics of high damping rubber bearings for seismic isolation." ASME Pressure Vessels and Piping Conference, PVP-Vol. 181, Hawaii, 23-28.

Gear, C. W. (1971). "The automatic integration of ordinary differential equations." Numerical Mathematics, Communications of ACM, 14(3), 176-190.

Hisano, M. et al. (1988). "Study on a sliding-type base isolation system: Tri-axial shaking table test and its simulation." Proc. of Ninth World Conf. on Earthquake Eng., Japan, V, 741-746.

Huffmann, G. K. (1986). "Full base isolation for earthquake protection by helical springs and viscodampers." Nuclear Engrg. and Design, 84, 331-338.

Ikonomou, A. S. (1985). "Alexisismon Isolation Engineering for Nuclear Power Plants." Nuclear Eng. Design, 85, 201-216.

Jagdish, K. S., Raghuprasad, B. K. and Rao, P. V. (1979). "The inelastic vibration absorber subjected to earthquake ground motion." Earthquake Engrg. and Struct. Dyn., 7(4), 317-326.

Kan, C. L. and Chopra, A. K. (1977). "Elastic earthquake analysis of torsionally coupled multistory building." Earthquake Engrg. and Struct. Dyn., 5(4), 395-412.

Kannan, A. M. and Powell, G. H. (1975). "DRAIN-2D a general purpose computer program for dynamic analysis of inelastic plane structures with users guide." Report No. UCB/EERC -73/22, Earthquake Engineering Research Center, University of California, Berkeley, Calif.

Kawamata, S. (1988). "Accelerated liquid mass dampers as tools of structural vibration control." Proc. of Ninth World Conf. on Earthquake Engrg., Japan, VIII, 421-426.

Kelly, J. M. and Beucke, K. E. (1983). "A friction damped base isolation system with fail safe characteristics." Earthquake Engrg. and Struct. Dyn., 11(1), 33-56.

Kelly, J. M., Buckle, I. G. and Tsai, H. C. (1986a) "Earthquake simulator testing of a base isolated bridge deck." Report no. UCB/EERC-85/09, Earthquake Engineering Research Center, University of California, Berkeley, Calif.

Kelly, J. M. (1986b). "Aseismic base isolation: review and bibliography." Soil Dyn. and Earthaquake Engrg., 5(4), 202-217.

Kelly, J. M. (1988). "Base Isolation in Japan, 1988." Report No. UCB.EERC-88/20, Earthquake Engineering Research Center, University of California, Berkeley, Calif.

Kelly, J. M. (1990). "Base isolation: Linear theory and design." Earthquake Spectra, 6(2), 244.

Koh, C. G. and Kelly, J. M. (1988). "A simple mechanical model for elastomeric bearings used in base isolation." Int. J. Mexh. Sci., 30(12), 933-943.

Koh, C. G. and Balendra, T. (1989). "Seismic response of base isolated buildings including $P-\Delta$ effects of isolation bearings." Earthquake Eng. Struct. Dyn., 18(4) , 461-473.

Lee, D. M. (1980). "Base isolation for torsion reduction in asymmetric structures under earthquake loading." Earthquake Engrg. Struct. Dyn., 8(3), 349-359.

Megget, L. M. (1978). "Analysis and design of a base isolated reinforced concrete frame building." Bull. of the New Zealand National Society for Earthquake Engineering, 11(4), 245-254.

Miyazaki, M. et al. (1988). "Design and its performance verification of a base isolated building using lead rubber bearings in Japan." Proc. of Ninth World Conf. on Earthquake Engrg., Japan, V, 717-722.

Mizukoshi, K. et al. (1989). "Torsional response behavior of base isolated FBR reactor building during earthquake excitation." ASME Pressure Vessels and Piping Conf., Hawaii, 121-127.

Mokha, A., Constantinou, M. C. and Reinhorn, A. M. (1990a). "Teflon bearings in base isolation I: Testing." J. struct. Engrg. ASCE, 116(2), 438-454.

Mokha, A., Constantinou, M. C. and Reinhorn, A. M. (1990b). "Experimental study and analytical prediction of earthquake response of the friction pendulum isolation system (FPS)." Report No. NCEER-90-20, National Center for Earthquake Engineering Research, State University of New York, Buffalo, New York (in print).

Mondkar, D. P. and Powell, G. H. (1975). "ANSR - General purpose program for analysis of nonlinear structural response." Report No. UCB/EERC-75/37, Earthquake Engineering Research Center, University of California, Berkeley, Calif.

Mostaghel, N. and Khodaverdian, M. (1987). "Dynamics of Resilient-Friction Base Isolator (R-FBI)." Earthquake Eng. Struct. Dyn., 15(3), 379-390.

Mostaghel, N. and Khodaverdian, M. (1988). "Seismic response of structures supported on R-FBI system." Earthquake Eng. Struct. Dyn. ,16(6), 839-854.

Mostaghel, N. and Mortazavi, A. R. (1989). "Code versus analysis design displacement of R-FBI system." ASME Pressure Vessels and Piping Conference, PVP-Vol. 181, Hawaii, 79-87.

Nagarajaiah, S., Reinhorn, A. M. and Constantinou, M. C. (1989). "Nonlinear dynamic analysis of three dimensional base isolated structures (3DBASIS)." Report No. NCEER-89-0019, National Center for Earthquake Engineering Research, State University of New York, Buffalo, New York.

Nagarajaiah, S., Reinhorn, A. M. and Constantinou, M. C. (1990a). "Analytical modeling of three dimensional behavior of base isolation devices." Proc. Fourth U. S. National Conf. on Earthquake Engrg., California, Vol. 3, 579-588.

Nagarajaiah, S. (1990b). "Nonlinear dynamic analysis of three dimensional base isolated structures" thesis presented to the state university of New York at Buffalo, New York, in partial fulfillment of the requirements of the degree of Doctor of Philosophy.

Nagarajaiah, S., Reinhorn, A. M. and Constantinou, M. C. (1990c). "Nonlinear dynamic analysis of three dimensional base isolated structures." J. Struct. Engrg., ASCE, to appear in July 91.

Nagarajaiah, S., Reinhorn, A. M. and Constantinou, M. C. (1990d). "Seismic response of asymmetric base isolated structures with biaxial interaction." J. Struct. Engrg., ASCE, to appear.

Nakamura, T. et al. (1988). "Study on base isolation for torsional response reduction in asymmetric structures under earthquake motion." Proc. of Ninth World Conf. on Earthquake Eng., Japan, V, 675-680.

Newmark, N. M. (1959). "A method of computation for structural dynamics." J. of Engrg. Mech. Div. ASCE, 85(EM3), 67-94.

Novak, M. and Henderson, P. (1989). "Base isolated buildings with soil-structure interaction." Earthquake Eng. Struct. Dyn. , 18(6), 751-765.

Ozdemir, H. (1976). "Nonlinear transient dynamic analysis of yielding structures," thesis presented to the University of California at Berkeley, California, in partial fulfillment of the degree of Doctor of Philosophy

Pan, T. C. and Kelly, J. M. (1983). "Seismic response of torsionally coupled base isolated structures." Earthquake Engrg. Struct. Dyn., 11(6), 749-770.

Pan, T. C. and Kelly, J. M. (1984). " Seismic response of base isolated structures with vertical-rocking coupling." Earthquake Engrg. and Struct. Dyn., 12(5), 681-702.

Park, Y. J.,Wen, Y. K. and Ang, A. H. S. (1986). "Random vibration of hysteretic systems under bidirectional ground motions." Earthquake Eng. Struct. Dyn., 14(4), 543-557.

Plichon, C. and Jolivet, F. (1978). "Aseismic foundation system of nuclear power plants." Proc. SMIRT Conf., Paper No. C190/78.

Plichon, C., Gueraud, R., Richli, W. H. and Casagrande, J. F. (1980). "Protection of nuclear power plants against seism." Nuclear Technology, 49, 295-306.

Ramberg, W. and Osgood, W. R. (1943). "Description of stress strain curve by three parameters." Technical note 902, National Advisory Committee on Aeronautics.

Reinhorn , A. M., Rutenberg, A. and Gluck, J. (1977). "Dynamic torsional coupling in asymmetric building structures." Building and Environment, 12, 251-261.

Rosenbrock, H. H. (1964). "Some general implicit processes for the numerical solution of differential equations." Computer J., 18, 50-64.

Schwahn, K. J.,Reinsch, K. H., and Weber, F. M. (1987). "Description of the features of viscous dampers on the basis of equivalent rheological models, presented for pipework dampers." ASME Pressure Vessels and Piping Conference, PVP-Vol. 127, Calif., 477-484.

Sharpe, R. D. and Carr, A. J. (1979). "Inelastic frame dynamic analysis." Computer programs library, Dept. of Civil Engrg., Unviersity of Canterbury, New Zealand.

Staudacher, K. (1985). "Protection for structures in extreme earthquakes: Full base isolation (3-d) by the Swiss seismafloat system." Nuclear Engrg. and Design, 84, 343-357.

Stricklin, J. A., Martinez, J. E., Tillerson, J. R., Hong, J. H. and Haisler, W. E. (1971). "Nonlinear dynamic analysis of shells of revolution by matrix displacement method." AIAA Journal, 9(4), 629-636.

Stricklin, J. A. and Haisler, W. E. (1977). "Formulations and solution procedures for nonlinear structural analysis." Computers and Structures, 7, 125-136.

Structural Engineering Association of California (1990). "Tentative general requirements for the design and construction of seismic isolated structures." Appendix IL of Recommended Lateral Force Requirements and Commentary (Blue Book), California.

Su, L., Ahmadi, G. and Tadjbakhsh, I. G. (1989). "A comparative study of performance of various base isolation systems, Part I: Shear beam structures." Earthquake Engrg. Struct. Dyn., 18(1), 11-32.

Sveinsson, B. I. et al. (1990). "Seismic isolation analysis of an existing eight story building." Proc. of Fourth U. S. National Conference on Earthquake Engrg., California, Vol. 3, 589-597.

Tarics, A. G., Way, D. and Kelly, J. M. (1984). "The implementation of base isolation for the foothill communities law and justice center." Report to the National Science Foundation.

Tsai, H. C. and Kelly, J. M. (1989). "Dynamic parameter identification for nonlinear isolation systems in response spectrum analysis." Earthquake Engrg. and Struct. Dyn., 18(8), 1119-1132.

Wada, A. et al. (1988). "Dynamic analysis of base isolated structure using various numerical models." Proc. of Ninth World Conf. on Earthquake Engrg., Japan, VII, 403-408.

Walters, M. and Elsesser, E. (1987). "Seismic isolation of existing structures with elastomeric bearings." ASME Pressure Vessels and Piping Conference, PVP-Vol. 127, California, 387-397.

Wang, Y. P. and Reinhorn, A. M. (1989). "Motion control of sliding isolated structures." 3rd Symposium on Seismic Vibrations and Shock Isolation, ASME/PVP - Vol. 181, 89-94.

Way, D. and Jeng, V. (1988). "NPAD - A computer program for the analysis of base isolated structures." ASME Pressure Vessels and Piping Conf., PVP-VOL.147, Pennsylvania, 65-69.

Wen, Y. K. (1976) "Method of random vibration of hysteretic systems." J. of Engrg. Mech. Div. ASCE, 102(EM2), 249-263.

Wilson, E. L. (1980). "SAP-80 Structural analysis programs for small or large computer systems." CEPA 1980 Fall Conf. and Annual Meeting, California, 13-15.

Wilson, E. L., Hollings, J. P. and Dovey, H. H. (1975). "ETABS - Three dimensional analysis of building systems." Report No. UCB/EERC -75/13, Earthquake Engineering Research Center, University of California, Berkeley, Calif.

Wolf, J. P. and Obernhuber, J. P. and Weber, B. T. (1983). "Response of a nuclear power plant on aseismic bearings to horizontally propagating waves." Earthquake Engrg. and Struct. Dyn., 11(4), 483-499.

Yasaka, A. et al. (1988). " Biaxial hysteresis model for base isolation devices." Summaries of Technical Papers of Annual Meeting - Architectural Institute of Japan, 1, 395-400.

Younis, C., Tadjbakhsh, I. G. and Saibel, E. A. (1983). "Analysis of general plane motion with coulomb friction." Wear, 91, 319-331.

Zayas, V., Low, S. and Mahin, S. (1987). "The FPS earthquake protection system: Experimental report." Report No. UCB/EERC-87/01, Earthquake Engineering Research Center, University of California, Berkeley, Calif.

APPENDIX A

3D-BASIS PROGRAM USER'S GUIDE

A.1 INPUT FORMAT FOR 3D-BASIS

Input file name is 3DBASIS.DAT and the output file is 3DBASIS.OUT. Free format is used to read all input data. Earthquake records are to be given in files WAVEX.DAT and/or WAVEY.DAT. Dynamic arrays are used. Double precision is used in the program for accuracy. Common block size has been set to 100,000 and should be changed if the need arises. All values are to be input unless mentioned otherwise. No blank cards are to be input.

A.2 PROBLEM TITLE

One card

TITLE TITLE upto 80 characters

A.3 UNITS

One card

UNITS UNITS upto 80 characters

A.4 CONTROL PARAMETERS

A.4.1 Control Parameters - Structure

One card

ISEV,NF,NP,NE

ISEV = 1 for option 1 - Data for Stiffness of the superstructure to be input.

ISEV = 2 for option 2 - Eigenvalues and eigenvectors of the superstructure (for

fixed base condition) to be input.

NF = Number of floors excluding the base.
(If NF<1 then NF set = 1)

NP = Number of bearings.
(If NP<4 then NP set = 4)

NE = Number of eigenvectors to be retained.
(If NE<3 then NE set = 3)

Notes: 1. For explanation of the option 1 and the option 2 refer to section 4.1.

2. Number of bearings refers to the total number of bearings which could be a combination of linear elastic elements, viscous elements, elastomeric bearings, steel dampers and sliding bearings.

3. Number of eigenvectors to be retained in the analysis should be in groups of three - the minimum being one set of three modes.

A.4.2 Control Parameters - Integration

one card
TSI,TOL,FMNORM,MAXMI,KVSTEP

TSI = Time step of integration.
(If TSI>TSR then TSI set = TSR;
refer to A.4.4 for details about TSR)

TOL = Tolerance for the nonlinear force

vector computation.

FMNORM = Reference moment at
the center of mass of the base
used for computing convergence.

MAXMI = Maximum number of iterations within
a time step.

KVSTEP = Index for time step variation.

KVSTEP = 1 for constant time step.
KVSTEP = 2 for variable time step.

Note: 1. The time step of integration cannot exceed the time step of earthquake record (given in A.4.4).

2. Tolerance for force computation may be 0.001.

3. The reference moment at the center of mass of the base can be calculated approximately by multiplying the base shear by one half the maximum dimension at the base.

4. If MAXMI is exceeded the program is terminated with an error message.

A.4.3 Control Parameters - Newmark's Method

One card

GAM,BET GAM = Parameter which produces numerical damping within a time step.
(Recommended value = 0.5)

BET = Parameter which controls the variation of acceleration within a time step.
(Recommended value = 0.25)

A.4.4 Control Parameters - Earthquake Input

One card
INDGACC,TSR,LOR,XTH,ULF

INDGACC = 1 for a single earthquake record at an angle of incidence XTH.

INDGACC = 2 for two independent earthquake records along the X and Y axes.

TSR = Time step of the earthquake record(s).

LOR = Length of the earthquake record(s).

XTH = Angle of incidence of the earthquake with respect to the X axis in anticlockwise direction (for INDGACC=1).

ULF = Load factor.

Notes: 1. Two options are available for the earthquake record input:

a. INDGACC = 1 refers to a single earthquake record input at any angle of incidence XTH with respect to the X axis. Input only one earthquake record (read through a single file WAVEX.DAT). Refer to D.2 for wave input information.

b. INDGACC = 2 refers to two independent earthquake records input in the X and Y directions, eg. El Centro N-S along the X direction and El Centro E-W along the Y direction. Input two independent earthquake records in the X and Y directions (read through two files WAVEX.DAT and WAVEY.DAT). Refer to D.2 and D.3 for wave input information.

2. The time step of earthquake record and the length of earthquake record has to be the same in both X and Y directions for INDGACC = 2.

3. Load factor is applied to the earthquake records in both X and Y directions.

B.1 SUPERSTRUCTURE DATA

Go to B.2 for option 1 - three dimensional shear building representation of the superstructure.

Go to B.3 for option 2 - full three dimensional representation of the superstructure. Eigenvalue analysis has to be done prior to the 3D-BASIS analysis using computer program ETABS.

B.2 Shear Stiffness Data for Three Dimensional Shear Building (for ISEV = 1)

B.2.1 Shear Stiffness - X Direction (Input only if ISEV = 1)

NF cards

SX(I),I=1,NF SX(I) = Shear stiffness of story I in the X direction.

Note: 1. Shear stiffness of each individual story in the X direction starting from the top story to the first story.

B.2.2 Shear stiffness - Y Direction (Input only if ISEV = 1)

NF cards

SY(I),I=1,NF SY(I) = Shear stiffness of story I in the Y direction.

Note: 1. Shear stiffness of each individual story in the Y direction starting from the top story to the first story.

B.2.3 Torsional stiffness - θ Direction
(Input only if ISEV = 1)

NF cards

ST(I),I=1,NF ST(I) = Torsional stiffness of story I in the θ direction about the center of mass of the floor.

Note: 1. Torsional stiffness of <u>each individual story</u> in the θ direction starting from the top story to the first story.

B.2.4 Eccentricity Data - X Direction (Input only if ISEV = 1)

NF cards

EX(I),I=1,NF EX(I) = Eccentricity of center of resistance from the center of mass of the floor I.

Note: 1. Eccentricity at each individual story in the X direction starting from the top story to the first story.

B.2.5 Eccentricity Data - Y direction (Input only if ISEV = 1)

NF cards

EY(I),I=1,NF EY(I) = Eccentricity of center of resistance from the center of mass of the floor I.

Note: 1. Eccentricity at each individual story in the Y direction starting from the top story to the first story.

B.3 Eigenvalues and Eigenvectors for Fully Three Dimensional Building (for ISEV = 2)

B.3.1 Eigenvalues (Input only if ISEV = 2)

NE cards

W(I),I=1,NE W(I) = Eigenvalue of mode I.

Note: 1. Input from the first mode to the NE mode.

B.3.2 Eigenvectors (Input only if ISEV =2)

NE cards

E(3*NF,I),I=1,NE

E(3*NF,I) = Eigenvector of mode I.

Note: 1. Input from the first mode to the NE mode.

B.4 Superstructure Mass Data

B.4.1 Translational Mass

NF Cards

CMX(I),I=1,NF CMX(I) = Translational mass at floor I.

Note: 1. Input from the top floor to the first floor.

B.4.2 Rotational Mass (Mass Moment of Inertia)

NF Cards

CMT(I),I=1,NF CMT(I) = Mass moment of inertia of floor I about the center of mass.

Note: 1. Input from the top floor to the first floor.

B.5 Superstructure Damping Data

NE Cards

DR(I),I=1,NE DR(I) = Damping ratio corresponding to mode I.

Note: 1. Input from the first mode to the NE mode.

B.6 Distance to the Center of Mass of the Floor

NF cards

XN(I),YN(I),I=1,NF

XN(I) = Distance of the center of mass of the floor I from the center of mass of the base in the X direction.

YN(I) = Distance of the center of mass of the floor I from the center of mass of the base in the Y direction.

(If ISEV = 1 then XN(I) and YN(I) set = 0)

Note: 1. Input from the top floor to the first floor.

B.7 Height of Different Floors and the Base

NF+1 cards

H(I),I=1,NF+1 H(I) = Height from the ground to the floor I.

Note: 1. Input from the top floor to the base.

C.1 ISOLATION SYSTEM DATA

C.2 Stiffness Data for Linear Elastic Isolation System

One card
SXE,SYE,STE,EXE,EYE

SXE = Resultant stiffness of the linear elastic isolation system in the X direction.

SYE = Resultant stiffness of the linear elastic isolation system in the Y direction.

STE = Resultant torsional stiffness of the linear elastic isolation system in the θ direction about the center of mass of the base.

EXE = Eccentricity of the center of resistance of the linear elastic isolation system in the X direction from the center of mass of the base.

EYE = Eccentricity of the center of resistance of the linear elastic isolation system in the Y direction from the center of mass of the base.

Note: 1. Data for linear elastic elements can also be input individually (refer to C.5.1).

C.3 Mass Data of the Base

One Card

CMXB,CMTB CMXB = Mass of the base in the translational direction.

CMTB = Mass moment of Inertia of the base about the center of mass of the base.

C.4 Global Damping Data

One card

CBX,CBY,CBT,ECX,ECY

CBX = Resultant global damping coefficient in the X direction.

CBY = Resultant global damping coefficient in the Y direction.

CBT = Resultant global damping coefficient in the θ direction about the center of mass of the base.

ECX = Eccentricity of the center of global damping of the isolation system in the X direction from the center of mass of the base.

ECY = Eccentricity of the center of global damping of the isolation system in the Y direction from the center of mass of the base.

Note: 1. Data for viscous elements can also be input individually (refer to C.5.2).

C.5 Isolation Element Data

(i). Data for NP isolation elements to be given using the elements in C.5.1,C.5.2,C.5.3 and C.5.4.

(ii). The following indices are used to identify the element type in the isolation system. INELEM(NP,2) described below is used in all the subsequent sections and will not be described in the subsequent sections.

INELEM(K,1:2)
= Indices for the isolation element K indicating its type and whether it is a uniaxial or biaxial element.

INELEM(K,1) = 1 for a uniaxial element in the X direction

INELEM(K,1) = 2 for a uniaxial element in the Y direction

INELEM(K,1) = 3 for a biaxial element

INELEM(K,2) = 1 for a linear elastic element

INELEM(K,2) = 2 for a viscous element

INELEM(K,2) = 3 for a hysteretic element
for elastomeric bearing or steel damper

INELEM(K,2) = 4 for a hysteretic element
for sliding bearing

C.5.1 Linear Elastic Element

One card
INELEM(K,1:2) INELEM(K,1) can be either 1,2 or 3
INELEM(K,2) = 1
(Refer to C.5 for further details).

One card
PS(K,1),PS(K,2)

PS(K,1) = Shear stiffness in the X direction for biaxial element or uniaxial element in the X direction
(leave blank if the uniaxial element is in the Y direction only).

PS(K,2) = Shear stiffness in the Y direction for biaxial element or uniaxial element in the Y direction
(leave blank if the uniaxial element is in the X direction only).

Note: 1. Biaxial element means elastic stiffness in both X and Y direcitons (no interaction between forces in the X and Y direction).

C.5.2 Viscous Element

One card

INELEM(K,1:2) INELEM(K,1) can be either 1,2 or 3
INELEM(K,2) = 2
(Refer to C.5 for further details).

One card

PC(K,1),PC(K,2)

PC(K,1) = Damping coefficient in the X direction for biaxial element or uniaxial element in the X direction (leave blank if the uniaxial element is in the Y direction only).

PC(K,2) = Damping coefficient in the Y direction for biaxial element or uniaxial element in the Y direction (leave blank if the uniaxial element is in the X direction only).

Note: 1. Biaxial element means damping in both X and Y direcitons (no interaction between forces in the X and Y direction).

C.5.3 Hysteretic Element for Elastomeric Bearings/Steel Dampers

One card

INELEM(K,1:2) INELEM(K,1) can be either 1,2 or 3
INELEM(K,2) = 3
(Refer to C.5 for further details).

One card

ALP(K,I),YF(K,I),YD(K,I),I=1,2

ALP(K,1) = Post-to-preyielding
stiffness ratio;
YF(K,1) = Yield force;
YD(K,1) = Yield displacement;
in the X direction
for biaxial element or uniaxial
element in the X direction
(leave blank if the uniaxial element
is in the Y direction only).

ALP(K,2) = Post-to-preyielding
stiffness ratio;
YF(K,2) = Yield force;
YD(K,2) = Yield displacement;
in the Y direction
for biaxial element or uniaxial
element in the Y direction
(leave blank if the uniaxial element
is in the X direction only).

C.5.4 Hysteretic Element for Sliding Bearings

One card
INELEM(K,1:2) INELEM(K,1) can be either 1,2 or 3
INELEM(K,2) = 4
(Refer to C.5 for further details).

One card
(FMAX(K,I),DF(K,I),PA(K,I),YD(K,I),I=1,2),FN(K)

FMAX(K,1) = Maximum coefficient
of sliding friction;
DF(K,1) = Difference between

the maximum and minimum
coefficient of sliding friction;
PA(K,1) = Constant which controls the
transition of coefficient of sliding
friction from maximum to minimum value;
in the X direction
for biaxial element or uniaxial
element in the X direction
(leave blank if the uniaxial element
is in the Y direction only).

FMAX(K,2) = Maximum coefficient
of sliding friction;
DF(K,2) = Difference between
the maximum and minimum
coefficient of sliding friction;
PA(K,2) = Constant which controls the
transition of coefficient of sliding
friction from maximum to minimum value;
in the Y direction
for biaxial element or uniaxial
element in the Y direction
(leave blank if the uniaxial element
is in the X direction only).

FN(K) = Initial normal force at the
sliding interface.

C.6 Coordinates of Isolation Elements

NP Cards

XP(I),YP(I),I=1,NP

XP(I) = X Coordinate of isolation element I from the center of mass of the base.

YP(I) = Y Coordinate of isolation element I from the center of mass of the base.

D.1 EARTHQUAKE DATA

D.2 Unidirectional Earthquake Record

File:WAVEX.DAT

LOR cards
X(I),I=1,LOR X(I) = Unidirectional acceleration component.

Note: 1.If INDGACC as specified in A.4.4 is 1, then the input will be assumed at an angle XTH specified in A.4.4. If INDGACC as specified in A.4.4 is 2, then X(LOR) is considered to be the X component of the bidirectional earthquake.

D.3 Earthquake Record in the Y Direction for the Bidirectional Earthquake

File:WAVEY.DAT (Input only if INDGACC = 2)

LOR cards
Y(I),I=1,LOR Y(I) = Acceleration component in the Y direction.

E.1 OUTPUT DATA

E.2 Output Parameters

One card
LTMH,KPD,IP1,IP2,IP3,IP4

LTMH = 0 for both the time history and peak response output.
LTMH = 1 for only peak response output.

KPD = No. of time steps before the next response quantity is output.

IP1,IP2, IP3, IP4 = Bearing numbers of four bearings at which the peak response values and the force - displacement time history response is desired.

E.3 Interstory drift output

Six cards
CORDX(K), CORDY(K),K=1,6

CORDX(K) = X coordinate of the column line K at which the interstory drift is desired.

CORDY(K) = Y coordinate of the column line K at which the interstory drift is desired.

Note: 1. The coordinates of the column lines are with respect to the reference axis at the center of mass of the base. Six column lines can be specified.

APPENDIX B
INPUT FILE FOR EXAMPLE 1
(Refer to section 8.2)

```
EXAMPLE 1: SIX STORY R. C. STRUCTURE WITH LEAD-RUBBER BEARING ISOLATION SYSTEM
Units tons-meters
2 6 22 6
0.01 0.001 10000 20 1
0.5 0.25
1 0.02 1000 1.5707963 9.81
51.96 57.024 247.246 580.031 719.228 2188.612
 -0.009522  0.105770  0.005537 -0.009752  0.085108  0.004543
 -0.009420  0.063397  0.003542 -0.007822  0.040315  0.002221
 -0.004639  0.016636  0.000748 -0.001864  0.006200  0.000284
  0.100908  0.013347  0.000731  0.088173  0.009824  0.000495
  0.072651  0.006506  0.000280  0.054303  0.003432  0.000085
  0.029818  0.000869 -0.000051  0.011884  0.000344 -0.000016
  0.004356 -0.042784  0.013871  0.001446 -0.028679  0.012522
 -0.001727 -0.016299  0.010895 -0.003289 -0.010052  0.008281
 -0.002702 -0.007866  0.004280 -0.001170 -0.003564  0.001813
  0.095580  0.005878  0.000123  0.022212 -0.001409 -0.000543
 -0.046944 -0.005707 -0.000925 -0.085458 -0.006066 -0.000845
 -0.074492 -0.003074 -0.000395 -0.037343 -0.001550 -0.000188
  0.007090 -0.077257 -0.006776  0.004214 -0.000701 -0.001227
 -0.000281  0.059408  0.002696 -0.005609  0.085899  0.004670
 -0.006811  0.065660  0.003402 -0.003486  0.031908  0.001493
 -0.066697  0.001406 -0.000595  0.043552  0.002344  0.000127
  0.084970  0.000045  0.000375  0.010653 -0.003358  0.000329
 -0.087084 -0.005079  0.000233 -0.072193 -0.003022  0.000159
35.665 35.665 35.665 39.245 41.918 36.571
1561.3 1561.3 1561.3 1718 1835.1 1601
0.05 0.05 0.05 0.05 0.05 0.05
0 0
0 0
0 0
0 0
0 0
0 0
20.3 17.1 13.9 10.7 6.9 3.7 0
0 0 0 0 0
36.571 1601
0  0  0 0 0
3 3
0.14407 5.909 0.004353  0.14407 5.909 0.004353
3 3
0.14407 5.909 0.004353 0.14407 5.909 0.004353
3 3
0.1465 3.64  0.005232 0.1465 3.64  0.005232
3 3
0.1538  7.732 0.007061 0.1538  7.732 0.007061
3 3
0.14407 5.909 0.004353 0.14407 5.909 0.004353
3 3
0.1538 7.732 0.007061 0.1538 7.732 0.007061
3 3
0.1538 7.732 0.007061 0.1538 7.732 0.007061
3 3
0.14407 5.909 0.004353 0.14407 5.909 0.004353
3 3
0.1465 3.64  0.005232 0.1465 3.64  0.005232
3 3
0.14407 5.909 0.004353 0.14407 5.909 0.004353
3 3
0.1538 7.732 0.007061 0.1538 7.732 0.007061
3 3
0.14407 5.909 0.004353 0.14407 5.909 0.004353
3 3
0.1465 3.64  0.005232 0.1465 3.64  0.005232
3 3
0.14407 5.909 0.004353 0.14407 5.909 0.004353
3 3
0.1538 7.732 0.007061 0.1538 7.732 0.007061
3 3
0.1538 7.732 0.007061 0.1538 7.732 0.007061
3 3
0.1538 7.732 0.007061 0.1538 7.732 0.007061
3 3
0.14407 5.909 0.004353 0.14407 5.909 0.004353
```

```
3 3
0.1538 7.732 0.007061 0.1538 7.732 0.007061
3 3
0.14407 5.909 0.004353 0.14407 5.909 0.004353
3 3
0.14407 5.909 0.004353 0.14407 5.909 0.004353
3 3
0.14407 5.909 0.004353 0.14407 5.909 0.004353
-9.15 -6.9
-9.15 -0.05
-9.15 6.6
-5.7 -6.9
-5.7 -0.05
-5.7 6.6
-2.1 -6.9
-2.1 -0.05
-2.1 6.6
0.3 -0.05
1.5 -6.9
1.5 -0.05
1.5  6.6
2.7 -0.05
5.1 -6.9
5.1 -0.05
5.1  6.6
6.4 -0.05
8.7 -6.9
8.7 -0.05
8.7  2.1
8.7  6.6
1 5 1 2 3 4
9 6.75
-9 -6.75
0 0
0 0
0 0
0 0
```

OUTPUT FILE FOR EXAMPLE 1
(Refer to section 8.2)

```
**************************************************

PROGRAM 3D-BASIS ... A GENERAL PROGRAM FOR THE NONLINEAR
          DYNAMIC ANALYSIS OF THREE DIMENSIONAL
          BASE ISOLATED BUILDINGS


DEVELOPED BY ... SATISH NAGARAJAIAH, ANDREI M. REINHORN
          AND MICHALAKIS C. CONSTANTINOU
          DEPARTMENT OF CIVIL ENGINEERING
          STATE UNIV. OF NEW YORK AT BUFFALO

          VAX VERSION , OCTOBER 1990

NATIONAL CENTER FOR EARTHQUAKE ENGINEERING RESEARCH
STATE UNIVERSITY OF NEW YORK, BUFFALO



**************************************************

EXAMPLE 1: SIX STORY R. C. STRUCTURE WITH LEAD-RUBBER BEARING ISOLATION SYSTEM

**************************************************


**************************************************

Units tons-meters

**************************************************



**********INPUT DATA**********


********** CONTROL PARAMETERS **********



NO. OF FLOORS(EXCL. BASE)..... =         6
NO. OF BEARINGS..... =        22
NO. OF EIGEN VECTORS CONSIDERED..... =         6
INDEX FOR  SUPERSTRUCTURE STIFFNESS DATA=         2

 INDEX = 1 FOR 3D SHEAR BUILDING  REPRES.
 INDEX = 2 FOR FULL 3D REPRESENTATION

TIME STEP OF INTEGRATION (NEWMARK)..... =     0.01000
INDEX FOR TYPE OF TIME STEP..... =         1

 INDEX = 1 FOR CONSTANT TIME STEP
 INDEX = 2 FOR VARIABLE TIME STEP

GAMA FOR NEWMARKS  METHOD..... =     0.50000
BETA FOR NEWMARKS  METHOD..... =     0.25000
TOLERANCE FOR FORCE COMPUTATION..... =     0.00100
REFERENCE MOMENT OF CONVERGENCE..... =  10000.00000
MAX NUMBER OF ITERATIONS WITHIN T.S..... =        20
INDEX FOR GROUND MOTION INPUT..... =         1

 INDEX = 1 FOR UNIDIRECTIONAL INPUT
 INDEX = 2 FOR BIDIRECTIONAL INPUT

TIME STEP OF RECORD ..... =     0.02000
```

LENGTH OF RECORD..... = 1000
LOAD FACTOR..... = 9.81000
ANGLE OF EARTHQUAKE INCIDENCE..... = 1.57080

POINTER WITHIN MASTER ARRAY MAX STORAGE 6296

********** SUPERSTRUCTURE DATA **********

SUPERSTRUCTURE STIFFNESS DATA.....

EIGENVALUES AND EIGENVECTORS (FULL THREE DIMENSIONAL REPRESENTATION)....
MODE NUMBER EIGENVALUE

1	51.960000
2	57.024000
3	247.246000
4	580.031000
5	719.228000
6	2188.612000

MODE SHAPES

FLOOR		1	2	3	4	5	6
6	X	-0.0095220	0.1009080	0.0043560	0.0955800	0.0070900	-0.0666970
6	Y	0.1057700	0.0133470	-0.0427840	0.0058780	-0.0772570	0.0014060
6	R	0.0055370	0.0007310	0.0138710	0.0001230	-0.0067760	-0.0005950
5	X	-0.0097520	0.0881730	0.0014460	0.0222120	0.0042140	0.0435520
5	Y	0.0851080	0.0098240	-0.0286790	-0.0014090	-0.0007010	0.0023440
5	R	0.0045430	0.0004950	0.0125220	-0.0005430	-0.0012270	0.0001270
4	X	-0.0094200	0.0726510	-0.0017270	-0.0469440	-0.0002810	0.0849700
4	Y	0.0633970	0.0065060	-0.0162990	-0.0057070	0.0594080	0.0000450
4	R	0.0035420	0.0002800	0.0108950	-0.0009250	0.0026960	0.0003750
3	X	-0.0078220	0.0543030	-0.0032890	-0.0854580	-0.0056090	0.0106530
3	Y	0.0403150	0.0034320	-0.0100520	-0.0060660	0.0858990	-0.0033580
3	R	0.0022210	0.0000850	0.0082810	-0.0008450	0.0046700	0.0003290
2	X	-0.0046390	0.0298180	-0.0027020	-0.0744920	-0.0068110	-0.0870840
2	Y	0.0166360	0.0008690	-0.0078660	-0.0030740	0.0656600	-0.0050790
2	R	0.0007480	-0.0000510	0.0042800	-0.0003950	0.0034020	0.0002330
1	X	-0.0018640	0.0118840	-0.0011700	-0.0373430	-0.0034860	-0.0721930
1	Y	0.0062000	0.0003440	-0.0035640	-0.0015500	0.0319080	-0.0030220
1	R	0.0002840	-0.0000160	0.0018130	-0.0001880	0.0014930	0.0001590

SUPERSTRUCTURE MASS.....

FLOOR	TRANSL. MASS	ROTATIONAL MASS	ECCENT X	ECCENT Y
6	35.66500	1561.30000	0.00000	0.00000
5	35.66500	1561.30000	0.00000	0.00000
4	35.66500	1561.30000	0.00000	0.00000
3	39.24500	1718.00000	0.00000	0.00000
2	41.91800	1835.10000	0.00000	0.00000
1	36.57100	1601.00000	0.00000	0.00000

SUPERSTRUCTURE DAMPING.....

MODE SHAPE DAMPING RATIO

1	0.05000
2	0.05000
3	0.05000
4	0.05000
5	0.05000
6	0.05000

HEIGHT.....
FLOOR HEIGHT

6	20.300
5	17.100
4	13.900
3	10.700
2	6.900
1	3.700
0	0.000

********** ISOLATION SYSTEM DATA **********

STIFFNESS DATA FOR LINEAR-ELASTIC ISOLATION SYSTEM.....

STIFFNESS OF LINEAR-ELASTIC SYS. IN X DIR. = 0.00000
STIFFNESS OF LINEAR ELASTIC SYS. IN Y DIR. = 0.00000
STIFFNESS OF LINEAR ELASTIC SYS. IN R DIR. = 0.00000
ECCENT. IN X DIR. FROM CEN. OF MASS..... = 0.00000
ECCENT. IN Y DIR. FROM CEN. OF MASS..... = 0.00000

MASS AT THE CENTER OF MASS OF THE BASE ....

	TRANSL. MASS	ROTATINAL MASS
MASS	36.57100	1601.00000

GLOBAL ISOLATION DAMPING AT THE CENTER OF MASS OF THE BASE.....

	X	Y	R	ECX	ECY
DAMPING	0.00000	0.00000	0.00000	0.00000	0.00000

ELASTOMERIC/DAMPER FORCE-DISPLACEMENT LOOP PARAMETERS.....

BEARING	ALPFA X	ALPFA Y	YIELD FORCE X	YIELD FORCE Y	YIELD DISPL. X	YIELD DISPL. Y
1	0.14407	0.14407	5.90900	5.90900	0.00435	0.00435
2	0.14407	0.14407	5.90900	5.90900	0.00435	0.00435
3	0.14650	0.14650	3.64000	3.64000	0.00523	0.00523
4	0.15380	0.15380	7.73200	7.73200	0.00706	0.00706
5	0.14407	0.14407	5.90900	5.90900	0.00435	0.00435
6	0.15380	0.15380	7.73200	7.73200	0.00706	0.00706
7	0.15380	0.15380	7.73200	7.73200	0.00706	0.00706
8	0.14407	0.14407	5.90900	5.90900	0.00435	0.00435
9	0.14650	0.14650	3.64000	3.64000	0.00523	0.00523
10	0.14407	0.14407	5.90900	5.90900	0.00435	0.00435
11	0.15380	0.15380	7.73200	7.73200	0.00706	0.00706

12	0.14407	0.14407	5.90900	5.90900	0.00435	0.00435
13	0.14650	0.14650	3.64000	3.64000	0.00523	0.00523
14	0.14407	0.14407	5.90900	5.90900	0.00435	0.00435
15	0.15380	0.15380	7.73200	7.73200	0.00706	0.00706
16	0.15380	0.15380	7.73200	7.73200	0.00706	0.00706
17	0.15380	0.15380	7.73200	7.73200	0.00706	0.00706
18	0.14407	0.14407	5.90900	5.90900	0.00435	0.00435
19	0.15380	0.15380	7.73200	7.73200	0.00706	0.00706
20	0.14407	0.14407	5.90900	5.90900	0.00435	0.00435
21	0.14407	0.14407	5.90900	5.90900	0.00435	0.00435
22	0.14407	0.14407	5.90900	5.90900	0.00435	0.00435

BEARING LOCATION .....

BEARING	X	Y
1	-9.1500	-6.9000
2	-9.1500	-0.0500
3	-9.1500	6.6000
4	-5.7000	-6.9000
5	-5.7000	-0.0500
6	-5.7000	6.6000
7	-2.1000	-6.9000
8	-2.1000	-0.0500
9	-2.1000	6.6000
10	0.3000	-0.0500
11	1.5000	-6.9000
12	1.5000	-0.0500
13	1.5000	6.6000
14	2.7000	-0.0500
15	5.1000	-6.9000
16	5.1000	-0.0500
17	5.1000	6.6000
18	6.4000	-0.0500
19	8.7000	-6.9000
20	8.7000	-0.0500
21	8.7000	2.1000
22	8.7000	6.6000

********** OUTPUT PARAMETERS **********

TIME HISTORY OPTION ..... = 1

INDEX = 0 FOR TIME HISTORY OUTPUT
INDEX = 1 FOR NO TIME HISTORY OUTPUT

NO. OF TIME STEPS AT WHICH TIME HISTORY
OUTPUT IS DESIRED ..... = 5
FORCE-DISPLACEMENT TIME HISTORY DESIRED
AT BEARINGS NUMBERED..... = 1 2 3 4

COORDINATES OF COLUMN LINES AT WHICH INTERSTORY DRIFTS ARE DESIRED

COL. LINE	X. CORD.	Y. CORD.
1	9.000000	6.750000
2	-9.000000	-6.750000
3	0.000000	0.000000
4	0.000000	0.000000
5	0.000000	0.000000
6	0.000000	0.000000

*****************OUTPUT****************

************** MAX. RESPONSE *************

MAX. REL. DISP. AT THE CENTER OF MASS OF FLOORS
(WITH RESPECT TO THE BASE)

FLOOR	X DISP.	Y DISP.	ROTN...
6	0.126061E-02	-.447928E-01	-.188709E-02
5	-.956010E-03	-.365397E-01	-.156477E-02
4	0.993690E-03	-.277203E-01	-.123003E-02
3	0.101032E-02	-.181371E-01	-.766164E-03
2	0.666496E-03	-.790795E-02	-.240127E-03
1	0.264250E-03	-.305054E-02	-.892772E-04

MAX INTERSTORY DRIFT

STORY	X DST.	Y DST.	TIME	X DRIFT/FL. HT.	TIME	Y DRIFT/FL. HT.
6	9.000000	6.750000	13.630000	0.000865	13.620000	0.003571
5	9.000000	6.750000	13.560000	0.000832	13.580000	0.003716
4	9.000000	6.750000	13.550000	0.000990	13.560000	0.004304
3	9.000000	6.750000	13.530000	0.000853	13.550000	0.003940
2	9.000000	6.750000	2.400000	0.000212	13.540000	0.001937
1	9.000000	6.750000	2.410000	0.000117	13.530000	0.001038
6	-9.000000	-6.750000	13.650000	0.000592	13.590000	0.001685
5	-9.000000	-6.750000	13.630000	0.000600	13.590000	0.001822
4	-9.000000	-6.750000	13.560000	0.000973	13.580000	0.001699
3	-9.000000	-6.750000	13.550000	0.001024	13.580000	0.001455
2	-9.000000	-6.750000	13.540000	0.000438	13.570000	0.001107
1	-9.000000	-6.750000	13.530000	0.000229	13.570000	0.000616
6	0.000000	0.000000	13.560000	0.000160	13.610000	0.002620
5	0.000000	0.000000	12.740000	0.000130	13.590000	0.002769
4	0.000000	0.000000	15.830000	0.000099	13.570000	0.002998
3	0.000000	0.000000	13.580000	0.000091	13.560000	0.002693
2	0.000000	0.000000	13.580000	0.000126	13.550000	0.001518
1	0.000000	0.000000	13.590000	0.000071	13.550000	0.000824
6	0.000000	0.000000	13.560000	0.000160	13.610000	0.002620
5	0.000000	0.000000	12.740000	0.000130	13.590000	0.002769
4	0.000000	0.000000	15.830000	0.000099	13.570000	0.002998
3	0.000000	0.000000	13.580000	0.000091	13.560000	0.002693
2	0.000000	0.000000	13.580000	0.000126	13.550000	0.001518
1	0.000000	0.000000	13.590000	0.000071	13.550000	0.000824
6	0.000000	0.000000	13.560000	0.000160	13.610000	0.002620
5	0.000000	0.000000	12.740000	0.000130	13.590000	0.002769
4	0.000000	0.000000	15.830000	0.000099	13.570000	0.002998
3	0.000000	0.000000	13.580000	0.000091	13.560000	0.002693
2	0.000000	0.000000	13.580000	0.000126	13.550000	0.001518
1	0.000000	0.000000	13.590000	0.000071	13.550000	0.000824
6	0.000000	0.000000	13.560000	0.000160	13.610000	0.002620
5	0.000000	0.000000	12.740000	0.000130	13.590000	0.002769
4	0.000000	0.000000	15.830000	0.000099	13.570000	0.002998
3	0.000000	0.000000	13.580000	0.000091	13.560000	0.002693
2	0.000000	0.000000	13.580000	0.000126	13.550000	0.001518
1	0.000000	0.000000	13.590000	0.000071	13.550000	0.000824

MAX. DISP. AT THE CENTER OF MASS OF BASE

X DISP.	Y DISP.	ROTN...
0.575676E-03	-.821524E-01	0.117162E-02

MAX RESULTANT DISP. AT THE CENTER OF MASS OF BASE

TIME	RES. DISP.	X COMP.	Y COMP
13.5400	0.082153	-0.000278	-0.082152

MAX RESULTANT BEARING DISP.

BEARING	TIME	MAX. DISP	ANG. WITH X AXIS
1	13.550000	0.091938	-1.494882
2	13.550000	0.091673	1.568197
3	13.550000	0.091959	1.491997
4	13.550000	0.088317	-1.491764

MAX BEARING DISP.

BEARING	TIME	MAX. DISP X
1	13.610000	0.007764
2	15.680000	0.000570
3	13.610000	-0.008053
4	13.610000	0.007764

MAX BEARING DISP.

BEARING	TIME	MAX. DISP Y
1	13.550000	-0.091673
2	13.550000	-0.091673
3	13.550000	-0.091673
4	13.550000	-0.088041

MAX. TOTAL ACCL. AT CENTER OF MASS OF FLOORS

FLOOR	ACCL. X	ACCL. Y	ACCL. R
6	0.177478E+00	0.246346E+01	-.124195E+00
5	-.108085E+00	0.198685E+01	0.681171E-01
4	0.791088E-01	0.185746E+01	0.635643E-01
3	-.113572E+00	0.162123E+01	-.742804E-01
2	0.170082E+00	-.159748E+01	-.817644E-01
1	0.142431E+00	-.159331E+01	0.940393E-01

MAX STORY SHEAR

STORY	TIME	X SHEAR	TIME	Y SHEAR
6	16.370000	6.329751	13.650000	87.859249
5	15.840000	-9.181454	13.630000	148.131992
4	15.840000	-10.446800	13.580000	208.785835
3	15.830000	-8.180457	13.570000	270.146570
2	16.180000	6.975167	13.540000	324.615474
1	16.180000	12.184029	13.530000	374.670575

MAX. STRUCTURE SHEAR (TOP OF BASE)

FORCE X	FORCE Y	Z MOMENT
0.121840E+02	0.374671E+03	0.431488E+03

MAX. BASE SHEAR (BEARING LEVEL)

FORCE X	FORCE Y	Z MOMENT
-.148706E+02	-.423744E+03	-.519536E+03

********** END OF OUTPUT **********

NATIONAL CENTER FOR EARTHQUAKE ENGINEERING RESEARCH
LIST OF TECHNICAL REPORTS

The National Center for Earthquake Engineering Research (NCEER) publishes technical reports on a variety of subjects related to earthquake engineering written by authors funded through NCEER. These reports are available from both NCEER's Publications Department and the National Technical Information Service (NTIS). Requests for reports should be directed to the Publications Department, National Center for Earthquake Engineering Research, State University of New York at Buffalo, Red Jacket Quadrangle, Buffalo, New York 14261. Reports can also be requested through NTIS, 5285 Port Royal Road, Springfield, Virginia 22161. NTIS accession numbers are shown in parenthesis, if available.

NCEER-87-0001 "First-Year Program in Research, Education and Technology Transfer," 3/5/87, (PB88-134275/AS).

NCEER-87-0002 "Experimental Evaluation of Instantaneous Optimal Algorithms for Structural Control," by R.C. Lin, T.T. Soong and A.M. Reinhorn, 4/20/87, (PB88-134341/AS).

NCEER-87-0003 "Experimentation Using the Earthquake Simulation Facilities at University at Buffalo," by A.M. Reinhorn and R.L. Ketter, to be published.

NCEER-87-0004 "The System Characteristics and Performance of a Shaking Table," by J.S. Hwang, K.C. Chang and G.C. Lee, 6/1/87, (PB88-134259/AS). This report is available only through NTIS (see address given above).

NCEER-87-0005 "A Finite Element Formulation for Nonlinear Viscoplastic Material Using a Q Model," by O. Gyebi and G. Dasgupta, 11/2/87, (PB88-213764/AS).

NCEER-87-0006 "Symbolic Manipulation Program (SMP) - Algebraic Codes for Two and Three Dimensional Finite Element Formulations," by X. Lee and G. Dasgupta, 11/9/87, (PB88-219522/AS).

NCEER-87-0007 "Instantaneous Optimal Control Laws for Tall Buildings Under Seismic Excitations," by J.N. Yang, A. Akbarpour and P. Ghaemmaghami, 6/10/87, (PB88-134333/AS).

NCEER-87-0008 "IDARC: Inelastic Damage Analysis of Reinforced Concrete Frame - Shear-Wall Structures," by Y.J. Park, A.M. Reinhorn and S.K. Kunnath, 7/20/87, (PB88-134325/AS).

NCEER-87-0009 "Liquefaction Potential for New York State: A Preliminary Report on Sites in Manhattan and Buffalo," by M. Budhu, V. Vijayakumar, R.F. Giese and L. Baumgras, 8/31/87, (PB88-163704/AS). This report is available only through NTIS (see address given above).

NCEER-87-0010 "Vertical and Torsional Vibration of Foundations in Inhomogeneous Media," by A.S. Veletsos and K.W. Dotson, 6/1/87, (PB88-134291/AS).

NCEER-87-0011 "Seismic Probabilistic Risk Assessment and Seismic Margins Studies for Nuclear Power Plants," by Howard H.M. Hwang, 6/15/87, (PB88-134267/AS).

NCEER-87-0012 "Parametric Studies of Frequency Response of Secondary Systems Under Ground-Acceleration Excitations," by Y. Yong and Y.K. Lin, 6/10/87, (PB88-134309/AS).

NCEER-87-0013 "Frequency Response of Secondary Systems Under Seismic Excitation," by J.A. HoLung, J. Cai and Y.K. Lin, 7/31/87, (PB88-134317/AS).

NCEER-87-0014 "Modelling Earthquake Ground Motions in Seismically Active Regions Using Parametric Time Series Methods," by G.W. Ellis and A.S. Cakmak, 8/25/87, (PB88-134283/AS).

NCEER-87-0015 "Detection and Assessment of Seismic Structural Damage," by E. DiPasquale and A.S. Cakmak, 8/25/87, (PB88-163712/AS).

NCEER-87-0016 "Pipeline Experiment at Parkfield, California," by J. Isenberg and E. Richardson, 9/15/87, (PB88-163720/AS). This report is available only through NTIS (see address given above).

NCEER-87-0017 "Digital Simulation of Seismic Ground Motion," by M. Shinozuka, G. Deodatis and T. Harada, 8/31/87, (PB88-155197/AS). This report is available only through NTIS (see address given above).

NCEER-87-0018 "Practical Considerations for Structural Control: System Uncertainty, System Time Delay and Truncation of Small Control Forces," J.N. Yang and A. Akbarpour, 8/10/87, (PB88-163738/AS).

NCEER-87-0019 "Modal Analysis of Nonclassically Damped Structural Systems Using Canonical Transformation," by J.N. Yang, S. Sarkani and F.X. Long, 9/27/87, (PB88-187851/AS).

NCEER-87-0020 "A Nonstationary Solution in Random Vibration Theory," by J.R. Red-Horse and P.D. Spanos, 11/3/87, (PB88-163746/AS).

NCEER-87-0021 "Horizontal Impedances for Radially Inhomogeneous Viscoelastic Soil Layers," by A.S. Veletsos and K.W. Dotson, 10/15/87, (PB88-150859/AS).

NCEER-87-0022 "Seismic Damage Assessment of Reinforced Concrete Members," by Y.S. Chung, C. Meyer and M. Shinozuka, 10/9/87, (PB88-150867/AS). This report is available only through NTIS (see address given above).

NCEER-87-0023 "Active Structural Control in Civil Engineering," by T.T. Soong, 11/11/87, (PB88-187778/AS).

NCEER-87-0024 Vertical and Torsional Impedances for Radially Inhomogeneous Viscoelastic Soil Layers," by K.W. Dotson and A.S. Veletsos, 12/87, (PB88-187786/AS).

NCEER-87-0025 "Proceedings from the Symposium on Seismic Hazards, Ground Motions, Soil-Liquefaction and Engineering Practice in Eastern North America," October 20-22, 1987, edited by K.H. Jacob, 12/87, (PB88-188115/AS).

NCEER-87-0026 "Report on the Whittier-Narrows, California, Earthquake of October 1, 1987," by J. Pantelic and A. Reinhorn, 11/87, (PB88-187752/AS). This report is available only through NTIS (see address given above).

NCEER-87-0027 "Design of a Modular Program for Transient Nonlinear Analysis of Large 3-D Building Structures," by S. Srivastav and J.F. Abel, 12/30/87, (PB88-187950/AS).

NCEER-87-0028 "Second-Year Program in Research, Education and Technology Transfer," 3/8/88, (PB88-219480/AS).

NCEER-88-0001 "Workshop on Seismic Computer Analysis and Design of Buildings With Interactive Graphics," by W. McGuire, J.F. Abel and C.H. Conley, 1/18/88, (PB88-187760/AS).

NCEER-88-0002 "Optimal Control of Nonlinear Flexible Structures," by J.N. Yang, F.X. Long and D. Wong, 1/22/88, (PB88-213772/AS).

NCEER-88-0003 "Substructuring Techniques in the Time Domain for Primary-Secondary Structural Systems," by G.D. Manolis and G. Juhn, 2/10/88, (PB88-213780/AS).

NCEER-88-0004 "Iterative Seismic Analysis of Primary-Secondary Systems," by A. Singhal, L.D. Lutes and P.D. Spanos, 2/23/88, (PB88-213798/AS).

NCEER-88-0005 "Stochastic Finite Element Expansion for Random Media," by P.D. Spanos and R. Ghanem, 3/14/88, (PB88-213806/AS).

NCEER-88-0006 "Combining Structural Optimization and Structural Control," by F.Y. Cheng and C.P. Pantelides, 1/10/88, (PB88-213814/AS).

NCEER-88-0007 "Seismic Performance Assessment of Code-Designed Structures," by H.H-M. Hwang, J-W. Jaw and H-J. Shau, 3/20/88, (PB88-219423/AS).

NCEER-88-0008 "Reliability Analysis of Code-Designed Structures Under Natural Hazards," by H.H-M. Hwang, H. Ushiba and M. Shinozuka, 2/29/88, (PB88-229471/AS).

NCEER-88-0009 "Seismic Fragility Analysis of Shear Wall Structures," by J-W Jaw and H.H-M. Hwang, 4/30/88, (PB89-102867/AS).

NCEER-88-0010 "Base Isolation of a Multi-Story Building Under a Harmonic Ground Motion - A Comparison of Performances of Various Systems," by F-G Fan, G. Ahmadi and I.G. Tadjbakhsh, 5/18/88, (PB89-122238/AS).

NCEER-88-0011 "Seismic Floor Response Spectra for a Combined System by Green's Functions," by F.M. Lavelle, L.A. Bergman and P.D. Spanos, 5/1/88, (PB89-102875/AS).

NCEER-88-0012 "A New Solution Technique for Randomly Excited Hysteretic Structures," by G.Q. Cai and Y.K. Lin, 5/16/88, (PB89-102883/AS).

NCEER-88-0013 "A Study of Radiation Damping and Soil-Structure Interaction Effects in the Centrifuge," by K. Weissman, supervised by J.H. Prevost, 5/24/88, (PB89-144703/AS).

NCEER-88-0014 "Parameter Identification and Implementation of a Kinematic Plasticity Model for Frictional Soils," by J.H. Prevost and D.V. Griffiths, to be published.

NCEER-88-0015 "Two- and Three- Dimensional Dynamic Finite Element Analyses of the Long Valley Dam," by D.V. Griffiths and J.H. Prevost, 6/17/88, (PB89-144711/AS).

NCEER-88-0016 "Damage Assessment of Reinforced Concrete Structures in Eastern United States," by A.M. Reinhorn, M.J. Seidel, S.K. Kunnath and Y.J. Park, 6/15/88, (PB89-122220/AS).

NCEER-88-0017 "Dynamic Compliance of Vertically Loaded Strip Foundations in Multilayered Viscoelastic Soils," by S. Ahmad and A.S.M. Israil, 6/17/88, (PB89-102891/AS).

NCEER-88-0018 "An Experimental Study of Seismic Structural Response With Added Viscoelastic Dampers," by R.C. Lin, Z. Liang, T.T. Soong and R.H. Zhang, 6/30/88, (PB89-122212/AS).

NCEER-88-0019 "Experimental Investigation of Primary - Secondary System Interaction," by G.D. Manolis, G. Juhn and A.M. Reinhorn, 5/27/88, (PB89-122204/AS).

NCEER-88-0020 "A Response Spectrum Approach For Analysis of Nonclassically Damped Structures," by J.N. Yang, S. Sarkani and F.X. Long, 4/22/88, (PB89-102909/AS).

NCEER-88-0021 "Seismic Interaction of Structures and Soils: Stochastic Approach," by A.S. Veletsos and A.M. Prasad, 7/21/88, (PB89-122196/AS).

NCEER-88-0022 "Identification of the Serviceability Limit State and Detection of Seismic Structural Damage," by E. DiPasquale and A.S. Cakmak, 6/15/88, (PB89-122188/AS).

NCEER-88-0023 "Multi-Hazard Risk Analysis: Case of a Simple Offshore Structure," by B.K. Bhartia and E.H. Vanmarcke, 7/21/88, (PB89-145213/AS).

NCEER-88-0024 "Automated Seismic Design of Reinforced Concrete Buildings," by Y.S. Chung, C. Meyer and M. Shinozuka, 7/5/88, (PB89-122170/AS).

NCEER-88-0025 "Experimental Study of Active Control of MDOF Structures Under Seismic Excitations," by L.L. Chung, R.C. Lin, T.T. Soong and A.M. Reinhorn, 7/10/88, (PB89-122600/AS).

NCEER-88-0026 "Earthquake Simulation Tests of a Low-Rise Metal Structure," by J.S. Hwang, K.C. Chang, G.C. Lee and R.L. Ketter, 8/1/88, (PB89-102917/AS).

NCEER-88-0027 "Systems Study of Urban Response and Reconstruction Due to Catastrophic Earthquakes," by F. Kozin and H.K. Zhou, 9/22/88, (PB90-162348/AS).

NCEER-88-0028 "Seismic Fragility Analysis of Plane Frame Structures," by H.H-M. Hwang and Y.K. Low, 7/31/88, (PB89-131445/AS).

NCEER-88-0029 "Response Analysis of Stochastic Structures," by A. Kardara, C. Bucher and M. Shinozuka, 9/22/88, (PB89-174429/AS).

NCEER-88-0030 "Nonnormal Accelerations Due to Yielding in a Primary Structure," by D.C.K. Chen and L.D. Lutes, 9/19/88, (PB89-131437/AS).

NCEER-88-0031 "Design Approaches for Soil-Structure Interaction," by A.S. Veletsos, A.M. Prasad and Y. Tang, 12/30/88, (PB89-174437/AS).

NCEER-88-0032 "A Re-evaluation of Design Spectra for Seismic Damage Control," by C.J. Turkstra and A.G. Tallin, 11/7/88, (PB89-145221/AS).

NCEER-88-0033 "The Behavior and Design of Noncontact Lap Splices Subjected to Repeated Inelastic Tensile Loading," by V.E. Sagan, P. Gergely and R.N. White, 12/8/88, (PB89-163737/AS).

NCEER-88-0034 "Seismic Response of Pile Foundations," by S.M. Mamoon, P.K. Banerjee and S. Ahmad, 11/1/88, (PB89-145239/AS).

NCEER-88-0035 "Modeling of R/C Building Structures With Flexible Floor Diaphragms (IDARC2)," by A.M. Reinhorn, S.K. Kunnath and N. Panahshahi, 9/7/88, (PB89-207153/AS).

NCEER-88-0036 "Solution of the Dam-Reservoir Interaction Problem Using a Combination of FEM, BEM with Particular Integrals, Modal Analysis, and Substructuring," by C-S. Tsai, G.C. Lee and R.L. Ketter, 12/31/88, (PB89-207146/AS).

NCEER-88-0037 "Optimal Placement of Actuators for Structural Control," by F.Y. Cheng and C.P. Pantelides, 8/15/88, (PB89-162846/AS).

NCEER-88-0038 "Teflon Bearings in Aseismic Base Isolation: Experimental Studies and Mathematical Modeling," by A. Mokha, M.C. Constantinou and A.M. Reinhorn, 12/5/88, (PB89-218457/AS).

NCEER-88-0039 "Seismic Behavior of Flat Slab High-Rise Buildings in the New York City Area," by P. Weidlinger and M. Ettouney, 10/15/88, (PB90-145681/AS).

NCEER-88-0040 "Evaluation of the Earthquake Resistance of Existing Buildings in New York City," by P. Weidlinger and M. Ettouney, 10/15/88, to be published.

NCEER-88-0041 "Small-Scale Modeling Techniques for Reinforced Concrete Structures Subjected to Seismic Loads," by W. Kim, A. El-Attar and R.N. White, 11/22/88, (PB89-189625/AS).

NCEER-88-0042 "Modeling Strong Ground Motion from Multiple Event Earthquakes," by G.W. Ellis and A.S. Cakmak, 10/15/88, (PB89-174445/AS).

NCEER-88-0043 "Nonstationary Models of Seismic Ground Acceleration," by M. Grigoriu, S.E. Ruiz and E. Rosenblueth, 7/15/88, (PB89-189617/AS).

NCEER-88-0044 "SARCF User's Guide: Seismic Analysis of Reinforced Concrete Frames," by Y.S. Chung, C. Meyer and M. Shinozuka, 11/9/88, (PB89-174452/AS).

NCEER-88-0045 "First Expert Panel Meeting on Disaster Research and Planning," edited by J. Pantelic and J. Stoyle, 9/15/88, (PB89-174460/AS).

NCEER-88-0046 "Preliminary Studies of the Effect of Degrading Infill Walls on the Nonlinear Seismic Response of Steel Frames," by C.Z. Chrysostomou, P. Gergely and J.F. Abel, 12/19/88, (PB89-208383/AS).

NCEER-88-0047 "Reinforced Concrete Frame Component Testing Facility - Design, Construction, Instrumentation and Operation," by S.P. Pessiki, C. Conley, T. Bond, P. Gergely and R.N. White, 12/16/88, (PB89-174478/AS).

NCEER-89-0001 "Effects of Protective Cushion and Soil Compliancy on the Response of Equipment Within a Seismically Excited Building," by J.A. HoLung, 2/16/89, (PB89-207179/AS).

NCEER-89-0002 "Statistical Evaluation of Response Modification Factors for Reinforced Concrete Structures," by H.H-M. Hwang and J-W. Jaw, 2/17/89, (PB89-207187/AS).

NCEER-89-0003 "Hysteretic Columns Under Random Excitation," by G-Q. Cai and Y.K. Lin, 1/9/89, (PB89-196513/AS).

NCEER-89-0004 "Experimental Study of 'Elephant Foot Bulge' Instability of Thin-Walled Metal Tanks," by Z-H. Jia and R.L. Ketter, 2/22/89, (PB89-207195/AS).

NCEER-89-0005 "Experiment on Performance of Buried Pipelines Across San Andreas Fault," by J. Isenberg, E. Richardson and T.D. O'Rourke, 3/10/89, (PB89-218440/AS).

NCEER-89-0006 "A Knowledge-Based Approach to Structural Design of Earthquake-Resistant Buildings," by M. Subramani, P. Gergely, C.H. Conley, J.F. Abel and A.H. Zaghw, 1/15/89, (PB89-218465/AS).

NCEER-89-0007 "Liquefaction Hazards and Their Effects on Buried Pipelines," by T.D. O'Rourke and P.A. Lane, 2/1/89, (PB89-218481).

NCEER-89-0008 "Fundamentals of System Identification in Structural Dynamics," by H. Imai, C-B. Yun, O. Maruyama and M. Shinozuka, 1/26/89, (PB89-207211/AS).

NCEER-89-0009 "Effects of the 1985 Michoacan Earthquake on Water Systems and Other Buried Lifelines in Mexico," by A.G. Ayala and M.J. O'Rourke, 3/8/89, (PB89-207229/AS).

NCEER-89-R010 "NCEER Bibliography of Earthquake Education Materials," by K.E.K. Ross, Second Revision, 9/1/89, (PB90-125352/AS).

NCEER-89-0011 "Inelastic Three-Dimensional Response Analysis of Reinforced Concrete Building Structures (IDARC-3D), Part I - Modeling," by S.K. Kunnath and A.M. Reinhorn, 4/17/89, (PB90-114612/AS).

NCEER-89-0012 "Recommended Modifications to ATC-14," by C.D. Poland and J.O. Malley, 4/12/89, (PB90-108648/AS).

NCEER-89-0013 "Repair and Strengthening of Beam-to-Column Connections Subjected to Earthquake Loading," by M. Corazao and A.J. Durrani, 2/28/89, (PB90-109885/AS).

NCEER-89-0014 "Program EXKAL2 for Identification of Structural Dynamic Systems," by O. Maruyama, C-B. Yun, M. Hoshiya and M. Shinozuka, 5/19/89, (PB90-109877/AS).

NCEER-89-0015 "Response of Frames With Bolted Semi-Rigid Connections, Part I - Experimental Study and Analytical Predictions," by P.J. DiCorso, A.M. Reinhorn, J.R. Dickerson, J.B. Radziminski and W.L. Harper, 6/1/89, to be published.

NCEER-89-0016 "ARMA Monte Carlo Simulation in Probabilistic Structural Analysis," by P.D. Spanos and M.P. Mignolet, 7/10/89, (PB90-109893/AS).

NCEER-89-P017 "Preliminary Proceedings from the Conference on Disaster Preparedness - The Place of Earthquake Education in Our Schools," Edited by K.E.K. Ross, 6/23/89.

NCEER-89-0017 "Proceedings from the Conference on Disaster Preparedness - The Place of Earthquake Education in Our Schools," Edited by K.E.K. Ross, 12/31/89, (PB90-207895).

NCEER-89-0018 "Multidimensional Models of Hysteretic Material Behavior for Vibration Analysis of Shape Memory Energy Absorbing Devices, by E.J. Graesser and F.A. Cozzarelli, 6/7/89, (PB90-164146/AS).

NCEER-89-0019 "Nonlinear Dynamic Analysis of Three-Dimensional Base Isolated Structures (3D-BASIS)," by S. Nagarajaiah, A.M. Reinhorn and M.C. Constantinou, 8/3/89, (PB90-161936/AS).

NCEER-89-0020 "Structural Control Considering Time-Rate of Control Forces and Control Rate Constraints," by F.Y. Cheng and C.P. Pantelides, 8/3/89, (PB90-120445/AS).

NCEER-89-0021 "Subsurface Conditions of Memphis and Shelby County," by K.W. Ng, T-S. Chang and H-H.M. Hwang, 7/26/89, (PB90-120437/AS).

NCEER-89-0022 "Seismic Wave Propagation Effects on Straight Jointed Buried Pipelines," by K. Elhmadi and M.J. O'Rourke, 8/24/89, (PB90-162322/AS).

NCEER-89-0023 "Workshop on Serviceability Analysis of Water Delivery Systems," edited by M. Grigoriu, 3/6/89, (PB90-127424/AS).

NCEER-89-0024 "Shaking Table Study of a 1/5 Scale Steel Frame Composed of Tapered Members," by K.C. Chang, J.S. Hwang and G.C. Lee, 9/18/89, (PB90-160169/AS).

NCEER-89-0025 "DYNA1D: A Computer Program for Nonlinear Seismic Site Response Analysis - Technical Documentation," by Jean H. Prevost, 9/14/89, (PB90-161944/AS).

NCEER-89-0026 "1:4 Scale Model Studies of Active Tendon Systems and Active Mass Dampers for Aseismic Protection," by A.M. Reinhorn, T.T. Soong, R.C. Lin, Y.P. Yang, Y. Fukao, H. Abe and M. Nakai, 9/15/89, (PB90-173246/AS).

NCEER-89-0027 "Scattering of Waves by Inclusions in a Nonhomogeneous Elastic Half Space Solved by Boundary Element Methods," by P.K. Hadley, A. Askar and A.S. Cakmak, 6/15/89, (PB90-145699/AS).

NCEER-89-0028 "Statistical Evaluation of Deflection Amplification Factors for Reinforced Concrete Structures," by H.H.M. Hwang, J-W. Jaw and A.L. Ch'ng, 8/31/89, (PB90-164633/AS).

NCEER-89-0029 "Bedrock Accelerations in Memphis Area Due to Large New Madrid Earthquakes," by H.H.M. Hwang, C.H.S. Chen and G. Yu, 11/7/89, (PB90-162330/AS).

NCEER-89-0030 "Seismic Behavior and Response Sensitivity of Secondary Structural Systems," by Y.Q. Chen and T.T. Soong, 10/23/89, (PB90-164658/AS).

NCEER-89-0031 "Random Vibration and Reliability Analysis of Primary-Secondary Structural Systems," by Y. Ibrahim, M. Grigoriu and T.T. Soong, 11/10/89, (PB90-161951/AS).

NCEER-89-0032 "Proceedings from the Second U.S. - Japan Workshop on Liquefaction, Large Ground Deformation and Their Effects on Lifelines, September 26-29, 1989," Edited by T.D. O'Rourke and M. Hamada, 12/1/89, (PB90-209388/AS).

NCEER-89-0033 "Deterministic Model for Seismic Damage Evaluation of Reinforced Concrete Structures," by J.M. Bracci, A.M. Reinhorn, J.B. Mander and S.K. Kunnath, 9/27/89.

NCEER-89-0034 "On the Relation Between Local and Global Damage Indices," by E. DiPasquale and A.S. Cakmak, 8/15/89, (PB90-173865).

NCEER-89-0035 "Cyclic Undrained Behavior of Nonplastic and Low Plasticity Silts," by A.J. Walker and H.E. Stewart, 7/26/89, (PB90-183518/AS).

NCEER-89-0036 "Liquefaction Potential of Surficial Deposits in the City of Buffalo, New York," by M. Budhu, R. Giese and L. Baumgrass, 1/17/89, (PB90-208455/AS).

NCEER-89-0037 "A Determinstic Assessment of Effects of Ground Motion Incoherence," by A.S. Veletsos and Y. Tang, 7/15/89, (PB90-164294/AS).

NCEER-89-0038 "Workshop on Ground Motion Parameters for Seismic Hazard Mapping," July 17-18, 1989, edited by R.V. Whitman, 12/1/89, (PB90-173923/AS).

NCEER-89-0039 "Seismic Effects on Elevated Transit Lines of the New York City Transit Authority," by C.J. Costantino, C.A. Miller and E. Heymsfield, 12/26/89, (PB90-207887/AS).

NCEER-89-0040 "Centrifugal Modeling of Dynamic Soil-Structure Interaction," by K. Weissman, Supervised by J.H. Prevost, 5/10/89, (PB90-207879/AS).

NCEER-89-0041 "Linearized Identification of Buildings With Cores for Seismic Vulnerability Assessment," by I-K. Ho and A.E. Aktan, 11/1/89.

NCEER-90-0001 "Geotechnical and Lifeline Aspects of the October 17, 1989 Loma Prieta Earthquake in San Francisco," by T.D. O'Rourke, H.E. Stewart, F.T. Blackburn and T.S. Dickerman, 1/90, (PB90-208596/AS).

NCEER-90-0002 "Nonnormal Secondary Response Due to Yielding in a Primary Structure," by D.C.K. Chen and L.D. Lutes, 2/28/90.

NCEER-90-0003 "Earthquake Education Materials for Grades K-12," by K.E.K. Ross, 4/16/90.

NCEER-90-0004 "Catalog of Strong Motion Stations in Eastern North America," by R.W. Busby, 4/3/90.

NCEER-90-0005 "NCEER Strong-Motion Data Base: A User Manuel for the GeoBase Release (Version 1.0 for the Sun3)," by P. Friberg and K. Jacob, 3/31/90.

NCEER-90-0006 "Seismic Hazard Along a Crude Oil Pipeline in the Event of an 1811-1812 Type New Madrid Earthquake," by H.H.M. Hwang and C-H.S. Chen, 4/16/90.

NCEER-90-0007 "Site-Specific Response Spectra for Memphis Sheahan Pumping Station," by H.H.M. Hwang and C.S. Lee, 5/15/90.

NCEER-90-0008 "Pilot Study on Seismic Vulnerability of Crude Oil Transmission Systems," by T. Ariman, R. Dobry, M. Grigoriu, F. Kozin, M. O'Rourke, T. O'Rourke and M. Shinozuka, 5/25/90.

NCEER-90-0009 "A Program to Generate Site Dependent Time Histories: EQGEN," by G.W. Ellis, M. Srinivasan and A.S. Cakmak, 1/30/90.

NCEER-90-0010 "Active Isolation for Seismic Protection of Operating Rooms," by M.E. Talbott, Supervised by M. Shinozuka, 6/8/9.

NCEER-90-0011 "Program LINEARID for Identification of Linear Structural Dynamic Systems," by C-B. Yun and M. Shinozuka, 6/25/90.

NCEER-90-0012 "Two-Dimensional Two-Phase Elasto-Plastic Seismic Response of Earth Dams," by A.N. Yiagos, Supervised by J.H. Prevost, 6/20/90.

NCEER-90-0013 "Secondary Systems in Base-Isolated Structures: Experimental Investigation, Stochastic Response and Stochastic Sensitivity," by G.D. Manolis, G. Juhn, M.C. Constantinou and A.M. Reinhorn, 7/1/90.

NCEER-90-0014 "Seismic Behavior of Lightly-Reinforced Concrete Column and Beam-Column Joint Details," by S.P. Pessiki, C.H. Conley, P. Gergely and R.N. White, 8/22/90.

NCEER-90-0015 "Two Hybrid Control Systems for Building Structures Under Strong Earthquakes," by J.N. Yang and A. Danielians, 6/29/90.

NCEER-90-0016 "Instantaneous Optimal Control with Acceleration and Velocity Feedback," by J.N. Yang and Z. Li, 6/29/90.

NCEER-90-0017 "Reconnaissance Report on the Northern Iran Earthquake of June 21, 1990," by M. Mehrain, 10/4/90.

NCEER-90-0018 "Evaluation of Liquefaction Potential in Memphis and Shelby County," by T.S. Chang, P.S. Tang, C.S. Lee and H. Hwang, 8/10/90.

NCEER-90-0019 "Experimental and Analytical Study of a Combined Sliding Disc Bearing and Helical Steel Spring Isolation System," by M.C. Constantinou, A.S. Mokha and A.M. Reinhorn, 10/4/90.

NCEER-90-0020 "Experimental Study and Analytical Prediction of Earthquake Response of a Sliding Isolation System with a Spherical Surface," by A.S. Mokha, M.C. Constantinou and A.M. Reinhorn, 10/11/90.

NCEER-90-0021 "Dynamic Interaction Factors for Floating Pile Groups," by G. Gazetas, K. Fan, A. Kaynia and E. Kausel, 9/10/90.

NCEER-90-0022 "Evaluation of Seismic Damage Indices for Reinforced Concrete Structures," by S. Rodríguez-Gómez and A.S. Cakmak, 9/30/90.

NCEER-90-0023 "Study of Site Response at a Selected Memphis Site," by H. Desai, S. Ahmad, G. Gazetas and M.R. Oh, 10/11/90.

NCEER-90-0024 "A User's Guide to Strongmo: Version 1.0 of NCEER's Strong-Motion Data Access Tool for PCs and Terminals," by P.A. Friberg and C.A.T. Susch, 11/15/90.

NCEER-90-0025 "A Three-Dimensional Analytical Study of Spatial Variability of Seismic Ground Motions," by L-L. Hong and A.H.-S. Ang, 10/30/90.

NCEER-90-0026 "MUMOID User's Guide - A Program for the Identification of Modal Parameters," by S. Rodríguez-Gómez and E. DiPasquale, 9/30/90.

NCEER-90-0027 "SARCF-II User's Guide - Seismic Analysis of Reinforced Concrete Frames," by S. Rodríguez-Gómez, Y.S. Chung and C. Meyer, 9/30/90.

NCEER-90-0028 "Viscous Dampers: Testing, Modeling and Application in Vibration and Seismic Isolation," by N. Makris and M.C. Constantinou, 12/20/90.

NCEER-90-0029 "Soil Effects on Earthquake Ground Motions in the Memphis Area," by H. Hwang, C.S. Lee, K.W. Ng and T.S. Chang, 8/2/90.

NCEER-91-0001 "Proceedings from the Third Japan-U.S. Workshop on Earthquake Resistant Design of Lifeline Facilities and Countermeasures for Soil Liquefaction, December 17-19, 1990," edited by T.D. O'Rourke and M. Hamada, 2/1/91.

NCEER-91-0002 "Physical Space Solutions of Non-Proportionally Damped Systems," by M. Tong, Z. Liang and G.C. Lee, 1/15/91.

NCEER-91-0003 "Kinematic Seismic Response of Single Piles and Pile Groups," by K. Fan, G. Gazetas, A. Kaynia, E. Kausel and S. Ahmad, 1/10/91, to be published.

NCEER-91-0004 "Theory of Complex Damping," by Z. Liang and G. Lee, to be published.

NCEER-91-0005 "3D-BASIS - Nonlinear Dynamic Analysis of Three Dimensional Base Isolated Structures: Part II," by S. Nagarajaiah, A.M. Reinhorn and M.C. Constantinou, 2/28/91.

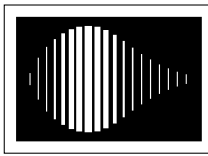

NATIONAL CENTER FOR EARTHQUAKE ENGINEERING RESEARCH

Headquartered at the State University of New York at Buffalo

State University of New York at Buffalo
Red Jacket Quadrangle
Buffalo, New York 14261
Telephone: 716/645-3391
FAX: 716/645-3399

ISSN 1088-3800